Multimodality imaging of coronary artery bypass grafts

Salm, L.P.

Multimodality Imaging of Coronary Artery Bypass Grafts

Multimodality Imaging of Coronary Artery Bypass Grafts

Proefschrift

ter verkrijging van
de graad van Doctor aan de Universiteit Leiden,
op gezag van de Rector Magnificus Dr. D.D. Breimer,
hoogleraar in de faculteit der Wiskunde en
Natuurwetenschappen en die der Geneeskunde,
volgens besluit van het College voor Promoties
te verdedigen op dinsdag 7 november 2006
klokke 13.45 uur

door
Liesbeth Pauline Salm
geboren te Amsterdam
in 1973

Promotiecommissie

Promotores	Prof. Dr. E.E. van der Wall Prof. Dr. A. de Roos
Co-promotor	Dr. H.W. Vliegen
Referent	Prof. Dr. P.J. de Feyter (Erasmus Universiteit, Rotterdam)
Overige leden	Prof. Dr. J.J. Bax Dr. J. Doornbos Prof. Dr. J.W. Jukema Prof. Dr. A.C. van Rossum (Vrije Universiteit, Amsterdam)

Cover design and lay-out by Wendy Karsten.
Printed by Drukkerij Macula b.v., Boskoop, the Netherlands.
Printed on Freelife paper, containing 50% recycled fibre.
ISBN-10: 90-9021156-X
ISBN-13: 978-90-9021156-5

The research described in this thesis was performed at the department of Cardiology and Radiology of the Leiden University Medical Center, Leiden, the Netherlands.
Financial support by the Netherlands Heart Foundation for the publication of this thesis is gratefully acknowledged.

Forever trusting who we are
and nothing else matters
Metallica

Aan Hugo

Table of Contents

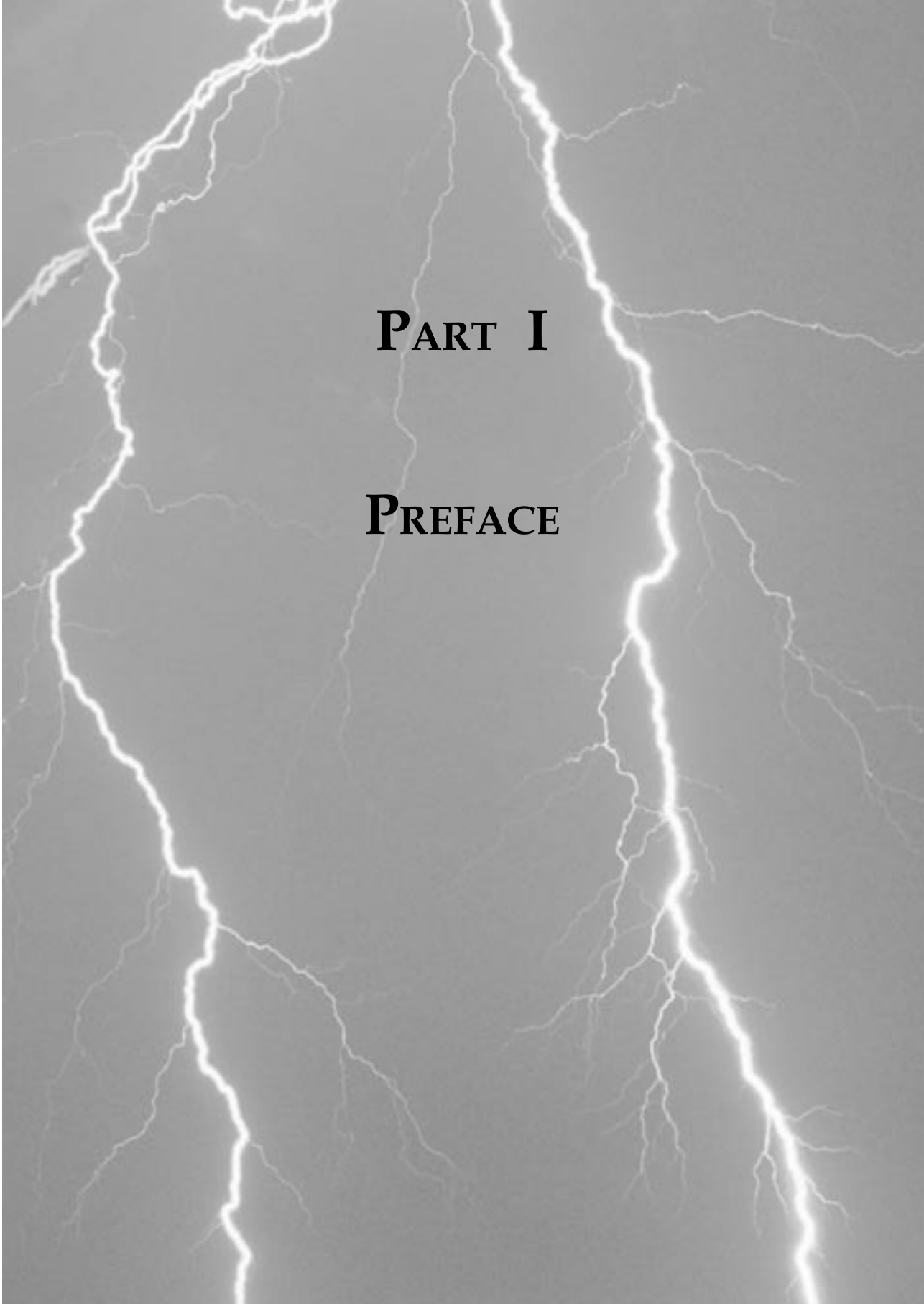

Part I

Preface

Chapter 1

Introduction

Coronary artery bypass graft surgery

Coronary heart disease (CHD) is the most common cause of death worldwide, accounting for nearly 2 million deaths each year in Europe alone (1). CHD is most commonly due to obstruction of the coronary arteries by an atheromatous plaque (2). Manifestations of CHD include unstable and chronic angina pectoris, and myocardial infarction. Therapeutic options for CHD are directed towards prevention of further progression of disease or symptom-relief. This is achieved by obtaining revascularization either by percutaneous coronary intervention or coronary artery bypass graft surgery (CABG), if pharmacological treatment alone is insufficient.

In CABG, revascularization of the myocardium is obtained by rerouting or bypassing the bloodstream around the coronary obstruction. Garrett et al. performed the first human CABG in 1967 as a "bailout" procedure (3). Since then, the surgical technique is further developed and refined. At first, graft material was harvested from the saphenous veins in the lower limbs. Subsequently, arteries were also used as bypass grafts, such as left and right internal mammary arteries (IMA), radial artery and gastro-epiploic artery.

CABG was demonstrated to be an effective treatment for CHD in short- and intermediate-term (4;5). However, graft disease occurs frequently, beginning with accelerated atherosclerosis early after surgery in vein grafts (6;7). Arterial grafts have a superior outcome compared with vein grafts, still obstruction and occlusion do occur (8;9). In a recent study, comparing the outcome of vein and IMA grafts, patency at 10 years was 61% for vein grafts compared with 85% for IMA grafts ($p<0.001$) (10).

The gold standard for evaluating bypass grafts is coronary angiography. Although coronary angiography offers a rapid and complete exploration of the native coronary arteries and grafts, it is an invasive procedure, requiring arterial puncture, x-ray exposition, and hospitalization. Complications include ventricular arrhythmias, myocardial infarction, cardiac perforation, necessary emergency CABG, and death, even though the risk is small (11;12). Furthermore, coronary angiography does not provide a functional assessment of the myocardial region, perfused by the respective coronary artery or graft. A noninvasive anatomical and functional examination of the coronary arteries and bypass grafts would be preferable to detect insufficiency and identify a target for re-intervention.

Noninvasive imaging of coronary artery bypass grafts

Several noninvasive imaging modalities are available in order to detect bypass graft insufficiency. Using cardiovascular magnetic resonance (CMR), anatomy and function of bypass grafts may be assessed. MR angiography allows an accurate evaluation of patency in both arterial and vein grafts (13-15). The degree of graft stenosis can, thus far, only be evaluated in vein graft bodies, excluding the recipient coronary arteries (16).

A functional parameter that may be evaluated by CMR is the blood flow velocity. Blood flow velocity of native coronary arteries and bypass grafts can be derived invasively at rest and during pharmacological stress using the Doppler flow wire (17). Subsequent calculation of the coronary flow velocity reserve (CFVR) by dividing the stress by the rest parameter provides insight in the physiological condition of the vessel (18;19). Previous studies have shown that flow velocity measurements may be used to evaluate the

hemodynamic consequences of stenoses in native coronary arteries (20;21), and bypass grafts (22), although studies focusing on bypass grafts are few. Using the phase-contrast MR technique, it is feasible to perform flow velocity measurements noninvasively by CMR in both vein (15;23) and arterial grafts (24). The value of CMR flow velocity measurements in predicting the presence of a stenosis in vein grafts was successfully researched (25;26). CMR flow velocity measurements of arterial grafts remain challenging because of the small luminal diameter of the internal mammary arteries, and metal clip artefacts. In earlier studies demonstrating the feasibility to measure flow in left IMA grafts, CMR sequences were limited by low spatial and temporal resolution (24;27;28).
With computed tomography (CT) angiography, assessment of bypass graft patency was extensively investigated (29-31).When it became possible to use multiple detectors in a single spiral CT acquisition, graft patency could be assessed with very high accuracy (32;33). The evaluation of stenoses in grafts by multi-detector row CT is still a challenge because of motion artefacts, metal clip artefacts or beam hardening from calcium deposits (32-34). Since a cardiac CT examination to evaluate native coronary arteries and bypass grafts requires scanning of the entire heart, reconstruction of the left ventricular (LV) function is also achievable. Several studies showed that 4-detector row CT allowed accurate assessment of global and regional LV function (35;36). Validation of the next generation CT equipment in assessing LV function has yet to be conducted.
Single-photon emission computed tomography (SPECT) perfusion imaging is a well-established technique by which to detect CHD by evaluating regional myocardial perfusion at rest and during stress. Excellent sensitivities and specificities of SPECT to detect stenoses in native coronary arteries (37;38) and bypass grafts (39) were demonstrated. More recently, for SPECT imaging the emphasis has shifted from detection of CHD to hemodynamic evaluation of stenoses. Comparative studies between SPECT imaging and invasive assessment using the Doppler flow wire have been performed, demonstrating a good agreement (ranging from 72% to 96%) between these two techniques for the evaluation of the hemodynamic consequence of an intermediate native coronary artery stenosis (21;40;41). Studies evaluating the hemodynamic consequences of bypass graft lesions are lacking.

OUTLINE OF THE THESIS

The aim of the thesis was to describe multiple modalities to examine coronary artery bypass grafts, and to further develop noninvasive imaging techniques to detect or exclude stenoses in native coronary arteries and bypass grafts in patients who experienced recurrent chest pain after CABG.

Part I of the thesis provides an introduction to noninvasive imaging. In chapter 2, noninvasive imaging of coronary artery bypass grafts by CMR and CT is reviewed in detail.
Part II of the thesis focuses on CMR flow velocity imaging in vein and arterial grafts. In chapter 3, a model to detect or exclude stenoses in vein grafts by CMR volumetric flow measurements is described. In chapter 4, two analysis methods for the CMR flow velocity maps, i.e. velocity and volumetric flow, are compared, using flow velocity

maps of vein grafts. In chapter 5, the functional significance of bypass graft stenoses is investigated by SPECT perfusion imaging and CMR, and compared with findings at coronary angiography. In chapter 6, a novel CMR phase-contrast sequence to measure flow velocity in arterial and vein grafts is introduced and validated.

Part III of the thesis concentrates on multi-detector row CT imaging of coronary artery bypass grafts. In chapter 7, a comprehensive assessment by 16-detector row CT of patients after CABG is investigated. In chapter 8, global and regional LV function evaluated by 16-detector row CT is compared with evaluation by echocardiography and CMR.

Part IV focuses on the hemodynamic consequences of vein graft lesions. In chapter 9, the relative merits of invasive Doppler flow velocity measurements and SPECT perfusion imaging are studied in assessing the hemodynamic significance of stenoses in vein grafts, and the results are related to coronary angiography.

REFERENCES

1. British Heart Foundation. European Cardiovascular Disease Statistics. 2000.
2. Morrow DA, Gersh BJ, Braunwald E. Chronic coronary artery disease. In: Braunwald's heart disease. A textbook of cardiovascular medicine. 2005.
3. Garrett HE, Dennis EW, DeBakey ME. Aortocoronary bypass with saphenous vein graft. Seven-year follow-up. Jama 1973;223:792-4.
4. Yusuf S, Zucker D, Peduzzi P et al. Effect of coronary artery bypass graft surgery on survival: overview of 10-year results from randomised trials by the Coronary Artery Bypass Graft Surgery Trialists Collaboration. Lancet 1994;344:563-70.
5. Davis KB, Chaitman B, Ryan T, Bittner V, Kennedy JW. Comparison of 15-year survival for men and women after initial medical or surgical treatment for coronary artery disease: a CASS registry study. Coronary Artery Surgery Study. J Am Coll Cardiol 1995;25:1000-9.
6. Motwani JG, Topol EJ. Aortocoronary saphenous vein graft disease: pathogenesis, predisposition, and prevention. Circulation 1998;97:916-31.
7. Fitzgibbon GM, Kafka HP, Leach AJ, Keon WJ, Hooper GD, Burton JR. Coronary bypass graft fate and patient outcome: angiographic follow-up of 5,065 grafts related to survival and reoperation in 1,388 patients during 25 years. J Am Coll Cardiol 1996;28:616-26.
8. Loop FD, Lytle BW, Cosgrove DM et al. Influence of the internal-mammary-artery graft on 10-year survival and other cardiac events. N Engl J Med 1986;314:1-6.
9. Cameron A, Kemp HG, Jr., Green GE. Bypass surgery with the internal mammary artery graft: 15 year follow-up. Circulation 1986;74:III30-III36.
10. Goldman S, Zadina K, Moritz T et al. Long-term patency of saphenous vein and left internal mammary artery grafts after coronary artery bypass surgery. Results from a department of Veteran Affairs Cooperative study. J Am Coll Cardiol 2004;44:2149-56.
11. Krone RJ, Johnson L, Noto T. Five year trends in cardiac catheterization: a report from the Registry of the Society for Cardiac Angiography and Interventions. Cathet Cardiovasc Diagn 1996;39:31-5.
12. Wyman RM, Safian RD, Portway V, Skillman JJ, McKay RG, Baim DS. Current complications of diagnostic and therapeutic cardiac catheterization. J Am Coll Cardiol 1988;12:1400-6.
13. Bunce NH, Lorenz CH, John AS, Lesser JR, Mohiaddin RH, Pennell DJ. Coronary artery bypass graft patency: assessment with true ast imaging with steady-state precession versus gadolinium-enhanced MR angiography. Radiology 2003;227:440-6.
14. Wintersperger BJ, Engelmann MG, von Smekal A et al. Patency of coronary bypass grafts: assessment with breath-hold contrast-enhanced MR angiography--value of a non-electrocardiographically triggered technique. Radiology 1998;208:345-51.
15. Galjee MA, van Rossum AC, Doesburg T, van Eenige MJ, Visser CA. Value of magnetic resonance imaging in assessing patency and function of coronary artery bypass grafts. An angiographically controlled study. Circulation 1996;93:660-6.
16. Langerak SE, Vliegen HW, de Roos A et al. Detection of Vein Graft Disease using High-resolution Magnetic Resonance Angiography. Circulation 2002;105:328-33.
17. Doucette JW, Corl PD, Payne HM et al. Validation of a Doppler guide wire for intravascular measurement of coronary artery flow velocity. Circulation 1992;85:1899-911.
18. Gould KL, Kirkeeide RL, Buchi M. Coronary flow reserve as a physiologic measure of stenosis severity. J Am Coll Cardiol 1990;15:459-74.
19. White CW, Wright CB, Doty DB et al. Does visual interpretation of the coronary arteriogram predict the physiologic importance of a coronary stenosis? N Engl J Med 1984;310:819-24.
20. Ofili EO, Labovitz AJ, Kern MJ. Coronary flow velocity dynamics in normal and diseased arteries. Am J Cardiol 1993;71:3d-9d.
21. Chamuleau SA, Tio RA, de Cock CC et al. Prognostic value of coronary blood flow velocity and myocardial perfusion in intermediate coronary narrowings and multivessel disease. J Am Coll Cardiol 2002;39:852-8.
22. White CW. Clinical applications of Doppler coronary flow reserve measurements. Am J Cardiol 1993;71:10d-6d.
23. Langerak SE, Kunz P, Vliegen HW et al. Improved MR flow mapping in coronary artery bypass grafts during adenosine-induced stress. Radiology 2001;218:540-7.
24. Ishida N, Sakuma H, Cruz BP et al. Mr flow measurement in the internal mammary artery-to-coronary artery bypass graft: comparison with graft stenosis at radiographic angiography. Radiology 2001;220:441-7.
25. Langerak SE, Vliegen HW, Jukema JW et al. Value of magnetic resonance imaging for the noninvasive detection of stenosis in coronary artery bypass grafts and recipient coronary arteries. Circulation 2003;107:1502-8.

26. Bedaux WL, Hofman MB, Vyt SL, Bronzwaer JG, Visser CA, van Rossum AC. Assessment of coronary artery bypass graft disease using cardiovascular magnetic resonance determination of flow reserve. J Am Coll Cardiol 2002;40:1848-55.
27. Debatin JF, Strong JA, Sostman HD et al. MR characterization of blood flow in native and grafted internal mammary arteries. J Magn Reson Imaging 1993;3:443-50.
28. Sakuma H, Globits S, O'Sullivan M et al. Breath-hold MR measurements of blood flow velocity in internal mammary arteries and coronary artery bypass grafts. J Magn Reson Imaging 1996;6:219-22.
29. Daniel WG, Dohring W, Stender HS, Lichtlen PR. Value and limitations of computed tomography in assessing aortocoronary bypass graft patency. Circulation 1983;67:983-7.
30. Bateman TM, Gray RJ, Whiting JS et al. Prospective evaluation of ultrafast cardiac computed tomography for determination of coronary bypass graft patency. Circulation 1987;75:1018-24.
31. Stanford W, Brundage BH, MacMillan R et al. Sensitivity and specificity of assessing coronary bypass graft patency with ultrafast computed tomography: results of a multicenter study. J Am Coll Cardiol 1988;12:1-7.
32. Ropers D, Ulzheimer S, Wenkel E et al. Investigation of aortocoronary artery bypass grafts by multislice spiral computed tomography with electrocardiographic-gated image reconstruction. Am J Cardiol 2001;88:792-5.
33. Nieman K, Pattynama PM, Rensing BJ, van Geuns RJ, de Feyter PJ. Evaluation of patients after coronary artery bypass surgery: CT angiographic assessment of grafts and coronary arteries. Radiology 2003;229:749-56.
34. Marano R, Storto ML, Maddestra N, Bonomo L. Non-invasive assessment of coronary artery bypass graft with retrospectively ECG-gated four-row multi-detector spiral computed tomography. Eur Radiol 2004;14:1353-62.
35. Dirksen MS, Bax JJ, de Roos A et al. Usefulness of dynamic multislice computed tomography of left ventricular function in unstable angina pectoris and comparison with echocardiography. Am J Cardiol 2002;90:1157-60.
36. Juergens KU, Grude M, Maintz D et al. Multi-detector row CT of left ventricular function with dedicated analysis software versus MR imaging: initial experience. Radiology 2004;230:403-10.
37. Mahmarian JJ, Boyce TM, Goldberg RK, Cocanougher MK, Roberts R, Verani MS. Quantitative exercise thallium-201 single photon emission computed tomography for the enhanced diagnosis of ischemic heart disease. J Am Coll Cardiol 1990;15:318-29.
38. Maddahi J, Kiat H, Van Train KF et al. Myocardial perfusion imaging with technetium-99m sestamibi SPECT in the evaluation of coronary artery disease. Am J Cardiol 1990;66:55E-62E.
39. Lakkis NM, Mahmarian JJ, Verani MS. Exercise thallium-201 single photon emission computed tomography for evaluation of coronary artery bypass graft patency. Am J Cardiol 1995;76:107-11.
40. Deychak YA, Segal J, Reiner JS et al. Doppler guide wire flow-velocity indexes measured distal to coronary stenoses associated with reversible thallium perfusion defects. Am Heart J 1995;129:219-27.
41. Verberne HJ, Piek JJ, van Liebergen RA, Koch KT, Schroeder-Tanka JM, van Royen EA. Functional assessment of coronary artery stenosis by doppler derived absolute and relative coronary blood flow velocity reserve in comparison with (99m)Tc MIBI SPECT. Heart 1999;82:509-14.

CHAPTER 2

Cardiovascular magnetic resonance and computed tomography of coronary artery bypass grafts

Liesbeth P. Salm
Jeroen J. Bax
Joanne D. Schuijf
Hildo J. Lamb
J.Wouter Jukema
Ernst E. van der Wall
Albert de Roos

Chapter 21 in: MRI and CT of the cardiovascular system. Second edition.
Lippincott Williams & Wilkins 2005

INTRODUCTION

Coronary artery bypass grafting (CABG) is a commonly performed surgical procedure for alleviation of symptoms and prolonging survival for patients with ischemic heart disease. Bypass graft disease is a common consequence, requiring x-ray coronary angiography for diagnosis. Coronary angiography is an invasive procedure that includes x-ray exposure, hospitalization, and a small risk of complications, including arrhythmias, coronary artery dissection, and cardiac death. A noninvasive diagnostic method for the assessment of bypass graft anatomy and function is of great benefit. This chapter reviews the research that has been performed in evaluating bypass grafts noninvasively using cardiovascular magnetic resonance (CMR) and computed tomography (CT).

CARDIOVASCULAR MAGNETIC RESONANCE OF CORONARY ARTERY BYPASS GRAFTS

Anatomy Assessment: Angiography

During the past decades, a considerable amount of effort has been invested to achieve noninvasive visualization of the coronary arteries and bypass grafts with CMR. The relatively larger size, straight course, and immobility during the cardiac cycle of coronary bypass grafts allowed the evaluation of graft patency even in the earliest studies, whereas assessment of the coronary arteries could not be achieved at that stage. In these initial investigations, two-dimensional (2D) spin-echo and gradient-echo techniques were

Author	Patients	Grafts	Graft type	Magnetic resonance technique	Assessable grafts (%)	Sensitivity (%)	Specificity (%)
White et al (4)	25	72	vein	2-D SE	90	72	91
Rubinstein et al (6)	20	47	vein	2-D SE	100	72	90
Jenkins et al (3)	22	45	vein	2-D SE	100	73	89
Frija et al (2)	28	52	vein and arterial	2-D SE	100	71	97
White et al (5)	10	28	vein and arterial	2-D GE	100	86	93
Aurigemma et al (1)	20	45	vein and arterial	2-D GE	100	100	88
Vanninen et al (7)	8	8	GEA	2-D GE	100	100	100
Galjee et al (8)	47	84	vein	2-D SE	92	84	98
				2-D GE	92	88	98
Weighted Mean 2D					95	81	94
Kessler et al (11)	8	21	vein and arterial	3-D NAV	90	100	87
Engelmann et al (9)	16	55	vein and arterial	3-D CE	100	85	95
Vrachliotis et al (14)	15	45	vein and arterial	3-D CE	98	93	97
Wintersperger et al (15)	27	76	vein and arterial	3-D CE	100	81	95
Kalden et al (10)	22	59	vein and arterial	3-D CE	100	93	93
Molinari et al (13)	18	51	vein and arterial	3-D NAV	96	92	97
Langerak et al (12)	38	56	vein	3-D NAV	100	83	98
Wittlinger et al (16)	34	82	vein and arterial	3-D NAV	90	78	96
Bunce et al (17)	34	79	vein and arterial	3-D CE	100	73	85
Weighted Mean 3D					96	85	94

SE = spin-echo; GE = gradient-echo; GEA = gastroepiploic artery; NAV = navigator; CE = contrast-enhanced

Table 2.1

Detection of occlusion in vein and arterial grafts by magnetic resonance angiography compared with invasive angiography

applied to acquire successive axial slices during repetitive breath-holds (1-8). With the spin-echo technique, absence of signal at different levels was considered to indicate the presence of a patent graft because in normal grafts, rapid blood movement is present. To obtain adequate contrast, however, sufficient flow between the graft lumen and the wall is needed, whereas the presence of metallic clips, stents, or calcifications may result in a signal void that can be mistaken for graft stenosis or occlusion. In contrast, flowing blood is depicted as a bright signal during imaging with gradient MR techniques. As shown in Table 2.1, both acquisition techniques have been evaluated in several studies with conventional angiography as the standard of reference, demonstrating sensitivities and specificities varying from 71% to 100% and 89% to 100%, respectively. Pooled analysis of these eight studies (with 180 patients and 381 grafts) revealed a weighted mean sensitivity and specificity of 81% and 94%, with inclusion of 95% of grafts. Despite these promising results in the distinction between patent and occluded grafts, these 2D techniques were still limited by their low signal-to-noise ratio and low spatial resolution. Substantial progress in image quality was achieved by the development of three-dimensional (3D) imaging techniques, allowing the acquisition of volume slabs containing several thin slices and imaging with high spatial resolution. To improve patient comfort, navigator techniques have been developed that permit real-time monitoring of diaphragm motion and thus free-breathing during data acquisition. In addition, improved enhancement of blood/muscle contrast can be expected by the administration of intravascular contrast agents. An example of a typical MR acquisition protocol with navigator respiratory gating is depicted in Figure 2.1. In Figure 2.2 a resulting 3D reconstruction is shown, and an example of a patent bypass graft as confirmed by conventional angiography is provided in Figure 2.3.

Pooled analysis of nine studies using 3D techniques, with more than 200 patients included, revealed a slight increase in weighted sensitivity from 81% to 85%, with no loss in specificity (Figure 2.4) (9-17). Sensitivity and specificity for the different types of grafts (as reported in seven studies) are shown in Figure 2.5. No difference in diagnostic accuracy for detection of graft occlusion was noted between arterial and vein grafts. In particular, the sensitivity and specificity of arterial grafts were 85% and 95% compared with 86% and 93% in vein grafts (9;10;12-14;16;17). These studies illustrate the potential of CMR to evaluate graft patency in clinical routine. Its safe and noninvasive nature in combination with the high specificity (~94%) and negative predictive value (~96%) suggests that in patients presenting with recurrent symptoms after bypass grafting, CMR may function as a first-line investigation tool to rule out graft occlusion before more invasive diagnostic procedures.

However, few attempts thus far have been made to evaluate graft stenosis in addition to assessment of patency. Langerak and colleagues observed a sensitivity and specificity of 82% and 88% for the detection of ≥50% luminal narrowing in vein bypass grafts (12). In contrast, a discouraging sensitivity of 38% was reported by Kalden et al. (10). Because the presence of graft stenosis rather than total occlusion of the graft may be the cause of recurrent complaints, the value of MR angiography (MRA) to evaluate graft stenosis needs to be further explored before routine use of the technique is feasible. In addition, recurrent anginal complaints may also be attributable to progression of coronary artery

disease in native coronary vessels, and assessment in these vessels is still severely hampered by the current spatial and temporal resolution. A possible solution to this limitation may lie in the combination of MRA with MR flow mapping, since the latter provides a functional measurement of the entire vascular tree beyond the level of the flow measurement. Moreover, because the functional graft status is not directly related to the degree of luminal narrowing, improved diagnostic accuracy and management may be expected by such a combined approach.

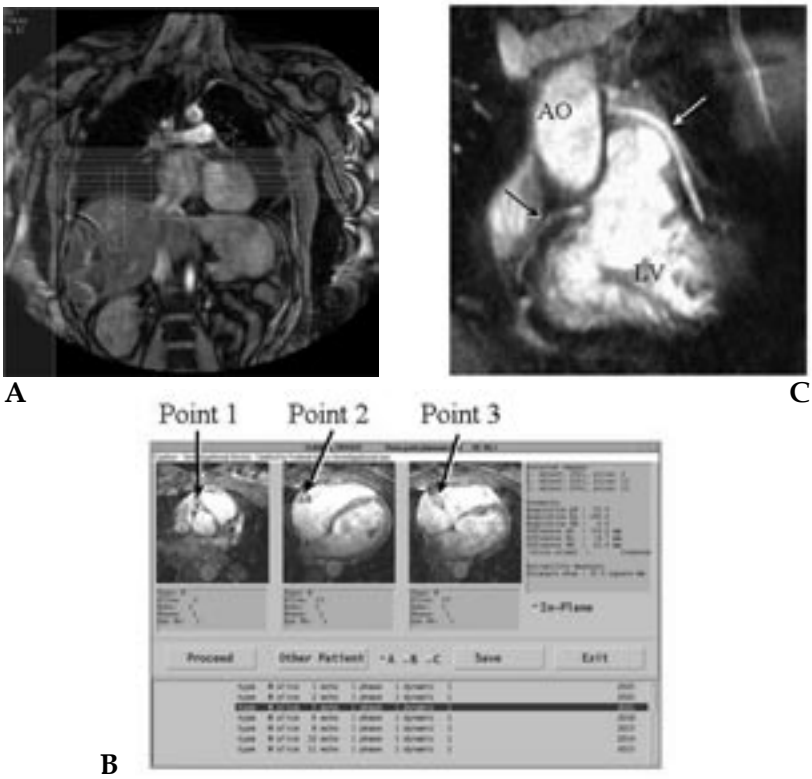

Figure 2.1

Typical magnetic resonance (MR) acquisition protocol. (A) Typical plan-scan for cardiovascular magnetic resonance (CMR) angiography. Axial imaging volume (horizontal lines); volume used for localized shimming (large box); position in the right hemidiaphragm of the respiratory navigator (rectangular box); position of a saturation band for suppression of image artifacts (left box). (B) With the use of axial scout images, the three-point plan-scan is used to select three points in space, one at the origin of the coronary artery or bypass graft, one at the most distal point, and one in the middle of the first two points. From this information, an imaging plane is automatically calculated in plane with the coronary artery or bypass graft of interest. (C) CMR angiography of a patient with a bypass of the left coronary system (white arrow) and a visible native right coronary artery (black arrow). This imaging approach can be used clinically to assess bypass graft patency. AO = aorta; LV = left ventricle. (Courtesy of H.J. Lamb) A full colour version of this illustration can be found in the full colour section (page 164).

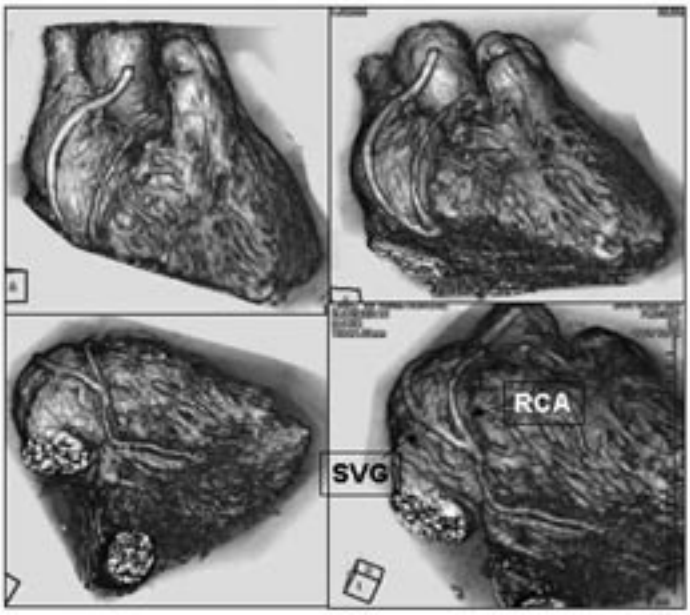

Figure 2.2
Whole-heart CMR angiography of a vein bypass graft to the right coronary artery at different rotation angles. (Courtesy of Dr. H. Sakuma) A full colour version of this illustration can be found in the full colour section (page 165).

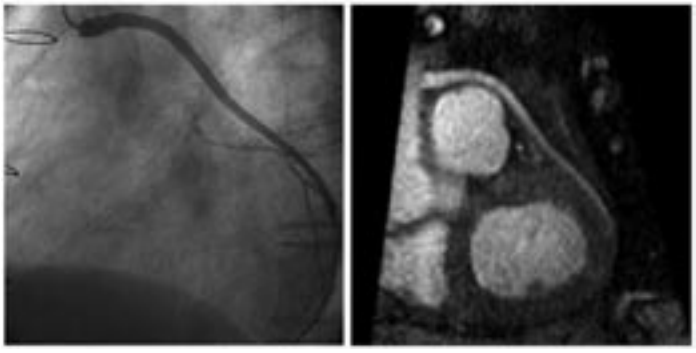

Figure 2.3
MR angiogram of a vein graft (right) in comparison with a coronary angiogram (left). Multiplanar reformat reconstruction is shown of a free-breathing, three-dimensional (3D), navigator-gated sequence used for acquisition of the MR angiogram.

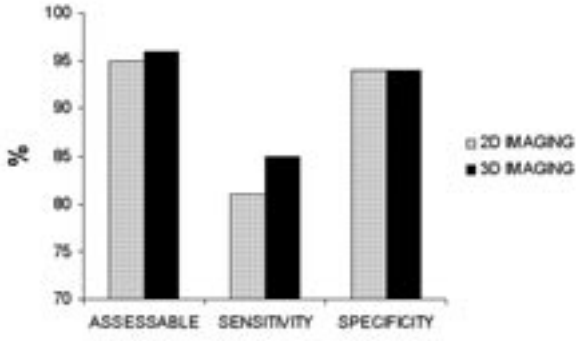

Figure 2.4
Sensitivities and specificities of two-dimensional (2D) and 3D MR angiography (MRA) acquisition techniques (data based on references 1-17).

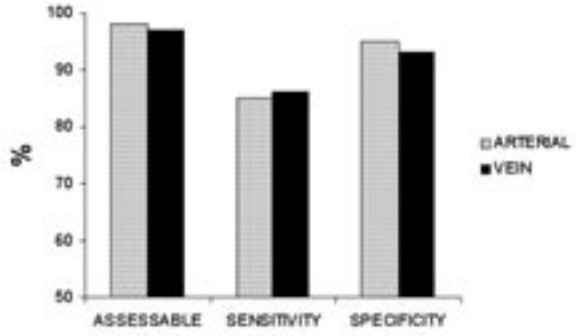

Figure 2.5
Performance of 3D MRA in arterial and vein grafts (data based on references 9,10,12-14,16,17).

Functional Assessment: Flow Velocity
A vessel narrowing, visualized by means of angiography, may or may not impair flow through that vessel (18;19). The assessment of blood flow through coronary arteries and bypass grafts has gained wide attention. To evaluate the hemodynamic impairment of a lesion, flow is measured at rest and during pharmacologically induced stress, for instance with adenosine or dipyridamole (20). By dividing the flow value during stress by the flow value at rest, the coronary flow reserve (CFR) is calculated (21;22). Flow-limiting stenoses cause a compensatory vasodilatation at rest to maintain sufficient blood flow to the myocardium. As a consequence, the vessel cannot respond adequately to an increase in absolute blood flow by vasodilatation during pharmacologically induced stress, and CFR will be reduced. At first, blood flow was determined by means of Doppler flow transducers at open-chest procedures (18;21-25), limitating extensive use

of CFR in clinical practice. When the diameter of intravascular catheter-based Doppler ultrasonographic devices could be reduced to 0.018 inch, it became feasible to measure the velocity of the blood flow and calculate the coronary flow velocity reserve (CFVR) for coronary arteries in patients during catheterization. Blood flow correlated well with Doppler-derived velocity of blood flow both in vitro and in vivo (26-28). Invasive Doppler-derived CFVR has proven its potential in numerous clinical applications, such as in identifying hemodynamic significant stenoses in native coronary arteries and vein grafts (29;30), in the functional assessment of stenoses of intermediate severity (31), in the determination of the need for and the outcome after coronary intervention (32-34) and in the prediction of restenosis (35).
With the use of MR, blood flow velocity can be measured using phase-contrast, velocity-encoded sequences (36). To use such a sequence accurately, an imaging plane perpendicular to the target vessel has to be selected by means of survey images. Throughout the cardiac cycle, the acquisition yields anatomic modulus images, paired with phase images, in which every pixel contains a different velocity value. Volume flow (in milliliters/min) can be obtained by calculating the integrated volumetric flow rate of all pixels in the vessel lumen per heartbeat and multiply it with the heart rate. To display the flow pattern, a flow rate-versus-time graph can be presented. Alternatively, the central peak velocity (in centimeters per second) can be obtained by selecting several pixels in the vessel center. Figure 2.6 depicts a typical example of a MR velocity mapping examination in a vein graft.

Early magnetic resonance studies in vein grafts
For vein grafts, feasibility to quantify flow and characterize the flow pattern noninvasively by MR was demonstrated (37;38). To establish feasibility, an attempt to measure flow in 49 vein grafts with ≤50% luminal stenosis at coronary angiography in 27 patients was made (38). In 84% of grafts, flow could be measured adequately. In another early study, 23 vein grafts in 18 patients were studied to distinguish normal from dysfunctional grafts by MR with flow mapping plus coronary angiography as the gold standard (39). They found that graft flow <20 ml/min and a loss of the biphasic flow pattern, typical for bypass grafts, would indicate a dysfunctional graft. On top of comparing spin-echo with cine gradient-echo MR assessment of vein graft patency, Galjee et al. (8) investigated vein graft function by phase-velocity imaging. In 62 of the 73 angiographically patent grafts (85%), adequate biphasic flow profiles could be obtained. A significant difference in flow between single grafts and sequential grafts to three vascular regions was demonstrated. These early vein graft flow studies were limited by the use of a gradient-echo sequence with limited spatial resolution (1.9x1.2x5 mm^3) and no compensation for respiratory motion on 0.5 to 0.6 Tesla (T) magnets.

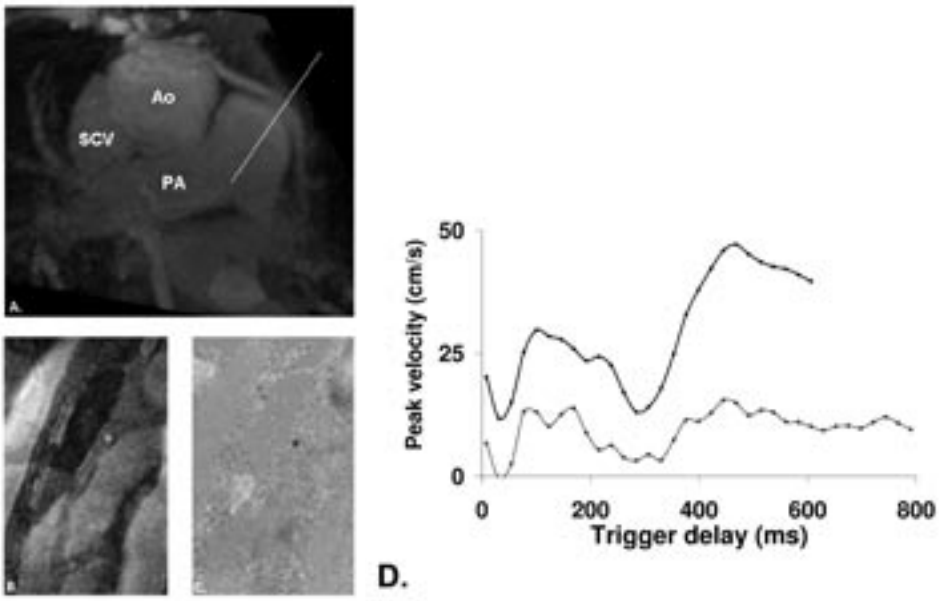

Figure 2.6

MR flow velocity study. Survey image visualizing a vein graft in plane (A). A plane perpendicular to the graft is selected, and modulus and phase images are acquired (B,C). The graft is pictured as a white, respectively black spot in the center of the image. In every image in the cardiac cycle 4 pixels in the center of the graft are selected to obtain a velocity curve (D). The MR flow velocity acquisition is repeated during adenosine-induced stress to obtain the stress velocity curve (black graph). Ao = aorta; PA = pulmonary artery; SCV = supracaval vein.

Early magnetic resonance studies in arterial grafts

Feasibility to quantify flow in native and grafted internal mammary arteries (IMAs) was demonstrated in 10 volunteers and 15 patients using a free-breathing gradient-echo sequence on a 1.5 T MR scanner (40). Patients had recently undergone IMA grafting; no control angiography of the arterial grafts was performed. A large intersubject variation of IMA graft flow (range 28-164 ml/min) was observed. Mean flow and peak velocity were lower in IMA grafts compared with native IMAs. In a different feasibility study, respiratory motion was compensated using a breath-hold segmented k-space gradient-echo sequence to quantify velocity in native and grafted IMAs (41). IMA grafts were investigated within 6 months after CABG; no control angiography was available. Comparison with a free-breathing techique in native IMAs demonstrated a higher peak velocity using the breath-hold sequence because of elimination of respiratory motion artifacts and averaging of velocities. This sequence allowed imaging time to decrease from approximately 4 minutes at free-breathing to a 20-second breath-hold. By means of a view-sharing reconstruction, an effective temporal resolution of 64 ms could be maintained, allowing an acquisition of 7 to 13 temporal phases in a cardiac cycle.

Angiographically controlled magnetic resonance studies in vein and arterial grafts

To evaluate the diagnostic value of MR flow velocity in bypass grafts, several angiographically controlled studies were performed. In addition to investigating the accuracy of contrast-enhanced MRA in the evaluation of bypass grafts postoperatively, Brenner et al. (42) performed additional MR velocity mapping of the grafts. Only 65% of the 247 obtained MR velocity images could be evaluated because of metal clip artifacts in IMA grafts. Concerning the MR velocity measurements, they concluded that this technique was not qualified for the detection of bypass graft stenoses.

With the use of breath-hold sequences, flow measurements at rest and during pharmacologically induced stress with determination of CFR in bypass grafts could be achieved. Langerak et al. (43) validated a breath-hold turbo-field echo-planar imaging sequence by demonstrating a good correlation with a free-breathing technique for aortic and native IMA flow in volunteers. This sequence was subsequently used to measure flow at rest and during adenosine-induced stress in 2 arterial and 18 vein grafts, which were patent at coronary angiography. A significant increase at adenosine-induced stress for flow and velocity parameters was observed, and CFR (mean 2.7 ± 1.1 for single grafts) could be calculated. In another study, MR-derived velocity measurements correlated well with invasive Doppler-derived velocity measurements in 27 grafts (26 vein/1 arterial graft) (44). A significant difference between grafts with <50% stenosis and ≥50% stenosis was demonstrated for MR-derived average peak velocity during adenosine-induced stress (20.2 ± 0.4 vs. 12.2 ± 0.4 cm/s), and diastolic peak velocity during adenosine-induced stress (35.3 ± 0.3 vs. 25.6 ± 0.3 cm/s). Measurements obtained at rest did not show a significant difference between grafts with <50% stenosis and ≥50% stenosis. The detection of ≥70% angiographic stenosis in IMA grafts by breath-hold MR flow velocity at rest and during dipyridamole-induced stress was investigated (45). In 24 early postoperative patients, successful MR flow measurements were performed in the mid-IMA graft. At CABG surgery, titanium clips were used to avoid metal artifacts at MR imaging. A significant difference between grafts with <70% and ≥70% stenosis was demonstrated for baseline mean blood flow (79.8 ± 38.2 ml/min vs. 16.9 ± 5.5 ml/min) and the diastolic-to-systolic velocity ratio (1.88 ± 0.96 vs. 0.61 ± 0.44). Threshold values of 35 ml/min for baseline mean flow and 1.0 for diastolic-to-systolic velocity ratio was proposed to separate IMA grafts with <70% and ≥70% stenosis. Respective sensitivity and specificity were 86% (95% confidence interval [CI]: 49.5-98.7%) and 94% (95% CI: 79.2-99.5%) for the threshold value of baseline mean flow, and 86% (95% CI: 48.6-99.2%) and 88% (95% CI: 72.9-93.8%) for the threshold value of diastolic-to-systolic velocity ratio. CFR did not differ significantly between IMA grafts with <70% and ≥70% stenosis.

The value of MR flow in the prediction of vein graft disease was assessed (46). Forty vein grafts in 21 patients were examined by contrast-enhanced MRA and breath-hold gradient-echo MR flow at rest and during adenosine-induced stress and coronary angiography. An algorithm was formulated combining baseline flow <20 ml/min or CFR<2 to detect grafts or run-offs with a significant stenosis (≥50%) or a myocardial infarction in the graft vascular territory, yielding a sensitivity of 78% with a specificity of 80%. The algorithm was designed to exclude normal-functioning vein grafts from further invasive examinations. A different approach for the detection of stenotic vein and arterial grafts

or recipient vessels by MR with velocity mapping was also developed (47). In this study, 166 grafts were examined by breath-hold MR velocity at rest and during adenosine-induced stress, controlled by coronary angiography. In 80% of grafts full MR examination was successful. Single and sequential vein and arterial grafts were separately analyzed. Marginal logistic regression was used to predict the probability for the presence of ≥50% or ≥70% stenosis per graft type using multiple MR velocity parameters, including CFVR. Sensitivity and specificity for detecting single vein grafts or recipient vessels with ≥50% and ≥70% stenosis were 94% (95% CI: 86-100%) and 63% (95% CI: 48-79%), and 96% (95% CI: 87-100%) and 92% (95% CI: 84-100%), respectively; for detecting ≥50% and ≥70% stenosis in sequential vein grafts these values were 91% (95% CI: 78-100%) and 82% (95% CI: 64-100%), and 94% (95% CI: 83-100%) and 71% (95% CI: 52-91%), respectively. A proposed cut-off point for separating <70% and ≥70% stenosis in single vein grafs was 1.43 for CFVR. Not enough stenoses in arterial grafts were present to formulate an adequate logistic regression model for those grafts.
These studies show that MR flow velocity assessment has high potential to become a valuable, diagnostic tool in predicting patency and even the presence or absence of a significant stenosis in both vein and IMA grafts in clinical practice. Future studies should focus on an integration of bypass graft and native coronary artery MR flow velocity assessment, by which an absence of significant stenosis can be predicted with high accuracy to avoid unnecessary invasive coronary angiographic examinations.

Applied studies using magnetic resonance flow velocity in bypass grafts
Some studies were conducted using MR flow velocity as a tool to evaluate a certain procedure (surgical or percutaneous intervention) or noninvasive modality. Miller et al. (48) used a comprehensive approach of breath-hold contrast-enhanced MRA, non-breath-hold MR flow quantification at rest, and MR cardiac function assessment to evaluate the status of IMA grafts after minimally invasive direct CABG surgery. The protocol was successfully completed in six patients postoperatively. Patency of the grafts was accurately assessed by this MR approach, compared with coronary angiography. To evaluate the value of color-Doppler echography and MRA with navigator-gated flow measurements to assess bypass graft patency postoperatively, a comparison with intraoperative flow measurements was performed (49). Only IMA grafts could be evaluated with color Doppler. They found that both modalities were useful to assess IMA graft patency after surgery, but MR flow measurements had the best correlation with intraoperative flow measurements. In one study, the success of percutaneous interventions in 15 veins was evaluated by breath-hold MR flow, and reference values for rest and adenosine-stress MR flow and velocity parameters were formulated using data of 39 single and 20 sequential vein grafts with <50% stenosis (50). Significant improvements by MR flow after a percutaneous intervention were observed for baseline (before: 9.2 ± 6.6 cm/s; after 12.9 ± 7.9 cm/s) and adenosine-induced stress (before: 12.9 ± 6.3 cm/s; after: 27.1 ± 13.9 cm/s) mean velocity. CFVR did not significantly improve after an intervention (before: 2.4 ± 1.4; after: 2.6 ± 0.9), as a result of an equal recovery of both baseline and stress mean velocity. Reference values confirmed a significant difference between single and sequential vein graft values, underscoring the need to evaluate

these grafts separately. Because a MR velocity map can be analyzed to evaluate both flow and velocity, the diagnostic accuracy of the flow and velocity analysis approach was investigated using velocity maps of 80 single vein grafts (51). A similar diagnostic accuracy was demonstrated for the flow (92%) and velocity analysis (93%) in the detection of ≥70% stenosis. Velocity analysis seemed to be the preferred method, because it is less time-consuming compared with flow analysis.
The functional significance of a bypass graft stenosis was evaluated by single-photon emission computed tomography (SPECT), breath-hold MR velocity at rest and during adenosine-induced stress, and coronary angiography (52). In 18 out of 20 (90%) grafts with a normal myocardial perfusion as determined by SPECT, preserved CFVR (≥2.0) was observed, whereas a reduced CFVR was noted in 19 of 26 grafts (69%) with abnormal perfusion on SPECT. Accordingly, agreement between SPECT perfusion imaging and MR velocity assessment was 80% (κ=0.61). In relation to invasive coronary angiography the following was observed: In grafts with a stenosis <50% and normal perfusion on SPECT, normal CFVR was observed in 86%, whereas reduced CFVR was observed in 78% of grafts with a stenosis ≥50% and abnormal perfusion. All grafts with a stenosis ≥50% and normal perfusion, suggesting no hemodynamic significance of the stenosis, had normal CFVR. Finally, reduced CFVR was observed in 33% of grafts with a stenosis <50% and abnormal perfusion (suggestive of microvascular disease).

Functional Assessment: Left Ventricular Function, Contrast-enhancement, Viability
Few studies have been performed evaluating patients after CABG surgery by a functional MR examination. In one study, global and regional left ventricular (LV) function by 3D MR served as the gold standard for the assessment of LV function by 99m-technetium-sestamibi gated SPECT in patients post-CABG surgery (53). After cardiac surgery, exaggerated systolic anteromedial translation of the entire heart within the chest has been observed, enhancing difficulties in assessing regional wall motion (especially in the septum). They demonstrated that an automated software algorithm (54;55) for the assessment of LV function by SPECT agreed well compared with MR functional assessment in this particular group of patients.
Several studies focused on evaluating myocardial injury by contrast-enhanced MR during off-pump and on-pump CABG surgery. Conventional on-pump surgery uses a cardiopulmonary bypass and aortic cross-clamping, which may lead to a systemic inflammatory response syndrome with multiorgan dysfunction (56) and myocardial damage as the result of ischemia (57). Selvanayagam et al. (58) randomized 60 patients to either off-pump or on-pump CABG surgery and examined those patients before and after surgery by contrast-enhanced MR. Troponin I measurements were also obtained, which correlated with mean mass of new myocardial hyperenhancement. The authors found that off-pump CABG resulted in a significantly better LV function early after surgery; however, it did not reduce the incidence or extent of irreverible myocardial injury. Correlation of elevated biochemical markers (creatinine kinase-MB, troponin I and T) after CABG with the amount of perioperatively infarcted myocardium was confirmed in another study (59). A 6-month follow-up contrast-enhanced MR examination was then performed in the same patient group to assess the diagnostic value of MR contrast

enhancement in predicting viability, and to assess late regional wall motion recovery (60). A strong correlation between the transmural extent of hyperenhancement and regional function recovery at 6 months was demonstrated, revealing contrast-enhanced MR as a powerful predictor of myocardial damage after CABG surgery.

Computed tomography of coronary artery bypass grafts

CT has been intensively investigated in its ability and value to visualize bypass grafts noninvasively. Early studies were using conventional CT scanners to assess bypass graft patency postoperatively, in comparison with coronary angiography. Repeated axial images were acquired at multiple levels of the graft. If the contrast agent was able to visualize the graft at two levels at least, a graft was scored as patent (61;62). This technique required an intravenous bolus of 20 to 50 ml contrast agent per image and therefore burdened the patient with a relatively large quantity of x-ray radiation. Then, CT scanners could be programmed to acquire multiple axial images after one bolus injection of contrast agent (dynamic scanning), allowing faster acquisition of images (63-69). Scans could be repeated after a 1- to 4-second interval, and per bolus injection four to six sequenced scans could be obtained. Diagnostic accuracy for this technique to detect bypass graft patency ranged from 45% to 95%. Ultrafast CT scanning allowed acquisition of one axial image in 50 ms, and repeating of scans after 8 ms (70-72). Total image acquisition time was 10 to 30 heartbeats, using electrocardiograph (ECG) triggering. Sensitivity to detect bypass graft patency using this technique was 93% to 96%, with a specificity of 89% to 100%. With spiral CT scanning the complete heart could be scanned in one breath-hold acquisition of 24 to 30 s (9;73-75). Optimal in-plane spatial resolution using this technique was 0.29 mm^2. Reported diagnostic accuracy for the detection of graft patency was 96% for vein grafts and 88% for arterial grafts (75). Then, it became feasible to use four detectors in a single spiral CT acquisition, allowing detection of graft patency with very high accuracy: 98% to100% for vein grafts and 97% to 100% for arterial grafts (76-82).

Another approach in assessing bypass graft patency is to estimate the graft blood flow. The contrast clearance curve of a contrast bolus injection is evaluated by cine CT (83). This technique was tested in patients, showing a good agreement with observations at coronary angiography (κ=0.75) (84). In addition to assessment of bypass graft patency, the extent of graft disease may be evaluated by CT. With four-detector row CT technology, adequate stenosis assessment of all grafts was prevented by motion artifacts, metal clip artifacts, or beam hardening from calcium deposits (80-82). Table 2.2 shows the percentage of graft segments that could be analyzed and the sensitivity, specificity, and diagnostic accuracy in detecting significant stenoses in patent bypass grafts. Bypass grafts have been examined by 16-detector row spiral CT, allowing a scanning range of the proximal IMA insertion to the heart apex. By using retrospective ECG gating and a segmental reconstruction algorithm, images with an in-plane spatial resolution of up to 0.35 mm^2 can be acquired in a single breath-hold (85-87). In Figure 2.7, a typical 16-slice multislice computed tomography (MSCT) protocol is explained, whereas the different image displays that are available for evaluation of the MSCT angiograms are shown in Figure 2.8.

Author	Patients	Grafts	Graft type	Assessable grafts (%)	Sensitivity (%)	Specificity (%)
Ropers et al (82)	65	124	vein and arterial	62	75	92
Nieman et al (81)	24	39	vein	95	83	90
Marano et al (80)	57	92	vein and arterial	67	80	96
Martuscelli et al (89)	96	278	vein and arterial	88	90	100
Salm et al (87)	25	67	vein and arterial	-	100	95
Weighted Mean		600		80	84	9

Table 2.2

Accuracy of multislice spiral computed tomography in the detection of significant stenoses (≥50% luminal narrowing) in bypass grafts, controlled by coronary angiography

In comparison with coronary angiography, the 16-detector row CT technique was demonstrated to detect bypass graft stenosis of 50% to 100% with a sensitivity of 96% and specificity of 95% (88). In another study, ≥50% angiographic stenoses in patent grafts were detected with a sensitivity of 90% with a specificity of 100% (89). Diagnostic accuracy to detect graft patency was 100%.

Multidetector row CT was used to preoperatively assess the surgical site before totally endoscopic CABG, and the results were correlated with findings at coronary angiography and during surgery (90). Multidetector row CT demonstrated extended information about the coronary target site and is recommended as a planning tool before complex cardiac surgery, such as endoscopic bypass grafting or minimally invasive direct CABG.

Retrospective ECG gating allows reconstruction of CT images at 0% to 90% during the cardiac cycle. The best reconstruction interval to view coronary artery bypass grafts anastomosed to the right coronary artery and branches was shown to be at 50%, whereas grafts anastomosed to the left anterior descending or circumflex artery (or branches) were best viewed at 60% to 70% of the cardiac cycle (79).

As illustrated in Figure 2.9, multidetector row CT (MDCT) technology allows a very accurate evaluation of vein and arterial bypass graft patency. Also, significant stenosis in bypass grafts may be assessed by MDCT. CT technology is rapidly evolving, with 32- and 64-detector row technology being readily available. A simultaneous assessment of native coronary arteries, coronary artery bypass grafts, and recipient vessels noninvasively by MDCT may soon be a part of daily clinical practice.

Summary

CMR and CT have made rapid progress in the last two decades in detecting patency/occlusion and eventually stenoses in coronary artery bypass grafts. Other applications of CMR and CT include pre- and postoperative assessment of the CABG procedure. Future studies should focus on integrating assessment of native coronary arteries and bypass grafts as a full noninvasive evaluation before coronary angiography.

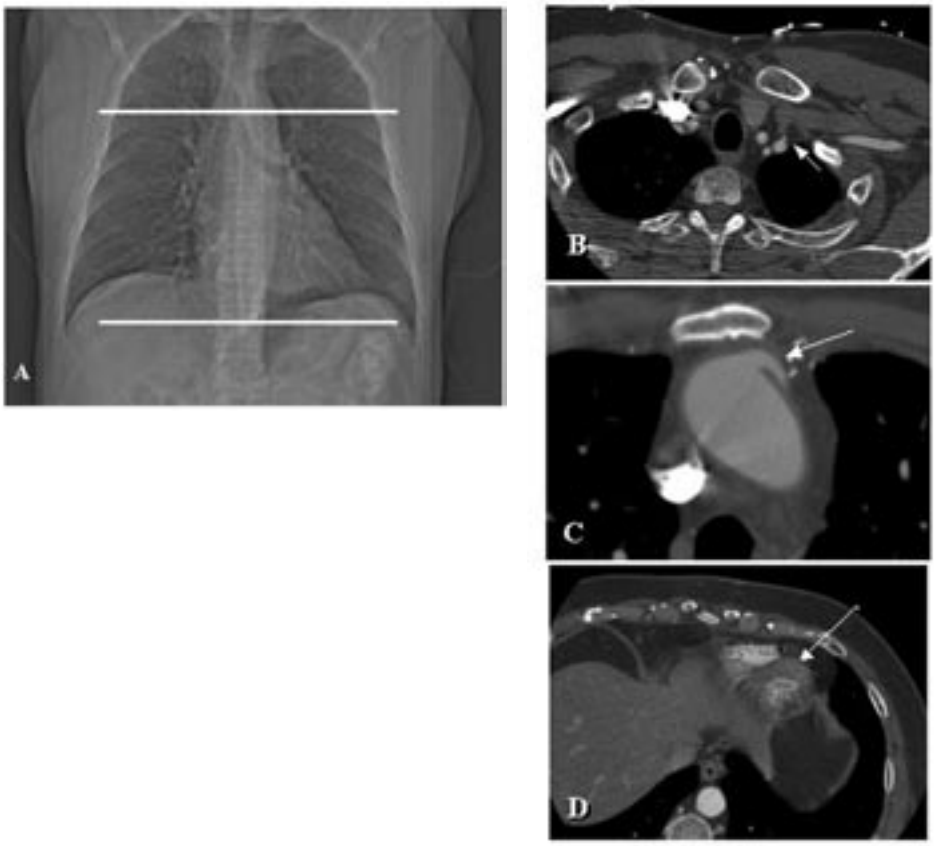

Figure 2.7

Typical 16-slice multislice computed tomography (MSCT) acquisition protocol. Typical coronary computed tomographic angiography (CTA) protocol starts with correct supine patient positioning, positioning of intravenous line, placement of three electrocardiograph (ECG) leads, and patient instruction concerning breath-holding. First, a scanogram for overview is acquired (A). Approximate cranial and caudal imaging margins (white lines) to acquire a second noncontrast localizer with prospective ECG triggering (30-40 slices, 3-mm slice thickness, 120 kV at 200 mA). (B) On the basis of the second localizer, the exact cranial and caudal margins are defined. These margins are depending on the clinical setting, for example, for CTA of arterial graft, such as the left internal mammary artery (IMA) graft, a higher cranial slice is needed (B, arrow) than for CTA of vein grafts (C, arrow). The actual contrast-enhanced helical acquisition should be planned from 1 cm above the defined cranial margin to 1 cm below the caudal margin, i.e. the apex of the heart (D, arrow). For optimal timing of the contrast arrival in the coronary arteries and bypass grafts, automated bolus tracking is applied by placement of a region of interest in the ascending aorta. (continues)

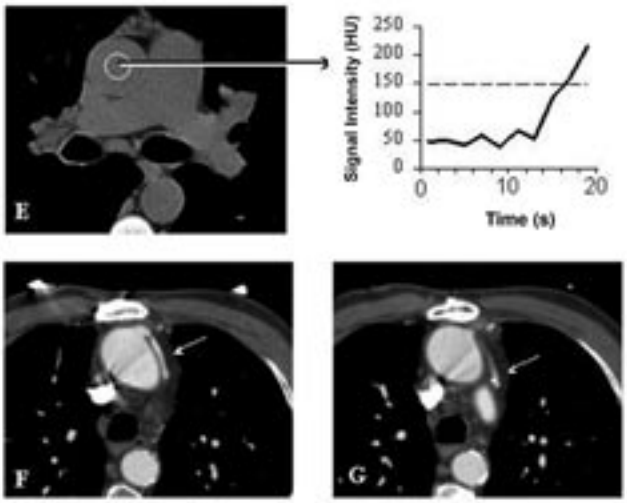

Figure 2.7 (continued)

(E) After the signal intensity reaches a predefined threshold (see graph), the final CTA scan starts automatically. Two levels are shown from the resulting CTA of a vein coronary artery bypass graft (F,G, arrows). CTA was performed with retrospective ECG gating (0.5-mm slice thickness, 120 kV at 250 mA, pitch and rotation time depending on heart rate).

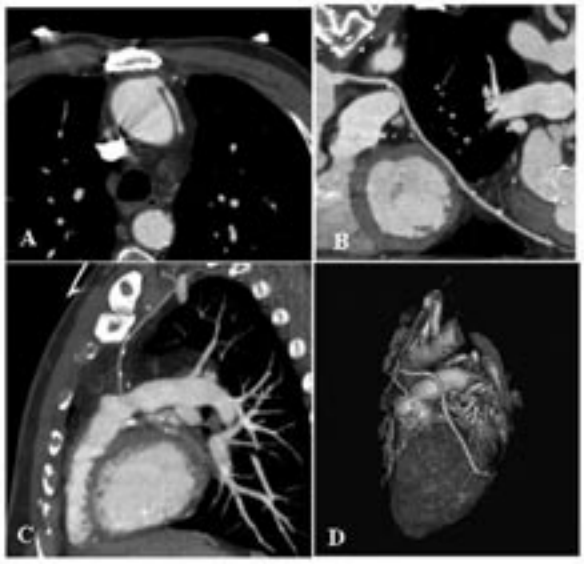

Figure 2.8

For the evaluation of MSCT angiograms, several imaging displays can be used. (A) Original axial slice. (B) Curved multiplanar reconstruction of a vein graft. (C) Maximum intensity projection of an arterial graft. (D) For an overview of the coronary arteries and bypass grafts, 3D volume-rendered reconstructions can be useful. A full colour version of this illustration can be found in the full colour section (page 166).

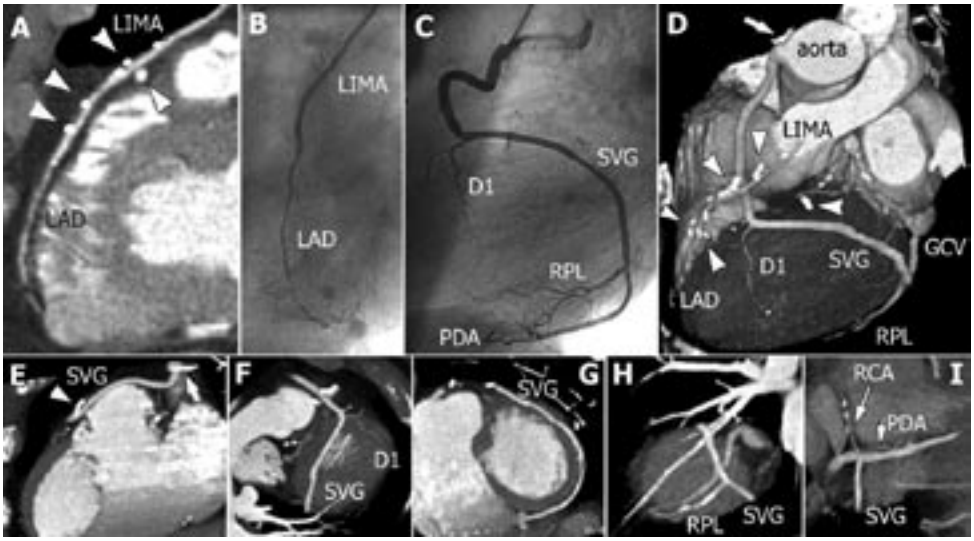

Figure 2.9

Arterial and vein bypass grafts. Images obtained with contrast-enhanced multidetector row CT angiography (A, E-I, maximum intensity projections; D, 3D volume rendering) and corresponding conventional angiography (B,C) show a left IMA graft (LIMA) connected to the left anterior descending coronary artery (LAD). Saphenous vein graft (SVG) runs from the aorta to the diagonal branch (D1), with consecutive jumps to the posterolateral branch (RPL) and posterior descending coronary artery (PDA). Surgical clips (arrowheads) and bypass indicator (arrow in D,E) appear as bright structures. Location of labeled right coronary and posterior descending coronary arteries (arrows in I). GCV = great cardiac vein; RCA = right coronary artery. (Reproduced with permission from Radiology)

REFERENCES

1. Aurigemma GP, Reichek N, Axel L, Schiebler M, Harris C, Kressel HY. Noninvasive determination of coronary artery bypass graft patency by cine magnetic resonance imaging. Circulation 1989;80:1595-602.
2. Frija G, Schouman Claeys E, Lacombe P, Bismuth V, Ollivier JP. A study of coronary artery bypass graft patency using MR imaging. J Comput Assist Tomogr 1989;13:226-32.
3. Jenkins JP, Love HG, Foster CJ, Isherwood I, Rowlands DJ. Detection of coronary artery bypass graft patency as assessed by magnetic resonance imaging. Br J Radiol 1988;61:2-4.
4. White RD, Caputo GR, Mark AS, Modin GW, Higgins CB. Coronary artery bypass graft patency: noninvasive evaluation with MR imaging. Radiology 1987;164:681-6.
5. White RD, Pflugfelder PW, Lipton MJ, Higgins CB. Coronary artery bypass grafts: evaluation of patency with cine MR imaging. AJR Am J Roentgenol 1988;150:1271-4.
6. Rubinstein RI, Askenase AD, Thickman D, Feldman MS, Agarwal JB, Helfant RH. Magnetic resonance imaging to evaluate patency of aortocoronary bypass grafts. Circulation 1987;76:786-91.
7. Vanninen RL, Vainio PA, Manninen HI, Suhonen M, Jaakola P. Gastroepiploic artery as an in situ coronary artery bypass graft: evaluation of MRI and colour Doppler ultrasound in follow-up. Scand J Thorac Cardiovasc Surg 1995;29:7-10.
8. Galjee MA, van Rossum AC, Doesburg T, van Eenige MJ, Visser CA. Value of magnetic resonance imaging in assessing patency and function of coronary artery bypass grafts. An angiographically controlled study. Circulation 1996;93:660-6.
9. Engelmann MG, Knez A, von Smekal A et al. Non-invasive coronary bypass graft imaging after multivessel revascularisation. Int J Cardiol 2000;76:65-74.
10. Kalden P, Kreitner KF, Wittlinger T et al. Assessment of coronary artery bypass grafts: value of different breath-hold MR imaging techniques. AJR Am J Roentgenol 1999;172:1359-64.
11. Kessler W, Achenbach S, Moshage W et al. Usefulness of respiratory gated magnetic resonance coronary angiography in assessing narrowings > or = 50% in diameter in native coronary arteries and in aortocoronary bypass conduits. Am J Cardiol 1997;80:989-93.
12. Langerak SE, Vliegen HW, de Roos A et al. Detection of Vein Graft Disease using High-resolution Magnetic Resonance Angiography. Circulation 2002;105:328-33.
13. Molinari G, Sardanelli F, Zandrino F, Balbi M, Masperone MA. Value of navigator echo magnetic resonance angiography in detecting occlusion/patency of arterial and venous, single and sequential coronary bypass grafts. Int J Card Imaging 2000;16:149-60.
14. Vrachliotis TG, Bis KG, Aliabadi D, Shetty AN, Safian R, Simonetti O. Contrast-enhanced breath-hold MR angiography for evaluating patency of coronary artery bypass grafts. AJR Am J Roentgenol 1997;168:1073-80.
15. Wintersperger BJ, Engelmann MG, von Smekal A et al. Patency of coronary bypass grafts: assessment with breath-hold contrast-enhanced MR angiography--value of a non-electrocardiographically triggered technique. Radiology 1998;208:345-51.
16. Wittlinger T, Voigtlander T, Kreitner KF, Kalden P, Thelen M, Meyer J. Non-invasive magnetic resonance imaging of coronary bypass grafts. comparison of the haste- and navigator techniques with conventional coronary angiography. Int J Cardiovasc Imaging 2002;18:469-77.
17. Bunce NH, Lorenz CH, John AS, Lesser JR, Mohiaddin RH, Pennell DJ. Coronary artery bypass graft patency: assessment with true ast imaging with steady-state precession versus gadolinium-enhanced MR angiography. Radiology 2003;227:440-6.
18. White CW, Wright CB, Doty DB et al. Does visual interpretation of the coronary arteriogram predict the physiologic importance of a coronary stenosis? N Engl J Med 1984;310:819-24.
19. Topol EJ, Nissen SE. Our preoccupation with coronary luminology. The dissociation between clinical and angiographic findings in ischemic heart disease. Circulation 1995;92:2333-42.
20. Uren NG, Melin JA, De Bruyne B, Wijns W, Baudhuin T, Camici PG. Relation between myocardial blood flow and the severity of coronary-artery stenosis. N Engl J Med 1994;330:1782-8.
21. Gould KL, Lipscomb K, Hamilton GW. Physiologic basis for assessing critical coronary stenosis. Instantaneous flow response and regional distribution during coronary hyperemia as measures of coronary flow reserve. Am J Cardiol 1974;33:87-94.
22. Gould KL, Kirkeeide RL, Buchi M. Coronary flow reserve as a physiologic measure of stenosis severity. J Am Coll Cardiol 1990;15:459-74.
23. Gould KL, Lipscomb K. Effects of coronary stenoses on coronary flow reserve and resistance. Am J Cardiol 1974;34:48-55.

24. Bittar N, Kroncke GM, Dacumos GC, Jr. et al. Vein graft flow and reactive hyperemia in the human heart. J Thorac Cardiovasc Surg 1972;64:855-60.
25. Wilson RF, White CW. Does coronary artery bypass surgery restore normal maximal coronary flow reserve? The effect of diffuse atherosclerosis and focal obstructive lesions. Circulation 1987;76:563-71.
26. Doucette JW, Corl PD, Payne HM et al. Validation of a Doppler guide wire for intravascular measurement of coronary artery flow velocity. Circulation 1992;85:1899-911.
27. Sudhir K, Hargrave VK, Johnson EL et al. Measurement of volumetric coronary blood flow with a Doppler catheter: validation in an animal model. Am Heart J 1992;124:870-5.
28. Labovitz AJ, Anthonis DM, Cravens TL, Kern MJ. Validation of volumetric flow measurements by means of a Doppler-tipped coronary angioplasty guide wire. Am Heart J 1993;126:1456-61.
29. Ofili EO, Labovitz AJ, Kern MJ. Coronary flow velocity dynamics in normal and diseased arteries. Am J Cardiol 1993;71:3d-9d.
30. White CW. Clinical applications of Doppler coronary flow reserve measurements. Am J Cardiol 1993;71:10d-6d.
31. Kern MJ, Donohue TJ, Aguirre FV et al. Assessment of angiographically intermediate coronary artery stenosis using the Doppler flowire. Am J Cardiol 1993;71:26d-33d.
32. Segal J. Applications of coronary flow velocity during angioplasty and other coronary interventional procedures. Am J Cardiol 1993;71:17d-25d.
33. Serruys PW, De Bruyne B, Carlier S et al. Randomized comparison of primary stenting and provisional balloon angioplasty guided by flow velocity measurement. Doppler Endpoints Balloon Angioplasty Trial Europe (DEBATE) II Study Group. Circulation 2000;102:2930-7.
34. Nishida T, Di Mario C, Kern MJ et al. Impact of final coronary flow velocity reserve on late outcome following stent implantation. Eur Heart J 2002;23:331-40.
35. Albertal M, Regar E, Van Langenhove G et al. Value of coronary stenotic flow velocity acceleration in prediction of angiographic restenosis following balloon angioplasty. Eur Heart J 2002;23:1849-53.
36. Lotz J, Meier C, Leppert A, Galanski M. Cardiovascular flow measurement with phase-contrast MR imaging: basic facts and implementation. Radiographics 2002;22:651-71.
37. van Rossum AC, Galjee MA, Doesburg T, Hofman M, Valk J. The role of magnetic resonance in the evaluation of functional results after CABG/PTCA. Int J Card Imaging 1993;9 Suppl 1:59-69.
38. Galjee MA, van Rossum AC, Doesburg T, Hofman MB, Falke TH, Visser CA. Quantification of coronary artery bypass graft flow by magnetic resonance phase velocity mapping. Magn Reson Imaging 1996;14:485-93.
39. Hoogendoorn LI, Pattynama PM, Buis B, van der Geest RJ, van der Wall EE, de Roos A. Noninvasive evaluation of aortocoronary bypass grafts with magnetic resonance flow mapping. Am J Cardiol 1995;75:845-8.
40. Debatin JF, Strong JA, Sostman HD et al. MR characterization of blood flow in native and grafted internal mammary arteries. J Magn Reson Imaging 1993;3:443-50.
41. Sakuma H, Globits S, O'Sullivan M et al. Breath-hold MR measurements of blood flow velocity in internal mammary arteries and coronary artery bypass grafts. J Magn Reson Imaging 1996;6:219-22.
42. Brenner P, Wintersperger B, von Smekal A et al. Detection of coronary artery bypass graft patency by contrast enhanced magnetic resonance angiography. Eur J Cardiothorac Surg 1999;15:389-93.
43. Langerak SE, Kunz P, Vliegen HW et al. Improved MR flow mapping in coronary artery bypass grafts during adenosine-induced stress. Radiology 2001;218:540-7.
44. Langerak SE, Kunz P, Vliegen HW et al. Magnetic resonance flow mapping in coronary artery bypass grafts: a validation study with Doppler flow measurements. Radiology 2002;222:127-35.
45. Ishida N, Sakuma H, Cruz BP et al. Mr flow measurement in the internal mammary artery-to-coronary artery bypass graft: comparison with graft stenosis at radiographic angiography. Radiology 2001;220:441-7.
46. Bedaux WL, Hofman MB, Vyt SL, Bronzwaer JG, Visser CA, van Rossum AC. Assessment of coronary artery bypass graft disease using cardiovascular magnetic resonance determination of flow reserve. J Am Coll Cardiol 2002;40:1848-55.
47. Langerak SE, Vliegen HW, Jukema JW et al. Value of magnetic resonance imaging for the noninvasive detection of stenosis in coronary artery bypass grafts and recipient coronary arteries. Circulation 2003;107:1502-8.
48. Miller S, Scheule AM, Hahn U et al. MR angiography and flow quantification of the internal mammary artery graft after minimally invasive direct coronary artery bypass. AJR Am J Roentgenol 1999;172:1365-9.
49. Walpoth BH, Muller MF, Genyk I et al. Evaluation of coronary bypass flow with color-Doppler and magnetic resonance imaging techniques: comparison with intraoperative flow measurements. Eur J Cardiothorac Surg 1999;15:795-802.
50. Langerak SE, Vliegen HW, Jukema JW et al. Vein graft function improvement after percutaneous intervention: evaluation with MR flow mapping. Radiology 2003;228:834-41.

51. Salm LP, Langerak SE, Vliegen HW et al. Blood flow in coronary artery bypass vein grafts: volume versus velocity at cardiovascular MR imaging. Radiology 2004;232:915-20.
52. Salm LP, Bax JJ, Vliegen HW et al. Functional significance of stenoses in coronary artery bypass grafts Evaluation by single-photon emission computed tomography perfusion imaging, cardiovascular magnetic resonance, and angiography. J Am Coll Cardiol 2004;44:1877-82.
53. Tadamura E, Kudoh T, Motooka M et al. Use of technetium-99m sestamibi ECG-gated single-photon emission tomography for the evaluation of left ventricular function following coronary artery bypass graft: comparison with three-dimensional magnetic resonance imaging. Eur J Nucl Med 1999;26:705-12.
54. Germano G, Kiat H, Kavanagh PB et al. Automatic quantification of ejection fraction from gated myocardial perfusion SPECT. J Nucl Med 1995;36:2138-47.
55. Germano G, Erel J, Kiat H, Kavanagh PB, Berman DS. Quantitative LVEF and qualitative regional function from gated thallium-201 perfusion SPECT. J Nucl Med 1997;38:749-54.
56. Ascione R, Lloyd CT, Underwood MJ, Lotto AA, Pitsis AA, Angelini GD. Inflammatory response after coronary revascularization with or without cardiopulmonary bypass. Ann Thorac Surg 2000;69:1198-204.
57. Taggart DP. Biochemical assessment of myocardial injury after cardiac surgery: effects of a platelet activating factor antagonist, bilateral internal thoracic artery grafts, and coronary endarterectomy. J Thorac Cardiovasc Surg 2000;120:651-9.
58. Selvanayagam JB, Petersen SE, Francis JM et al. Effects of off-pump versus on-pump coronary surgery on reversible and irreversible myocardial injury: a randomized trial using cardiovascular magnetic resonance imaging and biochemical markers. Circulation 2004;109:345-50.
59. Steuer J, Bjerner T, Duvernoy O et al. Visualisation and quantification of peri-operative myocardial infarction after coronary artery bypass surgery with contrast-enhanced magnetic resonance imaging. Eur Heart J 2004;25:1293-9.
60. Selvanayagam JB, Kardos A, Francis JM et al. Value of delayed-enhancement cardiovascular magnetic resonance imaging in predicting myocardial viability after surgical revascularization. Circulation 2004;110:1535-41.
61. Albrechtsson U, Stahl E, Tylen U. Evaluation of coronary artery bypass graft patency with computed tomography. J Comput Assist Tomogr 1981;5:822-6.
62. Daniel WG, Dohring W, Stender HS, Lichtlen PR. Value and limitations of computed tomography in assessing aortocoronary bypass graft patency. Circulation 1983;67:983-7.
63. Brundage BH, Lipton MJ, Herfkens RJ et al. Detection of patent coronary bypass grafts by computed tomography. A preliminary report. Circulation 1980;61:826-31.
64. Guthaner DF, Brody WR, Ricci M, Oyer PE, Wexler L. The use of computed tomography in the diagnosis of coronary artery bypass graft patency. Cardiovasc Intervent Radiol 1980;3:3-8.
65. Godwin JD, Califf RM, Korobkin M, Moore AV, Breiman RS, Kong Y. Clinical value of coronary bypass graft evaluation with CT. AJR Am J Roentgenol 1983;140:649-55.
66. Wilson PC, Gutierrez O, Moss A. Early evaluation of coronary artery bypass grafts: CT or selective angiography. Eur J Radiol 1984;4:22-7.
67. Foster CJ, Sekiya T, Brownlee WC, Isherwood I. Computed tomographic assessment of coronary artery bypass grafts. Br Heart J 1984;52:24-9.
68. Muhlberger V, Knapp E, zur ND. Predictive value of computed tomographic determination of the patency rate of aortocoronary venous bypasses in relation to angiographic results. Eur Heart J 1990;11:380-8.
69. Kahl FR, Wolfman NT, Watts LE. Evaluation of aortocoronary bypass graft status by computed tomography. Am J Cardiol 1981;48:304-10.
70. Bateman TM, Gray RJ, Whiting JS et al. Prospective evaluation of ultrafast cardiac computed tomography for determination of coronary bypass graft patency. Circulation 1987;75:1018-24.
71. Stanford W, Rooholamini M, Rumberger J, Marcus M. Evaluation of coronary bypass graft patency by ultrafast computed tomography. J Thorac Imaging 1988;3:52-5.
72. Stanford W, Brundage BH, MacMillan R et al. Sensitivity and specificity of assessing coronary bypass graft patency with ultrafast computed tomography: results of a multicenter study. J Am Coll Cardiol 1988;12:1-7.
73. Tello R, Costello P, Ecker C, Hartnell G. Spiral CT evaluation of coronary artery bypass graft patency. J Comput Assist Tomogr 1993;17:253-9.
74. Ueyama K, Ohashi H, Tsutsumi Y, Kawai T, Ueda T, Ohnaka M. Evaluation of coronary artery bypass grafts using helical scan computed tomography. Catheter Cardiovasc Interv 1999;46:322-6.

75. Engelmann MG, von Smekal A, Knez A et al. Accuracy of spiral computed tomography for identifying arterial and venous coronary graft patency. Am J Cardiol 1997;80:569-74.
76. Yoo KJ, Choi D, Choi BW, Lim SH, Chang BC. The comparison of the graft patency after coronary artery bypass grafting using coronary angiography and multi-slice computed tomography. Eur J Cardiothorac Surg 2003;24:86-91.
77. Ko YG, Choi DH, Jang YS et al. Assessment of coronary artery bypass graft patency by multislice computed tomography. Yonsei Med J 2003;44:438-44.
78. Burgstahler C, Kuettner A, Kopp AF et al. Non-invasive evaluation of coronary artery bypass grafts using multi-slice computed tomography: initial clinical experience. Int J Cardiol 2003;90:275-80.
79. Willmann JK, Weishaupt D, Kobza R et al. Coronary artery bypass grafts: ECG-gated multi-detector row CT angiography--influence of image reconstruction interval on graft visibility. Radiology 2004;232:568-77.
80. Marano R, Storto ML, Maddestra N, Bonomo L. Non-invasive assessment of coronary artery bypass graft with retrospectively ECG-gated four-row multi-detector spiral computed tomography. Eur Radiol 2004;14:1353-62.
81. Nieman K, Pattynama PM, Rensing BJ, van Geuns RJ, de Feyter PJ. Evaluation of patients after coronary artery bypass surgery: CT angiographic assessment of grafts and coronary arteries. Radiology 2003;229:749-56.
82. Ropers D, Ulzheimer S, Wenkel E et al. Investigation of aortocoronary artery bypass grafts by multislice spiral computed tomography with electrocardiographic-gated image reconstruction. Am J Cardiol 2001;88:792-5.
83. Rumberger JA, Feiring AJ, Hiratzka LF et al. Quantification of coronary artery bypass flow reserve in dogs using cine-computed tomography. Circ Res 1987;61:117-23.
84. Tello R, Hartnell GG, Costello P, Ecker CP. Coronary artery bypass graft flow: qualitative evaluation with cine single-detector row CT and comparison with findings at angiography. Radiology 2002;224:913-8.
85. Dewey M, Lembcke A, Enzweiler C, Hamm B, Rogalla P. Isotropic half-millimeter angiography of coronary artery bypass grafts with 16-slice computed tomography. Ann Thorac Surg 2004;77:800-4.
86. Gurevitch J, Gaspar T, Orlov B et al. Noninvasive evaluation of arterial grafts with newly released multidetector computed tomography. Ann Thorac Surg 2003;76:1523-7.
87. Salm LP, Bax JJ, Jukema JW et al. Comprehensive assessment of patients after coronary bypass grafting by 16-detector row computed tomography. Am Heart J 2005;150:775-81.
88. Schlosser T, Konorza T, Hunold P, Kuhl H, Schmermund A, Barkhausen J. Noninvasive visualization of coronary artery bypass grafts using 16-detector row computed tomography. J Am Coll Cardiol 2004;44:1224-9.
89. Martuscelli E, Romagnoli A, D'Eliseo A et al. Evaluation of Venous and Arterial Conduit Patency by 16-Slice Spiral Computed Tomography. Circulation 2004;110:3234-8.
90. Herzog C, Dogan S, Diebold T et al. Multi-detector row CT versus coronary angiography: preoperative evaluation before totally endoscopic coronary artery bypass grafting. Radiology 2003;229:200-8.

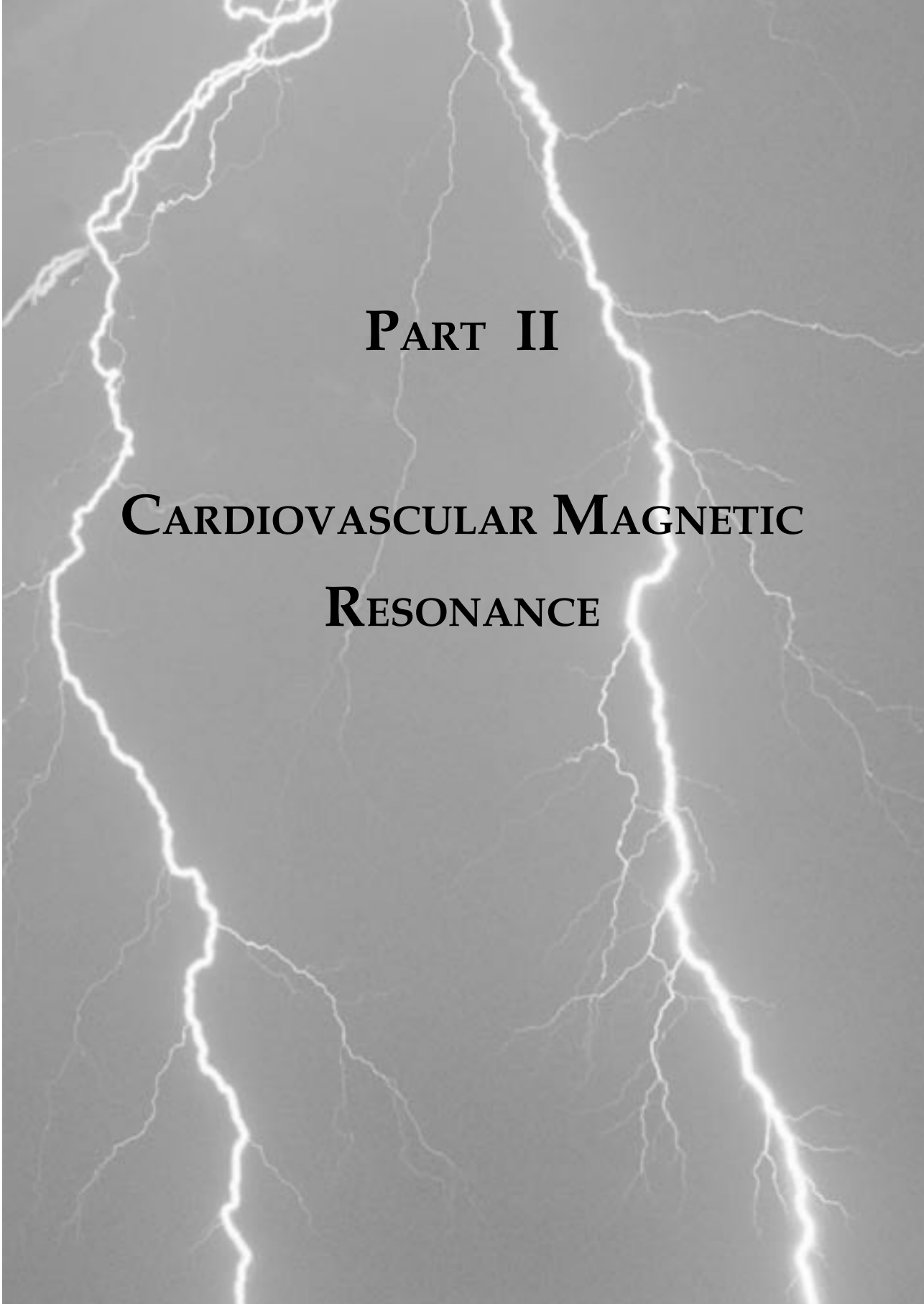

Part II

Cardiovascular Magnetic Resonance

CHAPTER 3

Evaluation of saphenous vein coronary artery bypass graft flow by cardiovascular magnetic resonance

Liesbeth P. Salm
Hubert W. Vliegen
Susan E. Langerak
Jeroen J. Bax
J. Wouter Jukema
Aeilko H. Zwinderman
Hildo J. Lamb
Albert de Roos
Ernst E. van der Wall

J Cardiovasc Magn Reson 2005; 7, 4, 631-637

ABSTRACT
Cardiovascular magnetic resonance (CMR) with flow velocity mapping has emerged as a noninvasive method to measure flow in saphenous vein coronary artery bypass grafts. The aim of the current study was to retrospectively test two previously described analysis methods on a large CMR data set, and compare their diagnostic accuracy in detecting diseased vein grafts. In 125 vein grafts of 68 patients volume flow parameters (volume flow, systolic and diastolic peak flow, diastolic-to-systolic flow ratio at rest and during adenosine stress, and flow reserve) were derived from the velocity maps. Method 1 implemented basal flow <20 ml/min or flow reserve <2, yielding a sensitivity and specificity of 70% and 38% in the detection of a diseased graft or recipient vessel. Method 2 used receiveroperating characteristic (ROC) curve analysis and implemented all significant volume flow parameters in a logistic regression model, yielding a sensitivity of 74% with a specificity of 68% in the detection of a diseased graft or recipient vessel. Evaluating single and sequential grafts separately, this method yielded a sensitivity and specificity of 79% and 87% for single grafts, and 62% and 94% for sequential grafts in the detection of ≥50% stenosis in grafts or recipient vessels. Cut-off values were formulated for the respective volume flow parameters, which maximally separate grafts with and without ≥50% stenosis.
Using ROC curve analysis with logistic regression the specificity of the analysis method improved considerably. For the current data set the best results were acquired when single and sequential grafts were separately analyzed.

INTRODUCTION

To determine the significance of a stenosis in coronary artery bypass grafts, flow velocity can be measured during catheterization using the Doppler flow wire (1). However, this invasive procedure carries a small risk of serious complications (2-4). Cardiovascular magnetic resonance (CMR) with flow velocity mapping has emerged as a potential noninvasive method to measure flow velocity in both arterial (5) and saphenous vein coronary artery bypass grafts (6-8). In one study (7) 40 vein grafts were analyzed by CMR and an algorithm was formulated to detect stenoses in vein grafts or recipient arteries by implementing basal volume flow <20 ml/min or flow reserve <2. Their algorithm yielded a sensitivity and specificity of 78% and 80%, respectively, in discrimination of grafts with a stenosis <50% and normal recipient vessel and grafts with a stenosis ≥50% or a diseased recipient vessel. A graft supplying a region with a prior myocardial infarction, considered to have an impaired flow reserve, was defined in the algorithm as a graft with a diseased recipient vessel.

Langerak et al. analyzed peak velocity of MR velocity maps in single and sequential vein grafts separately and described a model, developed using receiver operating characteristic (ROC) curve analysis and logistic regression, to detect a stenosis ≥50% and ≥70% in the graft or recipient vessel (8). For the detection of a stenosis ≥50% sensitivity and specificity were 94% and 63% in single vein grafts, and 91% and 82% in sequential vein grafts.

In native coronary arteries many studies have researched an optimal cut-off value for the coronary flow reserve (CFR) to separate normal from diseased arteries (9-12). In these invasive studies CFR cut-offs ranging from 1.7 to 2.0 have been used. An optimal cut-off value for CFR derived by CMR formulated to differentiate normal from diseased vein grafts has never been investigated.

Accordingly, the aim of the current study was 1) to retrospectively test two previously described analysis methods on a large, well documented CMR data set, and compare their diagnostic accuracy in detecting diseased vein grafts, and 2) to formulate cut-off values for the individual CMR flow parameters that maximally separate normal from diseased grafts.

METHODS

Patients

A total of 68 patients with a history of bypass surgery underwent coronary angiography because of recurrent chest pain. Patient characteristics are summarized in Table 3.1. These patients were part of a study describing the diagnostic value of CMR in detecting significant stenoses in both vein and arterial grafts by analyzing peak velocity on MR velocity maps (8). In the current study only vein grafts are described, and volume flow analysis has been used. Coronary angiography was performed according to a standard protocol using the Seldinger technique. In order to determine the stenosis severity of grafts and recipient vessels objectively quantitative coronary arteriography (QCA) was performed by an independent core lab (Heart Core, Leiden, the Netherlands). QCA was performed according to standardized methods (8;13;14).

CMR Examination

All patients underwent CMR examination, using a flow velocity mapping sequence to measure volume flow in bypass grafts. For the CMR examination a 1.5 T Gyroscan ACS-NT MR-scanner (Philips Medical Systems, Best, the Netherlands), equipped with Powertrak 6000 gradients, a cardiac research software patch and 5-element cardiac synergy coil was used. First, gross cardiac anatomy was visualized by means of a scout scan (Figure 3.1). Then, transverse ECG-gated 2D gradient-echo survey scans at the level of the ascending aorta were performed to localize the grafts. When a graft was not visualized on the survey scan, it was considered occluded at CMR examination, and defined to contain zero flow. When a graft was visualized, a plane perpendicular to the proximal section of the graft was planned on two differently angulated survey scans. A fast breathhold Turbo Field Echo Planar Imaging (TFEPI) sequence was used for the flow velocity mapping at rest and during stress (adenosine 140 µg/kg/min. intravenously), applying the following parameters: TR/TE of 11.0/4.6 ms, flip angle of 20°, temporal resolution of 23 ms, field of view of 200 x 100 mm, data acquisition matrix of 128 x 60 mm, in-plane spatial resolution of 1.6 x 1.6 mm, reconstructed to 0.8 x 0.8 mm by means of zero filling of k-space, section thickness of 6 mm, scan duration of 20 heart beats, velocity encoding of 75 cm/s and prospective ECG triggering. The CMR flow mapping sequence was previously validated against Doppler flow data in vitro, using a flow phantom, and in patients with vein grafts (15;16).

Image Analysis

Volume flow analysis of the bypass grafts was performed by means of an analytic software package (FLOW, Medis, Leiden, the Netherlands). Velocity maps consisted of paired modulus and phase images (Figure 3.1). For volume flow analysis contours of the cross-sectional area of each graft were traced manually on the modulus images and transferred to the phase images. In the phase images each pixel contained a velocity value, and the average velocity of the cross-sectional area was defined as the average velocity of all the pixels within the contour. The position and size of each contour was adjusted according to the cardiac phase. The flow rate (ml/s) was then calculated by multiplying the average velocity of the cross-sectional area with the cross-sectional area for each cardiac phase. Flow rate versus time curves were reconstructed and volume flow (ml/min) was obtained by multiplying the integrated volumetric flow per heart beat with the heart rate. Systolic peak flow rate (SPF; ml/s) and diastolic peak flow rate (DPF; ml/s) were defined as maximal flow rate during systole and diastole, respectively. CFR was calculated as the ratio of volume flow during adenosine stress and volume flow at rest. The ratio between DPF and SPF was regarded as the diastolic-to-systolic flow ratio (DSFR).

Assessment of Prior Myocardial Infarction

Myocardial infarction (MI) in the bypass graft region was evaluated by two cardiologists (H.W.V., J.W.J.) in consensus based on clinical investigations (patient history, electrocardiography, echocardiography, left ventricular contrast angiography, single-photon emission computed tomography (n = 20), if available).

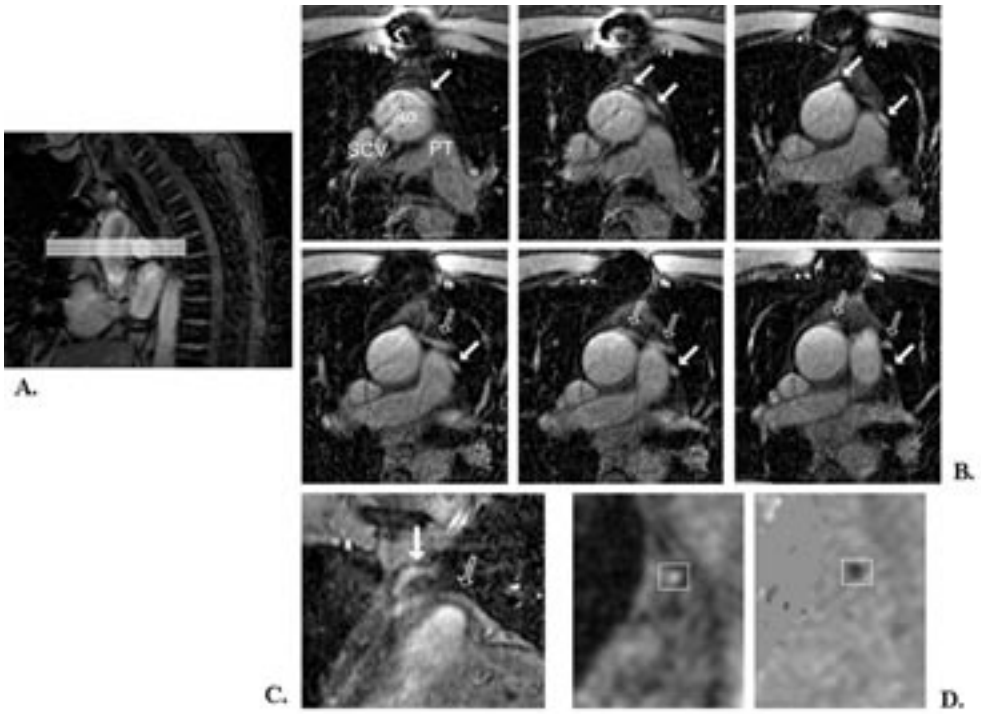

Figure 3.1

Example of a CMR study. Panel A shows a sagittal scout scan, on which the transversal survey scans at the level of the ascending aorta are planned. Panel B depicts the transversal survey scans showing two vein grafts, one sequential to the circumflex region (white arrow) and one single to the left anterior descending artery (outlined arrow). Panel C shows a coronal, oblique survey scan of the two vein grafts. Two differently orientated survey scans are used to plan the flow velocity scan.

Panel D illustrates the flow velocity scan (modulus and phase image) in mid-diastole of the sequential graft at rest, which is used to obtain volume flow. Ao = aorta; PT = pulmonary trunk; SCV = supra-caval vein

Statistical Analysis

Method 1

The aforementioned algorithm stated that basal volume flow <20 ml/min or CFR <2 would indicate a diseased graft or recipient vessel (7). A diseased graft or recipient vessel was defined as either showing a stenosis ≥50% or perfusing a region with previous MI. Grafts were not divided into single and sequential grafts. This algorithm was applied to our data set. Sensitivity and specificity were calculated in a 2 x 2 cross tabulation, in which sensitivity was defined as the proportion of diseased grafts that are correctly identified by the algorithm, and specificity as the proportion of normal grafts that are correctly identified by the algorithm.

Method 2

According to the second method (8) ROC curve analysis with logistic regression was performed on the CMR data set. To quantify the diagnostic performance of the individual flow parameters (volume flow, SPF, DPF, DSFR at rest and during stress, and CFR) ROC areas-under-the-curve (AUC) were calculated for each parameter (univariate analysis). Logistic regression analysis was performed using the parameters with significant AUC in univariate analysis to determine the diagnostic performance of the volume flow parameters (multivariate analysis). First, single and sequential grafts combined were analyzed in order to compare methods 1 and 2. A diseased graft or recipient vessel was defined as either showing a stenosis ≥50% or perfusing a region with previous MI. Sensitivities and specificities of methods 1 and 2 were compared by a McNemar test. Since prior MI may only partially compromise vein graft flow, ROC curve analysis with logistic regression was performed on the data set in separating grafts (and recipient vessels) with mild (<50%) and significant (≥50%) stenosis. Since significant differences in vein graft flow for single and sequential grafts were demonstrated previously (17), vein grafts were then divided into single and sequential grafts, and separately analyzed. Using the univariate ROC curves, a cut-off value for each parameter with significant AUC was formulated, defined as the intersection of sensitivities and specificities. Sensitivities and specificities are presented with their 95%-confidence intervals (95%-CI).

Influence of prior myocardial infarction

In order to assess whether a MI had an impact on the flow parameters, as formulated in method 1, single and sequential vein grafts with a stenosis <50% were divided into grafts supplying a region with and without MI, and the CMR flow parameters were compared using a Student t-test.

A p-value <0.05 was considered statistically significant.

RESULTS

Method 1

A total of 125 vein grafts were investigated by coronary angiography and CMR flow velocity mapping, including single and sequential grafts (Table 3.1). Of the 125 vein grafts, CMR flow velocity mapping either at rest or during stress was not completed in 15 grafts, due to artefacts or minor adenosine side-effects. Accordingly, these 15 grafts were discarded, since calculation of CFR requires both measurements at rest and during stress. On the 110 remaining grafts, the algorithm could be applied, discriminating between grafts and recipient vessels with a stenosis <50%, and grafts or recipient vessels with a stenosis severity ≥50% or a MI in the perfused region. The 2x2 cross tabulation is displayed in Table 3.2. Method 1 yielded a sensitivity of 70% (95%-CI 61-79%) and a specificity of 38% (95%-CI 29-47%).

Number of patients (n)	68
Male/female	57/11
Age (years)	66 ± 9
Time after CABG (years)	9 ± 5
Hypercholesterolemia	53 (77%)
Diabetes mellitus	13 (19%)
Hypertension	36 (52%)
Current smokers	9 (13%)
Positive family history for cardiovascular disease	42 (61%)
Bypass grafts included in analysis methods (n)	110
Single vein grafts	72
Sequential vein grafts	38
Bypass graft region	
Left anterior descending artery	29
Left circumflex artery	44
Right coronary artery	37
Prior myocardial infarction in bypass graft region	50 (45%)
Percentage diameter stenosis (QCA)	53 ± 39%
Stenosis <50%	55 (50%)
Stenosis ≥50%	55 (50%)

Table 3.1

Patient and graft characteristics

CABG = coronary artery bypass grafting; QCA = quantitative coronary arteriography

		QCA		
	Method 1	Diseased grafts	Nondiseased grafts	Totals
CMR volume flow	Basal volume flow <20 ml/min or CFR <2	51	23	74
	Basal volume flow ≥20 ml/min and CFR ≥2	22	14	36
	Totals	73	37	110

Table 3.2

2 x 2 table of CMR volume flow and QCA according to method 1

Diseased grafts are defined as vein grafts or recipient vessels with a stenosis severity ≥50% or a prior myocardial infarction in the bypass graft region. Nondiseased grafts represent vein grafts and recipient vessels with a stenosis <50%. QCA = quantitative coronary arteriography; CFR = coronary flow reserve

Single vein grafts			Sequential vein grafts		
Flow parameter	Cut-off	AUC	Flow parameter	Cut-off	AUC
Volume flow baseline (ml/min)	22.7	0.79 †	Volume flow baseline (ml/min)	40.9	0.75 *
Volume flow stress (ml/min)	47.9	0.82 †	Volume flow stress (ml/min)	93.6	0.77 *
SPF baseline (ml/s)	0.73	0.78 †	SPF baseline (ml/s)	1.17	0.80 *
SPF stress (ml/s)	1.49	0.81 †	SPF stress (ml/s)	2.28	0.78 *
DPF baseline (ml/s)	1.15	0.79 †	DPF stress (ml/s)	3.60	0.75 *
DPF stress (ml/s)	2.03	0.84 †			
CFR	1.56	0.81 †			
DSFR baseline	0.93	0.79 †			
DSFR stress	1.05	0.82 †			

Table 3.3

*Optimal cut-offs of significant flow parameters of vein grafts derived from univariate analysis. AUC = area-under-the-curve; SPF = systolic peak flow; DPF = diastolic peak flow; CFR = coronary flow reserve; DSFR = diastolic-to-systolic flow ratio; * p<0.01; † p<0.001*

Method 2

For method 2, the same 15 of 125 grafts were discarded, because either rest or stress flow velocity mapping was not completed. First, the remaining 110 grafts were analyzed to differentiate grafts with <50% stenosis from grafts with ≥50% or a MI in their perfused region. In univariate analysis all parameters had a significant AUC, and were included in the multivariate analysis. Using ROC curve analysis with logistic regression an AUC of 0.72 (p<0.001) was found with a sensitivity of 74% (95% CI 66-82%) and a specificity of 68% (95% CI 59-78%). Compared with method 1, method 2 yielded a similar sensitivity, however with a significantly higher specificity.

Second, the diagnostic performance of CMR volume flow was analyzed by determining its ability to separate grafts with <50% stenosis from grafts with ≥50% stenosis. In multivariate analysis an AUC of 0.80 (p<0.001) was demonstrated, yielding a sensitivity of 65% (95% CI 56-74%) and a specificity of 85% (95% CI 78-92%).

Third, grafts were divided into single (n = 72) and sequential grafts (n = 38). For single vein grafts in univariate analysis significant AUC were demonstrated for all parameters. For sequential vein grafts significant AUC were found for volume flow baseline and stress, SPF baseline and stress, and DPF stress. AUC and optimal cut-off values are shown in Table 3.3. In multivariate analysis using ROC curve analysis with logistic regression, implementing CMR flow parameters with significant AUC, the following regression equation was formulated for single vein grafts:

$$\text{logit}(P) = 0.009*\text{volume flow}_{baseline} - 0.002*\text{volume flow}_{stress} + 0.042*SPF_{baseline} - 1.48*SPF_{stress} + 1.44*DPF_{baseline} + 0.056*DPF_{stress} + 0.10*CFR - 0.35*DSFR_{baseline} - 1.68*DSFR_{stress} + 2.34 \quad (1)$$

in which P is the predicted probability for the presence of a stenosis ≥50% in the graft or recipient vessel. Optimal cut-off for P is for single vein grafts 0.411, yielding a sensitivity of 79% (95%-CI 70-88%) and specificity of 87% (95%-CI 79-95%). In the ROC curve analysis an AUC of 0.87 was found ($p<0.001$).
For sequential vein grafts the regression equation was formulated as follows:

$$\text{logit}(P) = -0.019*\text{volume flow}_{baseline} + 0.01*\text{volume flow}_{stress} - 0.40*SPF_{baseline} - 0.87*SPF_{stress} + 0.005*DPF_{stress} + 2.42 \quad (2)$$

Optimal cut-off for P is 0.696 for sequential vein grafts, generating a sensitivity and specificity of 62% (95%-CI 47-77%) and 94% (95%-CI 86-100%) with an AUC of 0.81 ($p=0.001$). ROC curves of the multivariate analysis are presented in Figure 3.2.

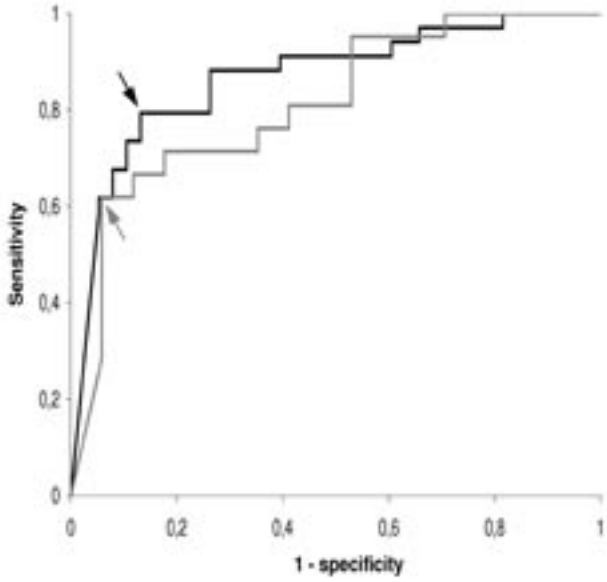

Figure 3.2
ROC curves of the multivariate analysis, including all significant CMR flow parameters from the univariate analysis, of single vein grafts (black line; AUC 0.87) and sequential vein grafts (grey line; AUC 0.81) in the detection of a stenosis ≥50%. Optimal cut-offs are indicated by an arrow. For single vein grafts the cut-off yielded a sensitivity and specificity of 79% and 87%, and for sequential vein grafts 62% and 94%, respectively.
ROC = receiver operating characteristic; AUC = area-under-the-curve

Influence of Prior Myocardial Infarction
When grafts with and without a MI in their vascular area were compared, for single and sequential grafts, respectively, no statistically significant differences were found for the flow parameters. In single vein grafts without a significant stenosis, and without a MI in their perfused territory (n = 25) mean CFR was 2.9 ± 2.9 versus 2.8 ± 0.9 in patients with sustained MI (n = 11; p = 0.84). When a vein graft has a sustained MI in its vascular area, vein graft flow is not necessarily impaired.

Discussion

In the present study two previously described analysis methods were retrospectively tested on a large, well documented CMR data set, and their diagnostic accuracy in detecting diseased vein grafts was compared. Method 1, using a previously described algorithm (7), yielded a sensitivity and specificity of 70% and 38% for discriminating between grafts without a significant stenosis (<50%) and grafts with a significant stenosis or a diseased recipient vessel. Using ROC curve analysis with logistic regression, method 2 yielded a sensitivity and specificity of 74% and 68% in the detection of a diseased graft. For the present data set the optimal approach for evaluating vein graft flow by CMR would be to analyze single and sequential grafts separately. For single grafts a sensitivity and specificity of 79% and 87% was demonstrated in the detection of ≥50% stenosis in grafts or recipient vessels. And for sequential grafts a sensitivity of 62% with a specificity of 94% was found.

Method 1
Method 1 stated that basal volume flow <20 ml/min or CFR <2 would indicate a diseased graft or recipient vessel, yielding a sensitivity of 78% and a specificity of 80% (7). When applied to a different, larger data set, similar sensitivity with a much lower specificity was demonstrated.
As a reference for the cut-off values, the study performed by Hoogendoorn et al. (18) was used, in which 23 vein grafts were investigated by CMR with flow mapping. Of the 23 grafts 6 were occluded, and one graft had a stenosis. The quantity of affected grafts in that study was too low to calculate cut-off values. In the present study a cut-off point of 22.7 ml/min was calculated for single vein grafts (n = 72), and 40.9 ml/min for sequential vein grafts (n = 38), underscoring the need to use separate reference values for single and sequential grafts, as was recently shown (17).

Method 2
The cut-off value <2 for CFR is commonly used when native coronary arteries are examined by Doppler flow wire (19;20). However, vein grafts display a different physiology than native coronary arteries (21;22), and therefore different cut-off values should be used. Using method 2, the best cut-off for CFR was demonstrated at 1.56 for single vein grafts. Several studies found a lower flow reserve in non-stenotic saphenous vein grafts, intra-operative, early and late after surgery, in comparison with non-stenotic native coronary arteries (23;24). Thus, a lower cut-off than 2 could be expected.
For sequential vein grafts CFR did not show a significant AUC at ROC analysis (p =

0.09). Absolute parameters (rest and stress volume flow, rest and stress SPF, stress DPF) did show significance in detecting bypass graft stenosis ≥50%, suggesting that absolute flow parameters, rather than relative parameters (CFR, DSFR), should be used in the evaluation of sequential vein grafts.

Influence of Prior Myocardial Infarction

In method 1 (7), a diseased graft run-off was defined as a distal coronary artery run-off with significant stenosis (≥50%) or a prior MI in the perfusion territory of the graft. However, the perfused territory may only partially be compromised by the MI, in particular in sequential grafts where the perfused area is large. In method 1 no distinction was made between subendocardial or transmural myocardial infarctions. In a study using a canine model small and large infarctions were induced and volume flow was measured invasively before occlusion and reperfusion of the left anterior descending artery, and one week after occlusion (25). Between the large and small infarctions (transmural extent 67-100% versus <50%) there was a significant difference in mean CFR after one week. Between small infarctions and the control group no significant differences in mean CFR were found. In our study no significant differences were found for the CMR flow parameters with or without sustained MI, in both single and sequential vein grafts. When a prior MI was not taken into account in method 2, the regression model improved for the data collected in the present study. Further research is required to quantify the extent of MI in the graft vascular area combined with a CFR determination, which could both be acquired by CMR (26;27).

Conclusion

Two previously described methods to evaluate vein graft flow by CMR display different results, when subjected to retrospective testing. Using ROC curve analysis and logistic regression the specificity of the analysis method improved considerably. For the current data set the best results were acquired when single and sequential grafts were separately analyzed, demonstrating a sensitivity of 79% and specificity of 87% for single grafts, and a sensitivity of 62% with a specificity of 94% for sequential grafts. Moreover, different cut-off values may be used for the individual CMR flow parameters in single and sequential vein grafts. Absolute parameters appear to be more discriminative than relative parameters.

REFERENCES

1. White CW. Clinical applications of Doppler coronary flow reserve measurements. Am J Cardiol 1993;71:10d-6d.
2. Chandrasekar B, Doucet S, Bilodeau L et al. Complications of cardiac catheterization in the current era: a single-center experience. Catheter Cardiovasc Interv 2001;52:289-95.
3. Laskey W, Boyle J, Johnson LW. Multivariable model for prediction of risk of significant complication during diagnostic cardiac catheterization. The Registry Committee of the Society for Cardiac Angiography & Interventions. Cathet Cardiovasc Diagn 1993;30:185-90.
4. Krone RJ, Johnson L, Noto T. Five year trends in cardiac catheterization: a report from the Registry of the Society for Cardiac Angiography and Interventions. Cathet Cardiovasc Diagn 1996;39:31-5.
5. Ishida N, Sakuma H, Cruz BP et al. Mr flow measurement in the internal mammary artery-to-coronary artery bypass graft: comparison with graft stenosis at radiographic angiography. Radiology 2001;220:441-7.
6. Galjee MA, van Rossum AC, Doesburg T, van Eenige MJ, Visser CA. Value of magnetic resonance imaging in assessing patency and function of coronary artery bypass grafts. An angiographically controlled study. Circulation 1996;93:660-6.
7. Bedaux WL, Hofman MB, Vyt SL, Bronzwaer JG, Visser CA, van Rossum AC. Assessment of coronary artery bypass graft disease using cardiovascular magnetic resonance determination of flow reserve. J Am Coll Cardiol 2002;40:1848-55.
8. Langerak SE, Vliegen HW, Jukema JW et al. Value of magnetic resonance imaging for the noninvasive detection of stenosis in coronary artery bypass grafts and recipient coronary arteries. Circulation 2003;107:1502-8.
9. Heller LI, Cates C, Popma J et al. Intracoronary Doppler assessment of moderate coronary artery disease: comparison with 201Tl imaging and coronary angiography. FACTS Study Group. Circulation 1997;96:484-90.
10. Deychak YA, Segal J, Reiner JS et al. Doppler guide wire flow-velocity indexes measured distal to coronary stenoses associated with reversible thallium perfusion defects. Am Heart J 1995;129:219-27.
11. Joye JD, Schulman DS, Lasorda D, Farah T, Donohue BC, Reichek N. Intracoronary Doppler guide wire versus stress single-photon emission computed tomographic thallium-201 imaging in assessment of intermediate coronary stenoses. J Am Coll Cardiol 1994;24:940-7.
12. Miller DD, Donohue TJ, Younis LT et al. Correlation of pharmacological 99mTc-sestamibi myocardial perfusion imaging with poststenotic coronary flow reserve in patients with angiographically intermediate coronary artery stenoses. Circulation 1994;89:2150-60.
13. Reiber JH, van der Zwet PM, Koning G et al. Accuracy and precision of quantitative digital coronary arteriography: observer-, short-, and medium-term variabilities. Cathet Cardiovasc Diagn 1993;28:187-98.
14. Reiber JH, Jukema W, van Boven A, van Houdt RM, Lie KI, Bruschke AV. Catheter sizes for quantitative coronary arteriography. Cathet Cardiovasc Diagn 1994;33:153-5.
15. Langerak SE, Kunz P, Vliegen HW et al. Magnetic resonance flow mapping in coronary artery bypass grafts: a validation study with Doppler flow measurements. Radiology 2002;222:127-35.
16. Langerak SE, Kunz P, Vliegen HW et al. Improved MR flow mapping in coronary artery bypass grafts during adenosine-induced stress. Radiology 2001;218:540-7.
17. Langerak SE, Vliegen HW, Jukema JW et al. Vein graft function improvement after percutaneous intervention: evaluation with MR flow mapping. Radiology 2003;228:834-41.
18. Hoogendoorn LI, Pattynama PM, Buis B, van der Geest RJ, van der Wall EE, de Roos A. Noninvasive evaluation of aortocoronary bypass grafts with magnetic resonance flow mapping. Am J Cardiol 1995;75:845-8.
19. Kern MJ, Meier B. Evaluation of the culprit plaque and the physiological significance of coronary atherosclerotic narrowings. Circulation 2001;103:3142-9.
20. Chamuleau SA, Meuwissen M, Eck-Smit BL et al. Fractional flow reserve, absolute and relative coronary blood flow velocity reserve in relation to the results of technetium-99m sestamibi single-photon emission computed tomography in patients with two-vessel coronary artery disease. J Am Coll Cardiol 2001;37:1316-22.
21. Motwani JG, Topol EJ. Aortocoronary saphenous vein graft disease: pathogenesis, predisposition, and prevention. Circulation 1998;97:916-31.
22. Chen L, Theroux P, Lesperance J, Shabani F, Thibault B, De Guise P. Angiographic features of vein grafts versus ungrafted coronary arteries in patients with unstable angina and previous bypass surgery. J Am Coll Cardiol 1996;28:1493-9.
23. Bates ER, Vogel RA, LeFree MT, Kirlin PC, O'Neill WW, Pitt B. The chronic coronary flow reserve provided by saphenous vein bypass grafts as determined by digital coronary radiography. Am Heart J 1984;108:462-8.
24. Campisi R, Czernin J, Karpman HL, Schelbert HR. Coronary vasodilatory capacity and flow reserve in normal myocardium supplied by bypass grafts late after surgery. Am J Cardiol 1997;80:27-31.

25. Klein LW, Agarwal JB, Schneider RM, Hermann G, Weintraub WS, Helfant RH. Effects of previous myocardial infarction on measurements of reactive hyperemia and the coronary vascular reserve. J Am Coll Cardiol 1986;8:357-63.
26. Wu E, Judd RM, Vargas JD, Klocke FJ, Bonow RO, Kim RJ. Visualisation of presence, location, and transmural extent of healed Q-wave and non-Q-wave myocardial infarction. Lancet 2001;357:21-8.
27. Fieno DS, Kim RJ, Chen EL, Lomasney JW, Klocke FJ, Judd RM. Contrast-enhanced magnetic resonance imaging of myocardium at risk: distinction between reversible and irreversible injury throughout infarct healing. J Am Coll Cardiol 2000;36:1985-91.

CHAPTER 4

Blood flow in coronary artery bypass vein grafts: volume versus velocity at cardiovascular MR imaging

Liesbeth P. Salm
Susan E. Langerak
Hubert W. Vliegen
J. Wouter Jukema
Jeroen J. Bax
Aeilko H. Zwinderman
Ernst E. van der Wall
Albert de Roos
Hildo J. Lamb

Radiology 2004; 232, 3, 915-920

ABSTRACT
Forty-nine patients with previous bypass surgery underwent coronary angiography and cardiovascular magnetic resonance (MR) imaging of single vein bypass grafts. Volume flow and velocity analyses were performed and compared on MR velocity maps. Bland-Altman analysis showed close agreement between the two types of analysis. Comparison of areas under the receiver operating characteristic curve revealed no significant differences between the analyses for detection of stenoses of 70% or greater. Diagnostic accuracy for volume flow and velocity parameters was 92% and 93%, respectively. Velocity analysis appears to be the preferred method, because it is less time-consuming and has a similar diagnostic accuracy to volume flow analysis.

Introduction

Volume flow and peak velocity measurements have been used as physiologic markers of stenosis severity in coronary arteries. Volume flow is of direct clinical value, since the quantity of blood flowing through a vessel within 1 minute is measured, and coronary flow reserve (CFR) is correlated with stenosis severity (1); however, direct invasive measurement is restricted to "open chest" procedures. Peak velocity measured by using a Doppler guidewire has been proven to correlate well with volume flow both in vitro and in vivo (2) and has evolved into a well-established method to evaluate stenoses in coronary arteries and bypass grafts in the catheterization laboratory (3,4). Cardiovascular magnetic resonance (MR) velocity mapping is a noninvasive technique used to measure coronary flow and velocity in native coronary arteries (5-8) and bypass grafts (9-12). Both volume flow and velocity can be analyzed on a MR velocity map. MR volume flow analysis has been validated as being an accurate noninvasive method of measuring volume flow (13-15). With this approach, the mean velocity for the whole luminal area of the vessel is multiplied by the luminal area. All pixels are included in the analysis; however, partial volume effects may occur at the edges of the lumen (16). Moreover, this analytical approach is time-consuming. In velocity analysis, the velocity in the center of the vessel is measured. This approach is less time-consuming and has been used successfully in several clinical studies (6,7,17,18). The present study was performed to evaluate whether MR volume flow analysis and MR velocity analysis have comparable diagnostic accuracies for the detection of significant (≥70%) stenosis in single vein coronary artery bypass grafts.

Materials and methods

Patients

A total of 49 patients, who had previously undergone bypass graft surgery, underwent coronary angiography because of recurrent chest pain and, in addition, underwent MR imaging according to the study protocol. Approval of the local medical ethics committee was obtained, and all patients gave informed consent. This study was prospective and was performed in a university hospital (Leiden University Medical Center). MR-related exclusion criteria included implanted metallic devices, unstable angina, irregular heart rhythm, claustrophobia, and the inability to lie flat. Adenosine-related exclusion criteria included chronic obstructive pulmonary disease and second- or third-degree atrioventricular block. Mean age (± standard deviation) in patients was 66.4 years ± 8.7 (range 43-79 years). There were 40 men and 9 women, with mean ages of 65.7 years ± 9.1 (range 43-79 years) and 69.7 years ± 6.3 (range 60-77 years), respectively. Table 4.1 gives pertinent information regarding the 49 patients.

Imaging and Analysis

Coronary Angiography

Coronary angiography was performed according to a standard protocol by using the Seldinger technique. Single vein grafts and recipient vessels (n = 80) were studied in 49 patients. To objectively determine the severity of stenosis, quantitative coronary arteriography was performed by members of an independent core laboratory (Heart Core,

Number of patients (n)	49
Male/female	40/9
Age (years)	66.4 ± 8.7
Time after bypass surgery (years)	13.5 ± 5.3
Number of grafts studied	80
Hypercholesterolemia	40 (82%)
Hypertension	24 (49%)
Current smokers	6 (12%)
Diabetes mellitus	8 (16%)
Family history for cardiovascular disease	28 (57%)

Table 4.1
Patient Characteristics

Leiden, the Netherlands). An experienced analyst from Heart Core, who was blinded to the results of the MR imaging, performed the quantitative coronary arteriography analyses. Quantitative coronary arteriography enabled digital measurement of the diameter of the stenosis (in millimeters) and of a nonstenotic segment of the same vessel (reference diameter). The percentage of stenosis was calculated as the ratio between the diameter of the stenosed segment and the reference diameter. This method of quantitative coronary arteriography was standardized and extensively validated by Reiber et al (19,20). A reduction in vessel diameter of 70% or greater was considered a significant stenosis.

MR Imaging
For MR imaging, a 1.5-T imager (Gyroscan ACS-NT; Philips Medical Systems, Best, the Netherlands) equipped with Powertrak 6000 gradient system, a cardiac research software patch, and a 5-element cardiac synergy coil was used. The investigator (S.E.L.) who performed the MR imaging was blinded to the results of coronary angiography. Information regarding the coronary artery bypass procedure was used as a reference for the course of the grafts. First, gross cardiac anatomy was visualized by means of a scout image. Then, transverse electrocardiographically gated 2-dimensional gradient-echo survey MR images were obtained at the level of the ascending aorta to localize the grafts. A plane perpendicular to the proximal section of the graft was planned on two differently angled survey images, and, for MR velocity mapping, a fast breath-hold turbo-field echo-planar imaging sequence was used at rest and during stress (140 µg of adenosine per kilogram of body weight per minute administered intravenously). The turbo-field echo-planar imaging sequence included the following parameters: 11.0/4.6 (repetition time msec/echo time msec), flip angle of 20°, temporal resolution of 23 msec, field of view of 200x100 mm, data acquisition matrix of 128x60, in-plane spatial resolution of 1.6x1.6 mm reconstructed to 0.8x0.8 mm by means of zero filling of k-space, section thickness of 6 mm, image duration of 20 heartbeats, velocity encoding of 75 cm/sec, and prospective electrocardiographic triggering (9,10).
Volume flow analysis and velocity analysis were performed with an analytic software

package (FLOW; Medis, Leiden, the Netherlands) by the same investigator (S.E.L.), and the flow and velocity analyses of the same velocity map were separated by a minimum of 4 weeks to avoid bias. The duration (in minutes) of the volume flow and velocity analyses per patient was registered from the start of the image analysis to report generation.
For the volume flow analysis, the luminal area was traced manually on the modulus image and transferred to the phase image (Figure 4.1). The position and size of each contour were adjusted according to the cardiac phase. The flow rate (in milliliters per second) was calculated by multiplying the average velocity over the luminal area with the luminal area for each cardiac phase. Flow rate-versus-time curves were reconstructed, and the volume flow rate (in milliliters per minute) was obtained by multiplying the integrated volumetric flow rate per heartbeat with the heart rate (Figure 4.2). Systolic peak flow rate and diastolic peak flow rate were defined as maximal flow rate during systole and diastole, respectively, both measured in milliliters per second. CFR was calculated as the ratio of volume flow during adenosine-induced stress and volume flow at rest. The ratio between diastolic and systolic peak flow rates was regarded as the diastolic-to-systolic flow ratio.
Velocity images consisted of paired modulus and phase images. For the velocity analysis, a region of interest of 2 x 2 pixels was placed in the center of the vessel in each phase image (Figure 4.1). The mean velocity of the 4 pixels was defined as the central velocity for that cardiac phase. Velocity-versus-time curves were drawn (Figure 4.2), which were similar to flow rate curves. Systolic peak velocity and diastolic peak velocity were defined as the maximal central velocity during systole and diastole, respectively, measured in centimeters per second. The mean central velocity was regarded as the average peak velocity. Coronary flow velocity reserve (CFVR) was calculated as the ratio between average peak velocities during adenosine-induced stress and at rest. Diastolic-to-systolic velocity ratio was the ratio between diastolic and systolic peak velocities.

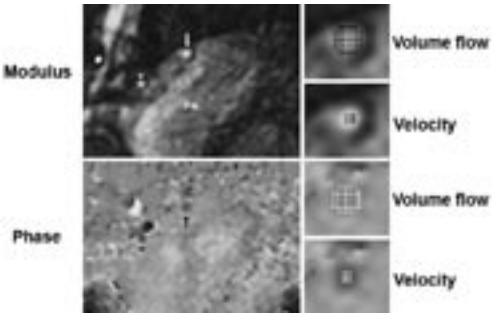

Figure 4.1
Sagittal oblique images from a typical phase-contrast MR examination. Modulus (top) and phase (bottom) images, obtained with a breath-hold turbo-field echo-planar (11.0/4.6) sequence, show the cross section of a vein graft (arrow) to the left anterior descending coronary artery and an arterial bypass graft (arrowhead) to the first diagonal branch during late diastole. Enlargements of the vein graft cross section (right) are shown to illustrate the volume flow and velocity analyses. PA = pulmonary artery; # = artefact derived from sternal wires on the chest wall

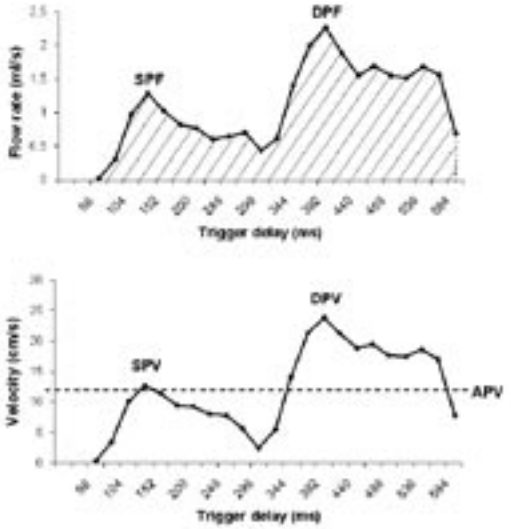

Figure 4.2

Top: Flow rate-versus-time curve. The integral of the curve (hatched area) indicates the volume flow per heartbeat. The volume flow per heartbeat multiplied with the heart rate results in the volume flow per minute. Bottom: Velocity-versus-time curve from the same bypass graft displays the velocity parameters that were distracted from the curve. Flow rate- and velocity-versus-time curves were used to quantify volume flow and velocity parameters. SPF = systolic peak flow; DPF = diastolic peak flow; SPV = systolic peak velocity; DPV = diastolic peak velocity; APV = average peak velocity

Statistical Analysis

Paired correlations of the flow and velocity parameters were determined by calculating the Pearson correlation coefficient. Limits of agreement between the volume flow and velocity analyses were evaluated by means of Bland-Altman analysis (21). Receiver operating characteristic (ROC) curve analysis was employed to determine the diagnostic performance of each flow and velocity parameter for demonstrating a significant stenosis using the Simpson rule (univariate analysis).

Significant parameters from the univariate analysis were subsequently used to perform stepwise multivariate logistic regression and ROC curve analyses to determine the diagnostic performance of the combined set of flow or velocity parameters, respectively, in the detection of a significant stenosis (multivariate analysis). Multiple single vein grafts in the same patient were possibly correlated (22), for instance, because they share the same risk of stenosis due to systemic factors. This correlation was investigated for the calculation of the correlations between the flow and velocity parameters, and for the logistic regression analysis by using a robust estimator of the standard errors and by the subsequent calculation of the p values. Results indicated no correlation between multiple grafts within a patient. Therefore, all grafts were treated independently for calculating correlations and areas under the curve in ROC analysis and for comparing ROC curves. The optimal cutoff values for flow and velocity parameters needed to

predict stenosis were defined as those providing the maximal sum of sensitivity and specificity. Sensitivity, specificity, and diagnostic accuracy were based on their standard definitions and are presented with 95% confidence intervals.
For all tests, $p<0.05$ was considered to indicate a statistically significant difference.

RESULTS

A total of 80 single vein grafts were analyzed. Sixteen grafts supplied the left anterior descending artery territory; 25 grafts, the left circumflex artery territory; and 39 grafts, the right coronary artery territory. By means of quantitative coronary arteriography, severity of stenosis was determined to range from 0% to 100% with a mean of 50% ± 39. Stenosis of 70% or greater was detected in 25 grafts (31%).
At MR imaging, 22 of 80 grafts were not visible in their expected course, and these grafts were regarded as occluded. MR velocity mapping was performed in the remaining 58 grafts. Baseline velocity mapping was unsuccessful in 1 graft because of artifacts. Adenosine-induced stress velocity mapping was not possible in 8 grafts because of side effects from adenosine.
Correlations for the volume flow and velocity parameters are shown in Table 4.2. Highly significant correlations were found for all paired parameters both at rest and during stress ($p<0.01$ for all correlations).
Agreement between CFR and CFVR and between diastolic-to-systolic flow ratio and diastolic-to-systolic velocity ratio was quantified by means of Bland-Altman analysis. Figure 4.3 displays the Bland-Altman plot for the CFR and CFVR. There was a close agreement between the two methods of analysis. The mean difference between the CFVR and CFR was not significant. Similar results were found for diastolic-to-systolic flow ratio and diastolic-to-systolic velocity ratio by using baseline and stress parameters. Direct comparison of the remaining parameters was not possible because units of measure were not equivalent; volume flow parameters were measured in milliliters per second, while velocity parameters were measured in centimeters per second.
At univariate analysis, all parameters for both volume flow and velocity methods were significantly different between grafts with and those without stenoses (≥70% stenosis; $p<0.001$). At multivariate analysis, the diagnostic value of all significant univariate flow parameters (volume flow; systolic and diastolic peak flow rates; diastolic-to-systolic flow ratio at baseline and during stress; CFR) were compared with all significant univariate velocity parameters (average, systolic, and diastolic peak velocities; diastolic-to-systolic velocity ratio at baseline and during stress; CFVR) in the detection of a graft stenosis of 70% or more. The estimated regression parameters, selected in the model, are given in Table 4.3. The area under the ROC curve was 0.93 (95% confidence interval: 0.87, 0.99) for the flow parameters and 0.96 (95% confidence interval: 0.92, 1.00) for the velocity parameters. Both ROC areas were significantly larger than 0.50 ($p<0.001$). When the ROC areas were compared, the results showed no significant difference ($p = 0.41$). Optimal cut-off points for the ROC curves are displayed in Figure 4.4. The optimal sensitivity, specificity and accuracy for the volume flow parameters were 90% (95% confidence interval: 83%, 97%), 92% (95% confidence interval: 86%, 98%), and 92% (95% confidence interval: 86%, 98%), respectively. The optimal sensitivity, specificity and accuracy for the

velocity parameters were 95% (95% confidence interval: 90%, 100%), 92% (95% confidence interval: 86%, 98%), and 93% (95% confidence interval: 87%, 99%), respectively. No significant differences in sensitivity, specificity, or accuracy were found between the methods of analysis for demonstrating a bypass graft stenosis of 70% or greater.
The mean duration for performing a volume flow analysis was 25.9 minutes ± 4.3, whereas a velocity analysis was performed in 11.1 minutes ± 2.2 ($p<0.05$).

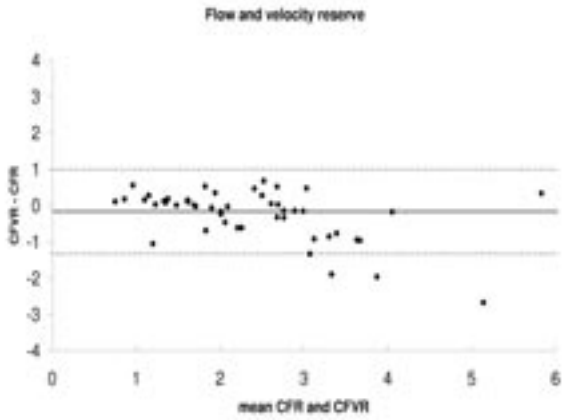

Figure 4.3
Bland-Altman plot of CFR and CFVR derived from the volume flow and velocity analysis, respectively. Solid horizontal line shows the mean difference between CFR and CFVR, and dashed lines are ± 2 standard deviations. The plot shows a close agreement between the two analysis methods. The mean difference between CFVR and CFR was not significant.

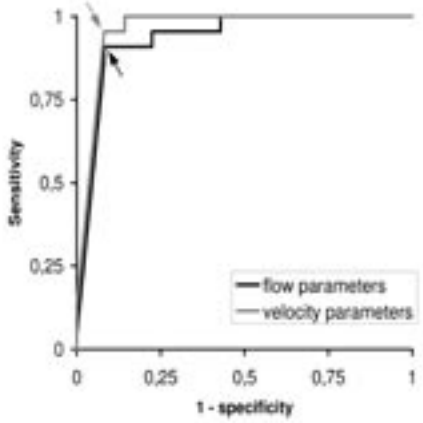

Figure 4.4
Graph shows ROC curves of single vein grafts with luminal stenosis 70% or greater derived from flow and velocity parameters. When the area under the ROC curve for flow parameters was compared with that for velocity parameters, no significant differences were found. Optimal cutoff points are indicated by arrows.

Paired parameters	Correlation coefficient
CFR and CFVR	0.85
Baseline	
Volume flow and average peak velocity	0.85
Systolic peak flow and velocity	0.84
Diastolic peak flow and velocity	0.86
Diastolic-to-systolic flow and velocity ratios	0.90
Adenosine-induced stress	
Volume flow and average peak velocity	0.95
Systolic peak flow and velocity	0.90
Diastolic peak flow and velocity	0.90
Diastolic-to-systolic flow and velocity ratios	0.83

Table 4.2

*Correlations for paired flow and velocity parameters**

** For all correlations p<0.01. Flow and velocity parameters are derived from the volume flow and velocity analysis of the MR velocity maps of 58 single vein bypass grafts.*

	Volume flow		Velocity	
Parameter	b	SEE	b	SEE
Average peak				
Baseline	0.054	0.036	1.72	0.55
Stress	-	-	-	-
Reserve *	-	-	3.12	1.01
Systolic peak				
Baseline	-	-	-0.82	0.28
Stress	-2.15	0.81	-0.28	0.12
Diastolic peak				
Baseline	-	-	-	-
Stress	-	-	-	-
Diastolic-to-systolic ratio	-	-	-	-
Baseline	-	-	-	-
Stress	-1.32	0.37	-7.74	2.14
Constant	1.50	0.58	1.51	0.60

Table 4.3

Estimated regression parameters of the forward stepwise multivariate logistic regression model

** Refers to the CFR or CFVR. b = regression coefficient; SEE = standard error of the estimate*

Discussion

In the present study, two approaches used to analyze MR velocity maps, MR volume flow analysis and MR velocity analysis, were compared in a head-to-head fashion in single vein bypass grafts. Close agreement was shown between the volume flow and velocity methods when comparing CFR, CFVR, diastolic-to-systolic flow ratio, and diastolic-to-systolic velocity ratio. Fair sensitivity, specificity, and diagnostic accuracy were shown for both approaches in depicting significant (≥70%) stenosis. Therefore, a single approach would be sufficient when analyzing MR velocity maps.

The concept of CFR was proposed by Gould et al (1) in the early 1970s, when the necessity arose for a hemodynamic assessment of coronary stenoses visualized on the coronary angiogram. Absolute coronary blood flow could be measured only by using perivascular flow transducers in "open chest" procedures. CFR was therefore validated in animal models or in patients undergoing bypass graft surgery (1,23,24); however, extensive use in the clinical setting was not possible. When the diameter of intravascular catheter-based Doppler ultrasonographic devices could be reduced to an 0.018-inch diameter, it became feasible to measure absolute velocity of blood flow and calculate CFVR in coronary arteries in patients during catheterization. Absolute blood flow correlated well with Doppler-derived absolute velocity and volume flow both in vitro and in vivo (2,25,26). Doppler-derived velocity and CFVR proved their potential in numerous clinical applications, such as in identification of hemodynamically significant stenoses in native coronary arteries and vein grafts (3,4), in the functional assessment of stenoses of intermediate severity (27), in the determination of the need for and the outcome after coronary intervention (28-30), and in the prediction of restenosis (31).

With MR imaging and a velocity mapping sequence, both CFR and CFVR can be calculated, as was described in Materials and Methods. In clinical studies, both the volume flow analysis (8,5,12) and the velocity analysis (7,17,18) have been used successfully. In our study, the accuracies of volume flow and velocity analyses were not significantly different when evaluating MR velocity maps. Other factors, such as errors in phase-contrast MR imaging and the time necessary to analyze the MR velocity maps, become important in choosing a method for analysis.

When obtaining flow measurements at phase-contrast MR imaging, several errors might occur (32). Some errors are dependent on the prescription of the MR velocity mapping sequence (eg. inadequate spatial and temporal resolution, mismatched encoding velocity, deviation of the perpendicular imaging plane from the flow direction). In the present study, an effort was made to keep the effects of errors minimal. Encoding velocity was adequately matched to avoid aliasing, and two survey images obtained at different angles were used to plan the imaging plane perpendicular to the graft. Phase-offset errors are dependent on local magnetic-field inhomogeneities and are usually small. In the analysis of MR velocity maps, all of these errors affect both volume flow and velocity analyses.

In volume flow analysis, all pixels in the cross-sectional area of the graft lumen are included. Pixels on the vessel edge may average signals both from the vessel lumen and from surrounding tissue. This type of error, known as partial volume effect, could either increase or decrease apparent flow (13,33). The extent of partial volume effect depends predominantly on spatial resolution and relative signal intensity of stationary tissue (16).

With the current MR imaging techniques, spatial resolution for flow measurements in small vessels is limited and, due to background noise velocity, is not zero in stationary tissue, enhancing partial volume effects. However, velocities at the vessel edge are expected to be low, as there is a pulsatile laminar flow pattern in bypass grafts with the highest velocity in the center of the vessel (34). Since diagnostic accuracy of the volume flow and velocity analyses did not differ significantly in our study, this might indicate that this type of error has a relatively minor role when MR imaging is used to measure flow in single vein bypass grafts.

In our study, a volume flow analysis required 25.9 minutes ± 4.3 to complete, whereas a velocity analysis required only 11.1 minutes ± 2.2. If clinical acceptance of a diagnostic test is to be achieved, performance and analysis of the test should be fast and straightforward. Since the diagnostic accuracy from both analyses was similar, velocity analysis appears to be the preferable method.

Our study had limitations in that other issues associated with MR velocity mapping, such as reference values of the MR flow and velocity parameters, spatial and temporal resolution of the acquired MR images, and proximal location of the imaging plane in the vessel were not addressed; this is because our purpose was to compare volume flow and velocity analyses of MR velocity maps. In addition, the sample size of our study was small. The study was not designed to test equivalence of the analysis methods. To demonstrate equivalence, a larger data set would be necessary.

Conclusion

In the evaluation of MR velocity maps of single vein coronary artery bypass grafts, there is close agreement between volume flow and velocity analyses. For detection of a stenosis 70% or greater, velocity analysis has a diagnostic accuracy similar to that of volume flow analysis, and is less time-consuming. Therefore, velocity analysis appears to be the method of preference in the analysis of MR velocity maps of bypass grafts.

REFERENCES

1. Gould KL, Lipscomb K, Hamilton GW. Physiologic basis for assessing critical coronary stenosis. Instantaneous flow response and regional distribution during coronary hyperemia as measures of coronary flow reserve. Am J Cardiol 1974; 33:87-94.
2. Doucette JW, Corl PD, Payne HM, et al. Validation of a Doppler guide wire for intravascular measurement of coronary artery flow velocity. Circulation 1992; 85:1899-1911.
3. Ofili EO, Labovitz AJ, Kern MJ. Coronary flow velocity dynamics in normal and diseased arteries. Am J Cardiol 1993; 71:3d-9d.
4. White CW. Clinical applications of Doppler coronary flow reserve measurements. Am J Cardiol 1993; 71:10d-16d.
5. Hundley WG, Hamilton CA, Clarke GD, et al. Visualization and functional assessment of proximal and middle left anterior descending coronary stenoses in humans with magnetic resonance imaging. Circulation 1999; 99:3248-3254.
6. Shibata M, Sakuma H, Isaka N, Takeda K, Higgins CB, Nakano T. Assessment of coronary flow reserve with fast cine phase contrast magnetic resonance imaging: comparison with measurement by Doppler guide wire. J Magn Reson Imaging 1999; 10:563-568.
7. Nagel E, Bornstedt A, Hug J, Schnackenburg B, Wellnhofer E, Fleck E. Noninvasive determination of coronary blood flow velocity with magnetic resonance imaging: comparison of breath-hold and navigator techniques with intravascular ultrasound. Magn Reson Med 1999; 41:544-549.
8. Kessler W, Moshage W, Galland A, et al. Assessment of coronary blood flow in humans using phase difference MR imaging. Comparison with intracoronary Doppler flow measurement. Int J Card Imaging 1998; 14:179-186.
9. Langerak SE, Kunz P, Vliegen HW, et al. Improved MR flow mapping in coronary artery bypass grafts during adenosine-induced stress. Radiology 2001; 218:540-547.
10. Langerak SE, Kunz P, Vliegen HW, et al. Magnetic resonance flow mapping in coronary artery bypass grafts: a validation study with Doppler flow measurements. Radiology 2002; 222:127-135.
11. Ishida N, Sakuma H, Cruz BP, et al. Mr flow measurement in the internal mammary artery-to-coronary artery bypass graft: comparison with graft stenosis at radiographic angiography. Radiology 2001; 220:441-447.
12. Bedaux WL, Hofman MB, Vyt SL, Bronzwaer JG, Visser CA, van Rossum AC. Assessment of coronary artery bypass graft disease using cardiovascular magnetic resonance determination of flow reserve. J Am Coll Cardiol 2002; 40:1848-1855.
13. Hofman MB, Visser FC, van Rossum AC, Vink QM, Sprenger M, Westerhof N. In vivo validation of magnetic resonance blood volume flow measurements with limited spatial resolution in small vessels. Magn Reson Med 1995; 33:778-784.
14. Sakuma H, Saeed M, Takeda K, et al. Quantification of coronary artery volume flow rate using fast velocity-encoded cine MR imaging. AJR Am J Roentgenol 1997; 168:1363-1367.
15. Lee VS, Spritzer CE, Carroll BA, et al. Flow quantification using fast cine phase-contrast MR imaging, conventional cine phase-contrast MR imaging, and Doppler sonography: in vitro and in vivo validation. AJR Am J Roentgenol 1997; 169:1125-1131.
16. Tang C, Blatter DD, Parker DL. Accuracy of phase-contrast flow measurements in the presence of partial-volume effects. J Magn Reson Imaging 1993; 3:377-385.
17. Saito Y, Sakuma H, Shibata M, et al. Assessment of coronary flow velocity reserve using fast velocity- encoded cine MRI for noninvasive detection of restenosis after coronary stent implantation. J Cardiovasc Magn Reson 2001; 3:209-214.
18. Langerak SE, Vliegen HW, Jukema JW, et al. Value of magnetic resonance imaging for the noninvasive detection of stenosis in coronary artery bypass grafts and recipient coronary arteries. Circulation 2003; 107:1502-1508.
19. Reiber JH, van der Zwet PM, Koning G, et al. Accuracy and precision of quantitative digital coronary arteriography: observer-, short-, and medium-term variabilities. Cathet Cardiovasc Diagn 1993; 28:187-198.
20. Reiber JH, Jukema W, van Boven A, van Houdt RM, Lie KI, Bruschke AV. Catheter sizes for quantitative coronary arteriography. Cathet Cardiovasc Diagn 1994; 33:153-155.
21. Bland JM, Altman DG. Statistical methods for assessing agreement between two methods of clinical measurement. Lancet 1986; 1:307-310.
22. Zeger SL, Liang KY. Longitudinal data analysis for discrete and continuous outcomes. Biometrics 1986; 42:121-130.
23. Gould KL, Kirkeeide RL, Buchi M. Coronary flow reserve as a physiologic measure of stenosis severity. J Am Coll Cardiol 1990; 15:459-474.
24. White CW, Wright CB, Doty DB, et al. Does visual interpretation of the coronary arteriogram predict the physiologic importance of a coronary stenosis? N Engl J Med 1984; 310:819-824.

25. Sudhir K, Hargrave VK, Johnson EL, et al. Measurement of volumetric coronary blood flow with a Doppler catheter: validation in an animal model. Am Heart J 1992; 124:870-875.
26. Labovitz AJ, Anthonis DM, Cravens TL, Kern MJ. Validation of volumetric flow measurements by means of a Doppler-tipped coronary angioplasty guide wire. Am Heart J 1993; 126:1456-1461.
27. Kern MJ, Donohue TJ, Aguirre FV, et al. Assessment of angiographically intermediate coronary artery stenosis using the Doppler flowire. Am J Cardiol 1993; 71:26d-33d.
28. Segal J. Applications of coronary flow velocity during angioplasty and other coronary interventional procedures. Am J Cardiol 1993; 71:17d-25d.
29. Serruys PW, De Bruyne B, Carlier S, et al. Randomized comparison of primary stenting and provisional balloon angioplasty guided by flow velocity measurement. Doppler Endpoints Balloon Angioplasty Trial Europe (DEBATE) II Study Group. Circulation 2000; 102:2930-2937.
30. Nishida T, Di Mario C, Kern MJ, et al. Impact of final coronary flow velocity reserve on late outcome following stent implantation. Eur Heart J 2002; 23:331-340.
31. Albertal M, Regar E, Van Langenhove G, et al. Value of coronary stenotic flow velocity acceleration in prediction of angiographic restenosis following balloon angioplasty. Eur Heart J 2002; 23:1849-1853.
32. Lotz J, Meier C, Leppert A, Galanski M. Cardiovascular flow measurement with phase-contrast MR imaging: basic facts and implementation. Radiographics 2002; 22:651-671.
33. Wolf RL, Ehman RL, Riederer SJ, Rossman PJ. Analysis of systematic and random error in MR volumetric flow measurements. Magn Reson Med 1993; 30:82-91.
34. Kajiya F, Tsujioka K, Ogasawara Y, et al. Analysis of flow characteristics in poststenotic regions of the human coronary artery during bypass graft surgery. Circulation 1987; 76:1092-1100.

CHAPTER 5

Functional significance of stenoses in coronary artery bypass grafts

Evaluation by single-photon emission computed tomography perfusion imaging, cardiovascular magnetic resonance, and angiography

Liesbeth P. Salm,
Jeroen J. Bax
Hubert W. Vliegen
Susan E. Langerak
Petra Dibbets
J. Wouter Jukema
Hildo J. Lamb
Ernest K.J. Pauwels
Albert de Roos
Ernst E. van der Wall

J Am Coll Cardiol 2004; 44, 9, 1877-1882

ABSTRACT

Objectives: This study was designed to perform a head-to-head comparison between single-photon emission computed tomography (SPECT) and cardiovascular magnetic resonance (CMR) to evaluate hemodynamic significance of angiographic findings in bypass grafts.

Background: The hemodynamic significance of a bypass graft stenosis may not always accurately be determined from the coronary angiogram. A variety of diagnostic tests (invasive or noninvasive) can further characterize the hemodynamic consequence of a lesion.

Methods: Fifty-seven arterial and vein grafts in 25 patients were evaluated by angiography, SPECT perfusion imaging, and coronary flow velocity reserve determination by CMR. Based on angiography and SPECT, four different groups could be identified: 1) no significant stenosis (<50%), normal perfusion; 2) significant stenosis (≥50%), abnormal perfusion; 3) significant stenosis, normal perfusion (no hemodynamic significance); and 4) no significant stenosis, abnormal perfusion (suggesting microvascular disease).

Results: A complete evaluation was obtained in 46 grafts. SPECT and CMR provided similar information in 37 of 46 grafts (80%), illustrating good agreement (κ=0.61, $p<0.001$). Eight grafts perfused a territory with scar tissue. When agreement between SPECT and CMR was restricted to grafts without scar tissue, it improved to 84% (κ=0.68). Integration of angiography with SPECT categorized 14 lesions in group 1, 23 in group 2, 6 in group 3, and 3 in group 4. SPECT and CMR agreement per group was 86%, 78%, 100%, and 33%, respectively.

Conclusions: Head-to-head comparison showed good agreement between SPECT and CMR for functional evaluation of bypass grafts. CMR may offer an alternative method to SPECT for functional characterization of angiographic lesions.

Introduction

Determination of stenosis severity by coronary angiography has been considered the gold standard for the assessment of obstructive coronary artery disease, but the hemodynamic significance of a stenosis may not be determined accurately from the coronary angiogram (1;2). In order to decide whether conservative (medical) treatment or a percutaneous intervention is required, further clinical evaluation may be necessary.

A variety of tests have been proposed for the evaluation of the hemodynamic significance of a stenosis in native coronary arteries and bypass grafts. One method is flow velocity measurement during cardiac catheterization, using the Doppler flow wire at rest and during pharmacologic stress. Subsequent calculation of the coronary flow velocity reserve (CFVR) is an invasive method that can be performed to assess the hemodynamic significance of a stenosis, but its use remains limited to centers with experience (3;4). Alternatively, noninvasive techniques may be of value; myocardial perfusion imaging with single-photon emission computed tomography (SPECT) in particular is a well-established technique to evaluate the hemodynamic significance of a stenosis (5;6). Based on the integration of angiographic findings and SPECT results, four different categories can be identified: 1) no significant stenosis, normal perfusion; 2) a significant stenosis, abnormal perfusion; 3) a significant stenosis, normal perfusion (no hemodynamic significance); and 4) no significant stenosis, abnormal perfusion (suggesting microvascular disease). Thus, integration of anatomical information (angiography) and functional information (SPECT) may allow more precise characterization of lesions.

More recently, the feasibility of CFVR assessment using cardiovascular magnetic resonance (CMR) with velocity mapping in coronary arteries and bypass grafts was demonstrated (7;8). The relative merits of SPECT and CMR to provide noninvasive information in addition to angiography are unknown.

Accordingly, the aim of the present study was to perform a head-to-head comparison between SPECT and CMR to assess the hemodynamic significance of angiographic findings in bypass grafts.

Methods

Study Population

Consecutive patients with a history of bypass surgery who underwent elective coronary angiography for recurrent chest pain were invited to participate in the study. All patients gave informed consent. The protocol was approved by the medical ethics committee of our institution. Coronary angiography was performed according to a standard protocol using the femoral approach. In order to determine the stenosis severity objectively, quantitative coronary arteriography (QCA) was performed by an independent core lab (Heart Core, Leiden, the Netherlands). QCA was performed according to standardized methods (8-10). If two or more stenoses were present in either the graft or recipient vessels, the most severe lesion was taken into account.

Gated SPECT

For the gated SPECT examination a two-day stress-rest protocol was used (11). The stress protocol included a symptom-limited treadmill exercise test. Whenever possible, beta-

blocking agents and calcium channel antagonists were discontinued at least 24 hours before scintigraphy. Test endpoints were physical exhaustion, dyspnea, angina pectoris, significant decrease in blood pressure (>10 mm Hg), or achievement of the maximum age-related heart rate. Blood pressure, heart rate, and electrocardiographic findings were monitored during the test. Technetium-99m tetrofosmin (500 MBq) was injected intravenously at peak exercise, which was continued for 1 minute after tracer injection. In patients unable to exercise (n = 11) adenosine stress was used. On the second day, resting images were obtained using 500 MBq technetium-99m tetrofosmin. The resting studies were acquired using electrocardiogram gating, allowing assessment of left ventricular (LV) ejection fraction and LV volumes (12).
Imaging was performed using a triple-head SPECT camera system (GCA 9300/HG, Toshiba Corp., Tokyo, Japan) equipped with low-energy, high-resolution collimators. A 20% window was used around the 140 keV energy-peak of technetium-99m tetrofosmin. A total of 90 projections (step-and-shoot mode, 35 s/projection, total imaging time 23 min) were obtained over a 360˚ circular orbit. Data were stored in a 64 x 64 matrix. The raw scintigraphic data were reconstructed by filtered back projection using a Butterworth filter (cutoff frequency at 0.26 cycle/pixel, of order 9). No attenuation correction was employed. Reconstruction of the images yielded standard long- and short-axis projections perpendicular to the heart axis. Reconstructed slices were 6.4 mm in all projections. The short-axis slices were displayed in polar map format, adjusted for peak myocardial activity (100%). The myocardium was divided into 17 segments, as recently proposed (13). Segmental tracer activity was expressed as percentage of maximum. Perfusion defects on stress images were considered present when tracer activity was <75% of maximum tracer uptake. Mild to moderate defects were defined as having 50% to 75% of normalized tracer uptake and severe defects as having <50% of normalized tracer uptake. When significant fill-in (>10% increase of normalized tracer activity) of perfusion defects was observed on the resting images, segments were classified as reversible (ischemic); defects without fill-in were classified as irreversible defects (scar) (14). The individual segments on the SPECT images were assigned to the distinct native coronary arteries, according to recently published guidelines (13). The anastomoses of the bypass graft on the different native coronary arteries then defined the vascular territory that the graft perfused.

Cardiovascular Magnetic Resonance
For the CMR examination a 1.5-T Gyroscan ACS-NT MR-scanner (Philips Medical Systems, Best, the Netherlands), equipped with Powertrak 6000 gradients, a cardiac research software patch, and five-element cardiac synergy coil was used. Transverse, electrocardiogram-gated, two-dimensional gradient-echo survey scans at the level of the ascending aorta were performed to localize the bypass grafts. A plane perpendicular to the proximal section of the graft was planned on two differently angulated survey scans, and for MR velocity mapping a fast breathhold Turbo field echo planar imaging (TFEPI) sequence was used at rest and during stress (adenosine 140 µg/kg/min intravenously). The TFEPI sequence is validated and described in more detail by Langerak et al. (15;16). Analyses of the velocity maps were performed with an analytic software package (FLOW, Medis, Leiden, the Netherlands) by an experienced investigator. A region

Number of patients (n)	25
Gender (M/F)	22/3
Age (years)	65 ± 9
Time after CABG (years)	11 ± 5
Hypercholesterolemia	22 (88%)
Diabetes mellitus	6 (24%)
Hypertension	15 (60%)
Current smokers	2 (8%)
Myocardial infarction	8 (32%)
Positive family history for cardiovascular disease	17 (68%)
Medication	
Beta-blockers	20 (80%)
Nitrates	19 (76%)
Calcium antagonists	18 (72%)
ACE inhibitors	10 (40%)
Statins	22 (88%)
Oral anticoagulants/aspirin	24 (96%)

Table 5.1
Patient Characteristics
CABG = coronary artery bypass grafting; ACE = angiotensin-converting enzyme

of interest of 2 x 2 pixels was placed in the center of the vessel in each phase image. The mean velocity of the four pixels was defined as the central velocity for that cardiac phase. The mean central velocity was regarded as the average peak velocity (APV; cm/s). CFVR was calculated as the ratio of APV during adenosine stress and APV at rest.

Statistical Analysis

Results are displayed as mean ± SD. Based on the integration of angiographic findings and SPECT results, four categories were distinguished: 1) a stenosis <50% on angiography and normal perfusion on SPECT; 2) a stenosis ≥50% and abnormal perfusion on SPECT, indicating a stenosis with hemodynamic consequences; 3) a stenosis ≥50% and normal perfusion on SPECT, indicating a stenosis without hemodynamic consequences; and 4) a stenosis <50% and abnormal perfusion, implying microvascular disease.
The agreement between SPECT and CMR results was evaluated using kappa statistics, with a kappa value <0.4, between 0.4 and 0.75, and >0.75 representing poor, fair to good, and excellent agreement, respectively. Grafts in which CFVR was not available were discarded. A p value <0.05 was considered significant.

RESULTS

Study Population

A total of 25 patients were included in the study. Patient characteristics are presented in Table 5.1. Fifty-seven bypass grafts were evaluated. Bypass graft characteristics are presented in Table 5.2. Stenosis severity, as measured by QCA, ranged from 0% to 100%

Number of bypass grafts (n)	57
Arterial/vein grafts	12/45
Single/sequential grafts	39/18
Vascular territory perfused by graft	
LAD	26 (46%)
LCX	13 (23%)
RCA	18 (32%)
Percentage diameter stenosis (QCA)	55 ± 36%
<50%	23
≥50%	34
Minimal luminal diameter (mm)	1.26 ± 0.50

Table 5.2
Bypass Graft Characteristics
LAD = left anterior descending artery; LCX = left circumflex artery; RCA = right coronary artery; QCA = quantitative coronary arteriography

with a mean percentage diameter stenosis of 55 ± 36%. Based on the QCA results, the grafts were divided into grafts with angiographically nonsignificant (<50%, n = 23), and significant stenoses (≥50%, n = 34).

Gated SPECT
Gated SPECT demonstrated an average LV ejection fraction of 53 ± 17% (range 24% to 85%). Mean end-systolic and end-diastolic volumes were 65 ± 50 ml and 122 ± 64 ml, respectively.
In the vascular territories supplied by the 57 grafts, stress myocardial perfusion was normal in the territories allocated to 25 grafts, mild or moderately reduced in territories of 17 grafts, and severely reduced in territories of 15 grafts. Rest perfusion was normal in 39 grafts, mild to moderately reduced in 15 grafts, and severely reduced in three grafts. Accordingly, perfusion was normal in the vascular territory of 25 grafts, ischemia was present in the territory of 22 grafts, and irreversible defects (indicating scar tissue) were present in the territory of 10 grafts. Perfusion defects per vascular territory are summarized in Table 5.3.

	Normal perfusion (n = 25)	Ischemia (n = 22)	Scar (n = 10)
LAD territory (n = 26)	13	9	4
LCX territory (n = 13)	4	5	4
RCA territory (n = 18)	8	8	2

Table 5.3
SPECT Perfusion Results per Vascular Territory of the Bypass Graft
SPECT = single-photon emission computed tomography; other abbreviations as in Table 5.2

SPECT Perfusion versus Angiographic Stenosis

Based on integration of the angiographic findings and SPECT results, 18 of 57 grafts (32%) were classified as stenosis <50% with normal perfusion; 27 (47%) had a stenosis ≥50% with abnormal perfusion, seven (12%) had a stenosis ≥50% with normal perfusion, indicating no hemodynamic significance of the stenosis; and five (9%) grafts had a stenosis <50% with abnormal perfusion, indicating microvascular disease. Mean percent diameter stenosis for the four categories were 16 ± 20%, 79 ± 20%, 65 ± 18%, and 36 ± 20%, respectively. Differences in percent diameter stenosis between the categories with equivalent stenosis percentages (<50% or ≥50%) were not significant. Mean minimal luminal diameter for the four categories were 1.51 ± 0.52 mm, 1.14 ± 0.50 mm, 1.33 ± 0.54 mm, and 1.03 ± 0.28 mm, respectively (p = NS).

Cardiovascular Magnetic Resonance

In 46 of 57 grafts, full CMR with velocity mapping at rest and during adenosine stress was successful. In 11 grafts velocity mapping failed for the following reasons. In one graft, the baseline velocity map could not be analyzed because of insufficient technical quality. In four grafts, stress velocity maps could not be obtained because of minor adverse reactions to adenosine, such as chest pain, dyspnea, headache, and flushing. All adverse reactions resolved within a few minutes after termination of adenosine infusion. In six grafts, velocity mapping could not be completed because of limitation of total research time, reserved for the CMR examination. One full CMR examination took approximately 1.5 hours to complete.

Fourteen of 57 grafts (25%) were not found in their expected course on the survey scan (zero flow) and were considered to be occluded.

Mean APV increased from 6.9 ± 5.5 cm/s (range 0 to 19.5 cm/s) at baseline to 15.2 ± 12.0 cm/s (range 0 to 35.6 cm/s) during stress, resulting in a mean CFVR of 1.7 ± 1.3 (range 0 to 3.7). When a cutoff value for CFVR of 2.0 was used (17), normal CFVR (≥2.0) was found in 25 grafts with a mean CFVR of 2.7 ± 0.5 and reduced CFVR (<2.0) in 21 grafts with a mean CFVR of 0.5 ± 0.8.

		CMR		
		CFVR ≥2.0	CFVR <2.0	Total
SPECT	Normal perfusion	18	2	20
	Abnormal perfusion	7	19	26
	Total	25	21	46

Table 5.4

Agreement of SPECT Perfusion and CMR

Only grafts with available CFVR (n = 46) were included.

SPECT = single-photon emission computed tomography; CMR = cardiovascular magnetic resonance; CFVR = coronary flow velocity reserve

SPECT/Angiography	CMR		
	CFVR ≥2.0	CFVR <2.0	Total
Stenosis <50% / normal SPECT perfusion	12	2	14
Stenosis ≥50% / abnormal SPECT perfusion	5	18	23
Stenosis ≥50% / normal SPECT perfusion	6	0	6
Stenosis <50% / abnormal SPECT perfusion	2	1	3
Total	25	21	46

Table 5.5
Agreement Between SPECT and CMR in Four Categories
Only grafts with available CFVR (n = 46) were included. Abbreviations as in Table 5.4

Relation between SPECT Perfusion and CMR
Grafts for which CFVR was not available (n = 11) were discarded. In 18 of the 20 grafts (90%) with normal perfusion on SPECT, CFVR was preserved (Table 5.4). Conversely, in 19 of 26 grafts (69%) with abnormal perfusion on SPECT, CFVR was reduced. Accordingly, SPECT and CMR provided similar information in 37 of 46 grafts (80%; κ = 0.61), illustrating a good agreement between SPECT and CMR ($p<0.001$).
The relation between SPECT and CMR in the four categories (see Statistical Analysis section) is depicted in Table 5.5. Grafts (n = 14) with a stenosis <50% and normal perfusion on SPECT had normal CFVR in 86%; 78% of grafts (n = 23) with a stenosis ≥50% and abnormal perfusion had reduced CFVR. Grafts with a stenosis ≥50% and normal perfusion, indicating no hemodynamic significance of the stenosis, also had normal CFVR in 100%. Finally, 33% of grafts with a stenosis <50% and abnormal perfusion (suggesting microvascular disease) also had reduced CFVR.

Influence of Scar Tissue
According to the SPECT results, scar tissue was present in the perfused territory of 8 of 46 grafts with available CFVR. When the analysis was restricted to grafts without scar tissue on SPECT, the agreement between SPECT and CMR improved to 84% (32 of 38 grafts; κ = 0.68).

Discussion
In the present study a head-to-head comparison between SPECT and CMR to evaluate the hemodynamic significance of angiographic findings in bypass grafts was performed. Similar results of SPECT perfusion and CFVR assessed by CMR were demonstrated in 80% of grafts (κ = 0.61), indicating that both noninvasive approaches provide similar information concerning the hemodynamic significance of the lesions detected invasively. Integration of an invasive and a noninvasive approach may allow optimal characterization of lesions.

Characterization of Angiographic Lesions by SPECT

SPECT perfusion imaging is a well-established technique to evaluate ischemic heart disease by assessing regional perfusion. A wealth of data is present demonstrating excellent sensitivities and specificities of (gated) SPECT to detect stenoses in native coronary arteries using coronary angiography as the gold standard (5;14). Less data are available in patients who underwent bypass surgery. A sensitivity of 80% with a specificity of 87% for the detection of >50% bypass graft stenosis has been reported (6). However, the hemodynamic significance of an angiographic stenosis cannot be determined on the coronary angiogram alone (1;2). A different approach is to use functional testing to further characterize the hemodynamic significance of an angiographic lesion. Chamuleau et al. (18) used this concept to further characterize intermediate stenoses (40% to 70%) in native coronary arteries by SPECT and by invasively acquired CFVR and used the results of the functional testing for deferral of a percutaneous coronary intervention in 191 patients. Safe deferral was demonstrated, when CFVR was ≥2.0 (event rate 6%). Both CFVR and SPECT were predictive of subsequent cardiac events. In the present study, SPECT was used to characterize angiographic findings into four categories: 1) both tests show normal results (n = 18); 2) both tests show abnormal results (n = 27); 3) discordance: angiographic significant stenosis but normal SPECT results, implying no hemodynamic consequence of the lesion (n = 7); and 4) discordance: no stenosis, but perfusion defects on SPECT, implying microvascular disease (n = 5).

Agreement between SPECT and CMR

It was previously demonstrated that SPECT perfusion imaging agreed well with CFVR established during cardiac catheterization using the Doppler guide wire. An agreement of 76% between SPECT perfusion and invasively acquired CFVR was demonstrated in patients with two-vessel coronary artery disease (17).

CMR with flow velocity mapping is a new noninvasive technique to assess CFVR, and evaluate the functional significance of a stenosis. Recently, the value of CMR with velocity mapping in the detection of stenoses in bypass grafts and recipient vessels was demonstrated. A sensitivity of 94% with a specificity of 63% for the detection of angiographically significant stenoses in single vein grafts has been reported (8). In another study, CMR with velocity mapping yielded a sensitivity and specificity of 78% and 80% for detecting vein grafts with a significant stenosis (19).

In the present study, agreement between SPECT perfusion imaging and CFVR acquired by CMR was assessed, showing both diagnostic tests to agree well in the identification of the hemodynamic significance of a stenosis in bypass grafts. In the aforementioned four categories of functional characterization of angiographic lesions, the agreement of SPECT and CMR results was evaluated. When angiography showed a nonsignificant (<50%) stenosis and SPECT showed normal perfusion, the agreement with CMR was good. Also, when angiography showed a significant stenosis and SPECT showed abnormal perfusion, the majority of lesions had reduced CFVR on CMR. Most importantly, 100% of the lesions with a significant stenosis on angiography but normal perfusion on SPECT (indicating no hemodynamic significance) had preserved CFVR on CMR, underscoring the capability of CMR with flow velocity mapping to accurately characterize angiographic lesions. The

category without a significant stenosis on angiography and abnormal SPECT, suggesting microvascular disease, contained few grafts. To draw any conclusions on this particular group, a larger sample size is needed.

Influence of Scar Tissue

A prior myocardial infarction, as evidenced by scar tissue on SPECT perfusion imaging, is known to affect CFVR (20;21). The extent of infarcted myocardium is an important factor in the impairment of CFVR. Conversely, when a graft is placed on a partially infarcted area, it can still display a preserved CFVR. Accordingly, when grafts with scar tissue in their perfused territory were eliminated from the analyses in the present study, agreement of SPECT and CFVR increased to 84%.

Study Limitations

Several limitations of the study need to be addressed. First, the current study did not investigate the safety of deferral of patients with significant stenoses in bypass grafts when negative test results were demonstrated by SPECT or CMR.

Full CMR examination with baseline and stress velocity mapping could not be completed in 11 grafts. In 10 grafts this was due either to minor adverse reactions to adenosine or a short period of time available for research in between the standard scanning procedures; only in one graft was it technically unfeasible to acquire CFVR.

Both exercise-induced and adenosine-induced stressors were used at SPECT imaging. However, previous studies with thallium-201 or technetium-99m tetrofosmin SPECT demonstrated comparable accuracies for both stressors to detect coronary artery disease (22;23). In the current study, exercise-induced and adenosine-induced stressors were equally distributed in the four distinguished categories and provided no source of disagreement between SPECT and CMR results.

In the present study sequential stenoses within a graft were not separately investigated. The most severe graft stenosis was considered the most flow-limiting lesion. Additional research is required to evaluate the influence of sequential stenoses in bypass grafts on SPECT perfusion imaging and CMR.

Our sample size is small. The category of grafts with a stenosis <50% and abnormal perfusion contained three grafts, which is inadequate to formulate a conclusion. Differences between groups based on specific disease categories could not be assessed.

In the current study multiple grafts in a single patient were investigated. A possible correlation of these grafts was not taken into account in the analysis.

CONCLUSIONS

The integration of anatomical and functional information obtained with angiography and SPECT, respectively, allows precise characterization of lesions. Head-to-head comparison showed good agreement between SPECT and CMR for this purpose in bypass grafts. CMR may offer an alternative method to SPECT for characterization of angiographic lesions.

REFERENCES

1. White CW, Wright CB, Doty DB et al. Does visual interpretation of the coronary arteriogram predict the physiologic importance of a coronary stenosis? N Engl J Med 1984;310:819-24.
2. Topol EJ, Nissen SE. Our preoccupation with coronary luminology. The dissociation between clinical and angiographic findings in ischemic heart disease. Circulation 1995;92:2333-42.
3. Ofili EO, Labovitz AJ, Kern MJ. Coronary flow velocity dynamics in normal and diseased arteries. Am J Cardiol 1993;71:3d-9d.
4. White CW. Clinical applications of Doppler coronary flow reserve measurements. Am J Cardiol 1993;71:10d-6d.
5. Mahmarian JJ, Boyce TM, Goldberg RK, Cocanougher MK, Roberts R, Verani MS. Quantitative exercise thallium-201 single photon emission computed tomography for the enhanced diagnosis of ischemic heart disease. J Am Coll Cardiol 1990;15:318-29.
6. Lakkis NM, Mahmarian JJ, Verani MS. Exercise thallium-201 single photon emission computed tomography for evaluation of coronary artery bypass graft patency. Am J Cardiol 1995;76:107-11.
7. Nagel E, Thouet T, Klein C et al. Noninvasive determination of coronary blood flow velocity with cardiovascular magnetic resonance in patients after stent deployment. Circulation 2003;107:1738-43.
8. Langerak SE, Vliegen HW, Jukema JW et al. Value of magnetic resonance imaging for the noninvasive detection of stenosis in coronary artery bypass grafts and recipient coronary arteries. Circulation 2003;107:1502-8.
9. Reiber JH, van der Zwet PM, Koning G et al. Accuracy and precision of quantitative digital coronary arteriography: observer-, short-, and medium-term variabilities. Cathet Cardiovasc Diagn 1993;28:187-98.
10. Reiber JH, Jukema W, van Boven A, van Houdt RM, Lie KI, Bruschke AV. Catheter sizes for quantitative coronary arteriography. Cathet Cardiovasc Diagn 1994;33:153-5.
11. Berman DS, Kiat HS, Van Train KF, Germano G, Maddahi J, Friedman JD. Myocardial perfusion imaging with technetium-99m-sestamibi: comparative analysis of available imaging protocols. J Nucl Med 1994;35:681-8.
12. Germano G, Berman DS. Quantitative gated SPECT. J Nucl Med 2001;42:528-9.
13. Cerqueira MD, Weissman NJ, Dilsizian V et al. Standardized myocardial segmentation and nomenclature for tomographic imaging of the heart: a statement for healthcare professionals from the Cardiac Imaging Committee of the Council on Clinical Cardiology of the American Heart Association. Circulation 2002;105:539-42.
14. Elhendy A, Bax JJ, Poldermans D. Dobutamine stress myocardial perfusion imaging in coronary artery disease. J Nucl Med 2002;43:1634-46.
15. Langerak SE, Kunz P, Vliegen HW et al. Improved MR flow mapping in coronary artery bypass grafts during adenosine-induced stress. Radiology 2001;218:540-7.
16. Langerak SE, Kunz P, Vliegen HW et al. Magnetic resonance flow mapping in coronary artery bypass grafts: a validation study with Doppler flow measurements. Radiology 2002;222:127-35.
17. Chamuleau SA, Meuwissen M, Eck-Smit BL et al. Fractional flow reserve, absolute and relative coronary blood flow velocity reserve in relation to the results of technetium-99m sestamibi single-photon emission computed tomography in patients with two-vessel coronary artery disease. J Am Coll Cardiol 2001;37:1316-22.
18. Chamuleau SA, Tio RA, de Cock CC et al. Prognostic value of coronary blood flow velocity and myocardial perfusion in intermediate coronary narrowings and multivessel disease. J Am Coll Cardiol 2002;39:852-8.
19. Bedaux WL, Hofman MB, Vyt SL, Bronzwaer JG, Visser CA, van Rossum AC. Assessment of coronary artery bypass graft disease using cardiovascular magnetic resonance determination of flow reserve. J Am Coll Cardiol 2002;40:1848-55.
20. Klein LW, Agarwal JB, Schneider RM, Hermann G, Weintraub WS, Helfant RH. Effects of previous myocardial infarction on measurements of reactive hyperemia and the coronary vascular reserve. J Am Coll Cardiol 1986;8:357-63.
21. Uren NG, Crake T, Lefroy DC, de Silva R, Davies GJ, Maseri A. Reduced coronary vasodilator function in infarcted and normal myocardium after myocardial infarction. N Engl J Med 1994;331:222-7.
22. Nguyen T, Heo J, Ogilby JD, Iskandrian AS. Single photon emission computed tomography with thallium-201 during adenosine-induced coronary hyperemia: correlation with coronary arteriography, exercise thallium imaging and two-dimensional echocardiography. J Am Coll Cardiol 1990;16:1375-83.
23. Levine MG, Ahlberg AW, Mann A et al. Comparison of exercise, dipyridamole, adenosine, and dobutamine stress with the use of Tc-99m tetrofosmin tomographic imaging. J Nucl Cardiol 1999;6:389-96.

CHAPTER 6

Validation of a high-resolution, phase contrast cardiovascular magnetic resonance sequence for evaluation of flow in coronary artery bypass grafts

Liesbeth P. Salm
Joanne D. Schuijf
Hildo J. Lamb
Jeroen J. Bax
Hubert W. Vliegen
J.Wouter Jukema
Ernst E. van der Wall
Albert de Roos
Joost Doornbos

Accepted for publication in J Cardiovasc Magn Reson

ABSTRACT
The aim was to validate a magnetic resonance high-resolution, phase-contrast sequence for quantifying flow in small and large vessels, and to demonstrate its feasibility to measure flow in coronary artery bypass grafts.
A breathhold, echo planar imaging (EPI) sequence was developed and validated in a flow phantom using a fast field echo (FFE) sequence as reference. In 17 volunteers aortic flow was measured using both sequences. In 5 patients flow in the left internal mammary artery (LIMA) and aorta was measured at rest and during adenosine stress, and coronary flow reserve (CFR) was calculated; in 7 patients vein graft flow velocity was measured.
In the flow phantom measurements, the EPI sequence yielded an excellent correlation with the FFE sequence ($r=0.99$; $p<0.001$ for all parameters). In healthy volunteers, aortic volume flow correlated well ($r=0.88$; $p<0.01$), with a minor overestimation. It was feasible to measure flow velocity in the LIMA and vein grafts of the 12 patients.
The high-resolution, breathhold MR velocity-encoded sequence correlated well with a free-breathing, FFE sequence in a flow phantom and in the aortae of healthy volunteers. Using the EPI sequence, it is feasible to measure flow velocity in both LIMA and vein grafts, and in the aorta.

INTRODUCTION

Coronary artery bypass grafting (CABG) is one of the therapeutic options in obstructive coronary artery disease. Over time, atherosclerosis may progress in these bypass grafts and graft stenosis may develop, requiring invasive angiography to assess the severity of the lesions. However, the hemodynamic consequences of the stenotic lesions cannot be assessed from angiography (1;2). Measurement of flow velocity and flow reserve by phase-contrast velocity-encoded cardiovascular magnetic resonance (CMR) has recently been demonstrated for the evaluation of vein graft disease (3;4). Imaging of arterial grafts remains challenging because of the small luminal diameter of the internal mammary arteries, and metal clip artefacts. Earlier studies demonstrated the feasibility to measure flow in left internal mammary artery (LIMA) grafts by free-breathing and breathhold CMR sequences, but these sequences generated a limited spatial and temporal resolution (5-7). The aim of the present study was to validate a recently developed velocity-encoded CMR sequence to measure flow velocity in small and large vessels, and to demonstrate its feasibility to measure flow in coronary artery bypass grafts.

METHODS

In Vitro Validation

In order to validate the velocity-encoded CMR sequence in small vessels, a calibrated flow simulator (UHDC flow simulator, Shelley Medical Imaging Technologies, London, Ontario, Canada) was used to create biphasic flow velocity patterns, such as observed in nonstenotic bypass grafts and coronary arteries, in a MRI compatible phantom. The design of the pump and its value in application for MR flow studies were described before (8;9). The simulator provided an ECG-signal to allow triggering by the MR-system. The phantom consisted of a cylindrical container filled with water, with a 4-mm-diameter glass tube running through the middle. The glass tube was connected to the flow simulator by two hoses, and filled with a blood-mimicking solution. The phantom was positioned in the bore of a 1.5 Tesla MRI scanner (Gyroscan ACS/NT, Philips Medical Systems, Best, the Netherlands) with Powertrak-6000 gradients (gradient strength 25mT/m, slow rate 100 T/m/s) and commercially available cardiac software (release 9). Scout scans of the glass tube were made, and a plane perpendicular to the tube was planned for the velocity measurements. A multishot echo planar imaging (EPI) velocity-encoded sequence yielded a field of view (FOV) of 60x150 mm with an acquisition matrix of 55x144 voxels. Per acquisition 55 k-lines were scanned. Multi-shot gradient echo EPI was performed by acquisition of 5 EPI-readouts twice per frame (Figure 6.1). For each time frame in the cardiac cycle a velocity-sensitive and a velocity-insensitive image was acquired, and for each image signals were averaged (NEx=2), resulting in an acquisition time of 22 heartbeats. Number of phases to be acquired during the cardiac cycle was set to 30 by retrospective ECG-gating. The repetition time (TR), defined as the time to acquire 5 k-lines after one RF pulse, was 15 ms, rendering a temporal resolution of 30 ms (2xTR). Additional scan parameters were: echo time (TE) of 7 ms, in-plane resolution of 1.0x1.0 mm, interpolated to 0.29x0.29 mm by zero padding, slice thickness of 6 mm, flip angle of 40°, velocity encoding of 50-150 cm/s.

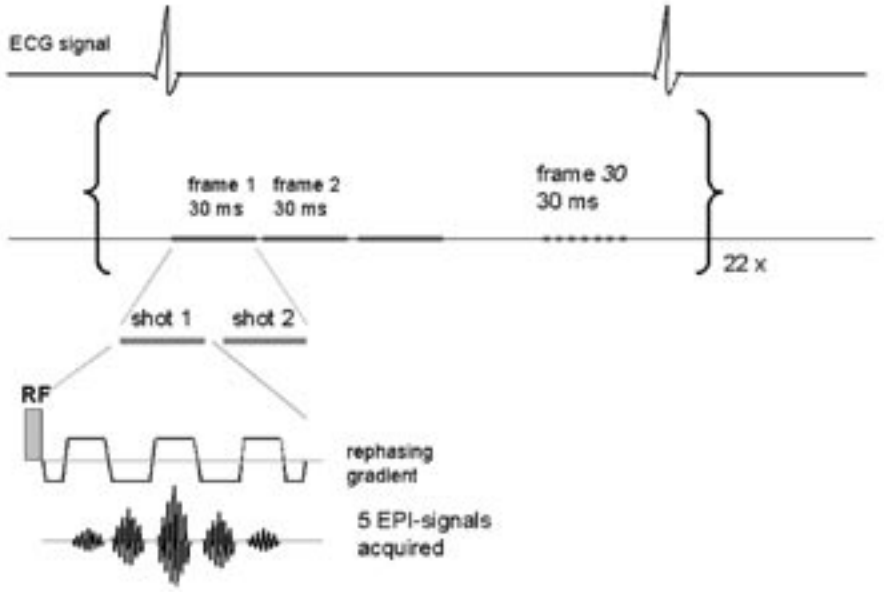

Figure 6.1.
Schematic presentation of the EPI sequence. Per heart beat 30 frames could be acquired, each consisting of two shots, each representing one radiofrequency pulse and 5 EPI-readouts. ECG-signal was recorded simultaneously for retrospective ECG-triggering.

Stepwise increasing velocities in a biphasic pattern resembling bypass graft flow were implemented in the simulator and subsequently imaged. The series of velocity measurements was repeated using a free-breathing fast field echo (FFE) sequence, previously validated at our institution (10), using the following parameters: TR/ TE 5.5/3.5, FOV of 370 mm, RFOV 60%, acquisition matrix 77x128 voxels, temporal resolution of 30 ms, pixel size of 3x3 mm, interpolated to 1.45x1.45 mm, slice thickness of 6 mm, flip angle of 20°, retrospective ECG gating, scan duration of 256 heart beats. For determination of interstudy variability the velocity measurements were repeated using the EPI sequence.

Image analysis
Velocity image acquisition consisted of paired modulus and phase images. For the velocity analysis a region of interest (ROI) of 1 pixel (2.1 mm^2) was placed in the center of the glass tube in each phase image for the free-breathing sequence, using FLOW software (version 4.0.4, Medis, Leiden, the Netherlands). Owing to the improved spatial resolution of the EPI sequence, 24 pixels (2.02 mm^2) were selected in the center of the tube in order to compare the two sequences. The peak velocity was defined as the mean velocity in the ROI for each time frame. The average peak velocity (APV; cm/s) was then defined as the average velocity measured in the ROIs over the cardiac cycle. Systolic peak velocity (SPV; cm/s) and diastolic peak velocity (DPV; cm/s) were defined as the maximal peak velocity during the first and second peak, respectively.

In Vivo Validation

In 17 healthy volunteers aortic flow was measured using the EPI and FFE sequence. A scout scan in three planes of the thorax was made. Aortic flow was acquired in a transverse plane planned through the ascending aorta by both free-breathing FFE and EPI sequence. For this measurement FOV was increased to 370 mm in the EPI sequence, resulting in a voxel size of 2.6x2.6 mm, interpolated to 0.7x0.7 mm. All breathholds were initiated at end-expiration in order to avoid aortic flow changes due to high intrathoracic pressures (11).

Feasibility Study

In 10 healthy volunteers LIMA and aortic flow were measured using the EPI sequence. Two surface coils were used, one placed at the proximal native LIMA and one placed at the center of the thorax to measure aortic flow. First, a scout scan in three planes of the thorax was made. A transversal balanced turbo field echo (bTFE) survey scan of the proximal part of the LIMA was made to identify the arterial anatomy. The proximal portion of the LIMA was selected in order to avoid artefacts derived from metal clips in patients with LIMA grafts. The proximal part of the LIMA was scanned in plane in two perpendicular planes in order to plan a third plane orthogonally. The EPI sequence was applied to measure velocity in a single breathhold. The sequence validated in the phantom study was used. Then, aortic flow was acquired as described in the previous section.

In 5 randomly selected patients with LIMA grafts, who underwent coronary angiography because of recurrent chest pain, aortic and proximal LIMA graft flow was measured in the same manner. After acquiring the baseline aortic and LIMA flow, adenosine was administered intravenously in dosage of 140 µg/kg/min in order to achieve maximal hyperemia (12). Aortic and LIMA flow velocity scans were repeated during adenosine stress.

In 7 randomly selected patients with vein grafts, baseline flow velocity was measured. By means of the bTFE survey scan, vein grafts were visualized at the level of the ascending aorta. On two perpendicular survey images showing the graft in plane, a plane was planned perpendicular to the graft and velocity was obtained using the EPI sequence. Beforehand, the nature of the study was fully explained to the patients, and all patients gave informed consent. The study was approved by the medical ethics committee of our institution.

All patients underwent coronary angiography because of recurrent chest pain by a standard procedure prior to the CMR examination. The MR operators were blinded to the results of invasive angiography. Angiograms were evaluated by an experienced cardiologist for potential stenoses in the examined bypass grafts and recipient vessels. If more than one stenosis was present in either bypass graft or recipient vessel, the most severe stenosis was taken into account.

Image analysis

For the image analysis aortic and LIMA contours were traced by automatic contour detection, using FLOW 4.0.4 (Medis, Leiden, the Netherlands) (13;14). In the flow rate-

versus-time curves the area-under-the-curve was multiplied with the heart rate to obtain aortic and LIMA volume flow (ml/min). The maximal flow rate at systole and diastole were defined as the systolic peak flow (SPF; ml/s) and diastolic peak flow (DPF; ml/s), respectively. The diastolic-to-systolic flow ratio (DSFR) was defined as the ratio of DPF and SPF. The ratio of hyperemic to baseline volume flow was defined as coronary flow reserve (CFR). As values of LIMA flow are known to vary widely between individuals (5), LIMA flow was also expressed as a percentage of the aortic flow at rest and during stress.
For vein grafts it has been demonstrated previously that the accuracy of volume flow analysis and peak velocity analysis is similar (15). Therefore, only peak velocity analysis was performed, in which 4 pixels at the center of the vessel were selected and defined as the peak velocity for every phase in the cardiac cycle. APV, SPV, and DPV were derived from the velocity-versus-time curves, such as described for the flow simulator.

Statistical Analysis
Parameters were expressed as mean ± SD. The velocity parameters, measured by the flow phantom, and the flow parameters, measured in healthy volunteers, were compared using Pearson correlation and Bland-Altman analysis. Interstudy variability was expressed as correlation and calculated as the mean difference divided by the mean of the two measurements. Baseline and stress values in LIMA grafts were compared using a paired Student t-test. A p-value <0.05 was considered significant.

RESULTS
In Vitro Validation
When comparing the FFE and EPI sequence with the flow simulator, an excellent correlation was demonstrated for APV ($y=1.06x-2.6$; $r=0.99$; $p<0.001$), as for SPV and DPV ($y=1.05x-2.1$; $r=0.99$ and $y=1.05x-1.3$; $r=0.99$; $p<0.001$). In the Bland-Altman analysis, the mean differences (95% limits of agreement) were for APV –1.26 cm/s (-2.89 to 0.36), for SPV –1.05 cm/s (-2.64 to 0.55), and for DPV 0.19 cm/s (-2.84 to 3.23), indicating good agreement. A good reproducibility of the EPI sequence was demonstrated, expressed by the following correlations: $y=x+0.2$ for APV, $y=x-0.5$ for SPV and $y=x+2.2$ for DPV ($r=0.99$ and $p<0.001$ for all correlations). Interstudy variabilities were –0.2% for APV, -2.4% for SPV, and 5.5% for DPV.

In Vivo Validation
In 17 healthy volunteers (mean age 30 years, range 20 to 60, male/female 7/10) aortic flow was measured by free-breathing FFE and breathhold EPI sequence. For 2 volunteers, image quality was insufficient due to inability to sustain the obligatory breathhold, and these individuals were excluded from further analysis. A good correlation was shown for the FFE and EPI sequences (Figure 6.2). The regression equation, $y=1.2x-301$, demonstrated a slight overestimation of volume flow, when the EPI sequence was used ($r=0.88$; $p<0.01$). The EPI sequence correlated well with the FFE sequence for SPF ($y=1.04x-21$; $r=0.94$; $p<0.001$). Bland-Altman analysis illustrated the overestimation of aortic flow with the EPI sequence with a mean difference of 560 ml/min (95% limits of agreement –872 to 1992). For SPF mean difference was –4.5 ml/s (95% limits of agreement –75.0 to 66.0).

Feasibility Study

In 10 volunteers native LIMA flow was adequately measured using the EPI sequence. Mean LIMA flow was 66.5±22.3 ml/min (range 32.0 to 106.2), mean SPF was 5.2±1.4 ml/s (range 3.1 to 7.3), and mean aortic flow was 5365±1302 ml/min (range 3331 to 7493). When LIMA flow was expressed as percentage of aortic flow, the mean percentage was 1.2±0.4% (range 0.6 to 2.0).

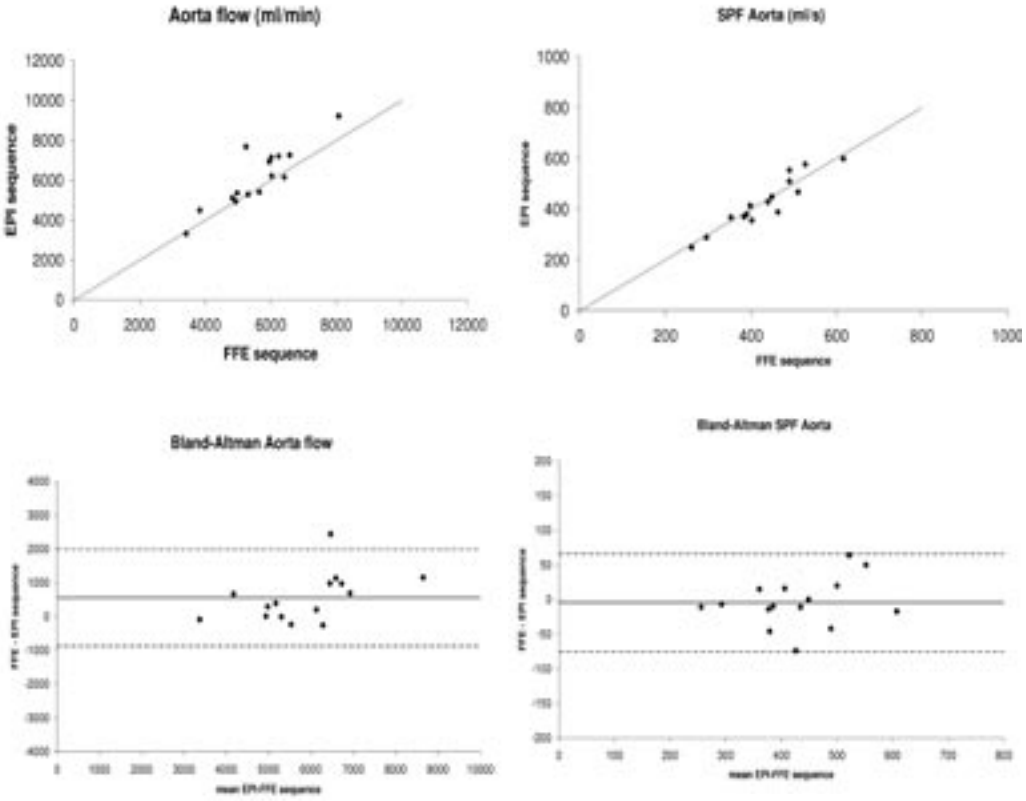

Figure 6.2.

Correlation and Bland-Altman analysis of the comparison of FFE and EPI sequence for aortic flow in healthy volunteers. Identity lines (y=x) are shown in the correlation plots in gray. In the Bland-Altman plots, solid lines represent the mean, and dotted lines represent the 95% limits of agreement.

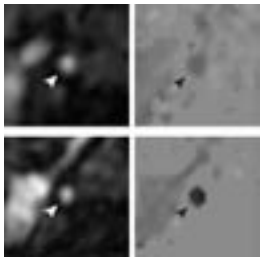

Figure 6.3.
Modulus (left) and phase (right) images of a sequential LIMA graft (arrowheads) to anterolateral and obtuse marginal branch in diastole, acquired using the EPI sequence. Top images represent baseline flow velocity and bottom images flow velocity during adenosine stress.

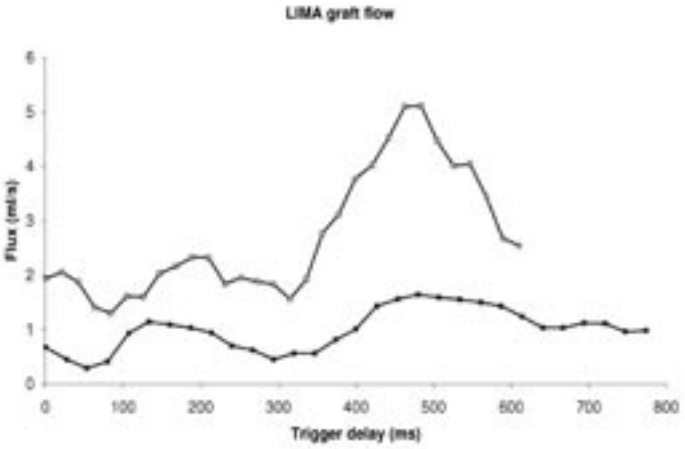

Figure 6.4.
Flow curve of the LIMA graft depicted in Figure 3. Black squares represent the flow rate at baseline. Open squares characterize adenosine stress flow rate. LIMA volume flow was 58.3 ml/min at baseline and 159.5 ml/min during adenosine stress, resulting in a CFR of 2.7.

In 5 male patients (mean age 56 years, range 43 to 73) with 5 LIMA grafts, proximal LIMA graft and aortic flow were successfully measured at rest and during adenosine stress, see Figure 6.3. Grafts were anastomosed to the left anterior descending (LAD) artery (n=1), first diagonal branch and LAD (n=2), anterolateral branch and obtuse marginal (OM) branch (n=1). In one patient the LIMA was anastomosed to the first diagonal branch and LAD, and a free right IMA was anastomosed from the LIMA to the OM and posterior descending branch. Mean interval between bypass surgery and CMR examination was 48 months (range 8 to 104). A biphasic flow pattern was obtained in all grafts (Figure 6.4). The measured flow parameters are summarized in Table 6.1. All LIMA grafts were patent at coronary angiography. Stenoses in LIMA grafts or recipient vessels distal from the anastomosis were not observed.

In 7 male patients (mean age 67 years, range 57 to 75 years) flow velocity in 9 vein grafts at rest was obtained (mean time interval after CABG 9 years, range 5 to 15). Single vein grafts perfused the LAD (n=3), OM (n=2), or posterolateral branch (n=1). Sequential vein grafts were anastomosed to OM and posterior descending branch (n=3). The velocity parameters are presented in Figure 6.5. At coronary angiography 7 grafts had no significant stenosis (≥50%), in 2 single grafts a diameter stenosis of 80% was observed. In concordance with previous studies (3;16), the velocity parameters of single vein grafts were lower than sequential vein graft values. Two grafts with significant stenosis showed low velocity values at rest. Using the EPI sequence it is feasible to measure flow velocity in both arterial and vein grafts.

Discussion

In this study validation of a high-resolution, phase contrast CMR sequence was described. This sequence correlated well with a previously validated FFE sequence in a flow phantom and for aortic flow measured in healthy volunteers. In addition, the feasibility to measure LIMA and vein graft flow velocity using the proposed sequence was demonstrated.

In Vitro and in Vivo Validation

MR phase contrast imaging has succesfully been used before to measure flow velocity in arterial and vein bypass grafts (3-7). In the current study an improved phase contrast EPI sequence was validated in vitro and in vivo against an established FFE sequence (10), and the feasibility to measure bypass graft flow velocity was demonstrated. The EPI sequence used segmented filling of k-space (factor 5), and had an in-plane resolution of 1.0x1.0 mm, interpolated to 0.29x0.29 mm, with a temporal resolution of 30 ms. The measurements were obtained at breathholding, and with the use of retrospective ECG-gating, data could be collected during the full cardiac cycle.

	Baseline	**Stress**
LIMA flow (ml/min)	37.1±13.9 (22.3-58.3)	101.1±45.6 (39.7-159.5) *
SPF LIMA (ml/s)	1.28±0.49 (0.70-2.03)	2.88±0.72 (2.33-4.05) *
DPF LIMA (ml/s)	1.03±0.42 (0.54-1.64)	2.79±1.55 (0.96-5.11) *
DSFR	0.89±0.44 (0.38-1.44)	1.03±0.70 (0.31-2.19)
Aortic flow (ml/min)	5142±901 (4116-6185)	6275±1208 (4237-7116)
SPF aorta (ml/s)	406±51 (334-473)	442±59 (397-524)
LIMA/aortic flow (%)	0.71±0.17 (0.52-0.94)	1.56±0.52 (0.94-2.27) †
CFR	2.70±0.88 (1.78-4.14)	

Table 6.1.
LIMA graft and aortic flow
*Results are presented as mean ± SD (range). LIMA= left internal mammary artery, SPF= systolic peak flow, DPF= diastolic peak flow, DSFR= diastolic-to-systolic flow ratio, CFR= coronary flow reserve. * p<0.05, † p<0.01.*

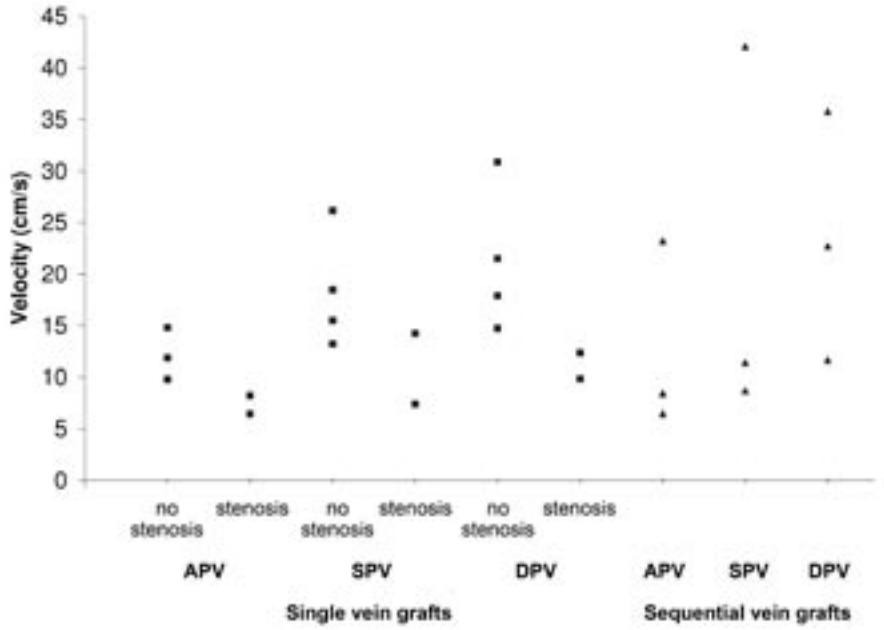

Figure 6.5.
Diagram of the velocity parameters, measured in the vein grafts. APV = average peak velocity, SPV = systolic peak velocity, DPV = diastolic peak velocity.

In comparison, spatial and temporal resolution of formerly established breathhold phase contrast sequences were 2.5x1.9 mm and 128 ms (6), 1.6x0.8 mm and 112 ms (7), 1.6x1.6 mm and 23 ms (3), and 0.9x1.5 mm and 125 ms(4), respectively. In LIMA grafts with a mean diameter of 2.42±0.45 mm (17), an improvement of 0.5 mm in in-plane spatial resolution is of important benefit. A temporal resolution of 30 ms is adequate to accurately measure the systolic and diastolic peak in peak flow velocity measurements (18). The formerly established breathhold sequences all used prospective ECG-triggering, with which the flow of late diastole may not be measured correctly. The presented sequence used retrospective gating, providing data collection throughout the whole cardiac cycle. Particularly in bypass grafts, where flow is maximal during diastole, this is an important improvement.
For validation purposes, quantitative flow velocity measurements with FFE phase contrast imaging have been shown to be accurate (19-22). An excellent agreement between the EPI sequence and the conventional sequence was demonstrated in vitro, and the sequences correlated well in vivo.
In healthy volunteers aortic volume flow showed a minor overestimation using the EPI sequence, which may be explained in part by the fact that the EPI sequence had a better spatial resolution, causing partial volume effects to be less prominent (23). Also, eddy current effects or Maxwell concomitant terms may be more prominent using an EPI

approach. These artefacts were not specifically investigated in this study. Moreover, at end-expiration left ventricle stroke volume was previously demonstrated to be higher than the average stroke volume in healthy volunteers (24). Thus, when aortic volume flow is measured over 22 heart beats in an end-expiratory breathhold, measured volume flow may be higher than averaged over 256 heart beats in normal breathing, due to low intrathoracic pressure.
The phase-contrast EPI sequence was initially developed for measuring flow velocity in bypass grafts. The results of the current study showed that this sequence may additionally be used in large arteries as part of an integrated CMR approach.

CMR Flow Velocity in Bypass Grafts

Arterial grafts

Absolute LIMA graft flow ranged considerably between patients without stenoses in the graft or recipient vessel of the graft. Standardized thresholds of the flow parameters are necessary to be able to detect flow-limiting stenoses. Ishida et al. studied volume flow by CMR in 24 LIMA grafts at rest and during dipyridamole stress in patients shortly after CABG, and the authors proposed threshold values for the detection of >70% stenosis of 35 ml/min for baseline LIMA volume flow, 1.0 for diastolic-to-systolic velocity ratio, and 1.5 for CFR (7). These parameters however are known to change over time (17;25). Langerak et al. formulated a regression model to detect ≥50% and ≥70% stenoses in vein grafts by using CMR with velocity mapping (3). Arterial grafts (n=41) were additionally investigated, but a sufficient number of stenoses to formulate a model for the identification of graft disease was lacking. Future studies are necessary to formulate a model to detect significant stenoses in arterial grafts noninvasively by velocity-encoded CMR. Such a study may be performed using the currently presented sequence.
Another application of LIMA flow measurements by CMR is assessment before and after surgical revascularization to evaluate patency of the graft. Stauder et al. (26) demonstrated the feasibility of a combined CMR protocol, including contrast-enhanced MR angiography and phase contrast flow measurements, for assessment of patency in 42 LIMA grafts. The presented CMR flow velocity sequence may also be used for this purpose.
Metal clips used in bypass graft surgery formed no obstacle in the present study, since proximal CMR measurements were performed. Metal clip artefacts did however prevent the acquisition of distal flow measurements. As CMR imaging gains acceptance as noninvasive follow-up after surgery, MR compatible clips, e.g. titanium clips, may be used at CABG in a standard fashion.

Vein grafts

Vein graft flow velocity has been studied more extensively by CMR in previous studies (3;4;27;28). Two models were described to identify diseased vein grafts yielding a sensitivity and specificity of 94% and 63%, and 78% and 80%, respectively, using velocity-encoded CMR (3;4). Measurement of flow velocity in vein grafts using this sequence was demonstrated to be feasible.

Study Limitations

In this study the results in patients are to show the feasibility of the EPI sequence to be used to measure flow velocity in bypass grafts. A future study validating this sequence to measure bypass grafts flow compared with a prospectively-triggered, breathhold sequence with similar spatial resolution is needed.

Also, artefact sensitivity of EPI was not specifically investigated. Future studies may further focus on this issue.

CONCLUSION

In conclusion, the presented velocity-encoded CMR sequence allows accurate measurements of velocity in small vessels with good reproducibility, demonstrated by means of a flow simulator. The presented sequence correlated well with a conventional sequence for measurement of aortic flow in healthy volunteers. In addition, the feasibility to quantify flow velocity in LIMA and vein grafts was demonstrated.

REFERENCES

1. Topol EJ, Nissen SE. Our preoccupation with coronary luminology. The dissociation between clinical and angiographic findings in ischemic heart disease. Circulation 1995;92:2333-42.
2. White CW, Wright CB, Doty DB et al. Does visual interpretation of the coronary arteriogram predict the physiologic importance of a coronary stenosis? N Engl J Med 1984;310:819-24.
3. Langerak SE, Vliegen HW, Jukema JW et al. Value of magnetic resonance imaging for the noninvasive detection of stenosis in coronary artery bypass grafts and recipient coronary arteries. Circulation 2003;107:1502-8.
4. Bedaux WL, Hofman MB, Vyt SL, Bronzwaer JG, Visser CA, van Rossum AC. Assessment of coronary artery bypass graft disease using cardiovascular magnetic resonance determination of flow reserve. J Am Coll Cardiol 2002;40:1848-55.
5. Debatin JF, Strong JA, Sostman HD et al. MR characterization of blood flow in native and grafted internal mammary arteries. J Magn Reson Imaging 1993;3:443-50.
6. Sakuma H, Globits S, O'Sullivan M et al. Breath-hold MR measurements of blood flow velocity in internal mammary arteries and coronary artery bypass grafts. J Magn Reson Imaging 1996;6:219-22.
7. Ishida N, Sakuma H, Cruz BP et al. Mr flow measurement in the internal mammary artery-to-coronary artery bypass graft: comparison with graft stenosis at radiographic angiography. Radiology 2001;220:441-7.
8. Frayne R, Holdsworth DW, Gowman LM et al. Computer-controlled flow simulator for MR flow studies. J Magn Reson Imaging 1992;2:605-12.
9. Holdsworth DW, Rickey DW, Drangova M, Miller DJ, Fenster A. Computer-controlled positive displacement pump for physiological flow simulation. Med Biol Eng Comput 1991;29:565-70.
10. Rebergen SA, Chin JG, Ottenkamp J, van der Wall EE, de Roos A. Pulmonary regurgitation in the late postoperative follow-up of tetralogy of Fallot. Volumetric quantitation by nuclear magnetic resonance velocity mapping. Circulation 1993;88:2257-66.
11. Sakuma H, Kawada N, Kubo H et al. Effect of breath holding on blood flow measurement using fast velocity encoded cine MRI. Magn Reson Med 2001;45:346-8.
12. Wilson RF, Wyche K, Christensen BV, Zimmer S, Laxson DD. Effects of adenosine on human coronary arterial circulation. Circulation 1990;82:1595-606.
13. van der Geest RJ, Niezen RA, van der Wall EE, de Roos A, Reiber JH. Automated measurement of volume flow in the ascending aorta using MR velocity maps: evaluation of inter- and intraobserver variability in healthy volunteers. J Comput Assist Tomogr 1998;22:904-11.
14. van der Geest RJ, Reiber JH. Quantification in cardiac MRI. J Magn Reson Imaging 1999;10:602-8.
15. Salm LP, Langerak SE, Vliegen HW et al. Blood flow in coronary artery bypass vein grafts: volume versus velocity at cardiovascular MR imaging. Radiology 2004;232:915-20.
16. Langerak SE, Vliegen HW, Jukema JW et al. Vein graft function improvement after percutaneous intervention: evaluation with MR flow mapping. Radiology 2003;228:834-41.
17. Gurne O, Chenu P, Polidori C et al. Functional evaluation of internal mammary artery bypass grafts in the early and late postoperative periods. J Am Coll Cardiol 1995;25:1120-8.
18. Lotz J, Meier C, Leppert A, Galanski M. Cardiovascular flow measurement with phase-contrast MR imaging: basic facts and implementation. Radiographics 2002;22:651-71.
19. Boesiger P, Maier SE, Kecheng L, Scheidegger MB, Meier D. Visualization and quantification of the human blood flow by magnetic resonance imaging. J Biomech 1992;25:55-67.
20. Meier D, Maier S, Boesiger P. Quantitative flow measurements on phantoms and on blood vessels with MR. Magn Reson Med 1988;8:25-34.
21. Firmin DN, Nayler GL, Kilner PJ, Longmore DB. The application of phase shifts in NMR for flow measurement. Magn Reson Med 1990;14:230-41.
22. Hoogeveen RM, Bakker CJ, Viergever MA. MR phase-contrast flow measurement with limited spatial resolution in small vessels: value of model-based image analysis. Magn Reson Med 1999;41:520-8.
23. Tang C, Blatter DD, Parker DL. Accuracy of phase-contrast flow measurements in the presence of partial-volume effects. J Magn Reson Imaging 1993;3:377-85.
24. van den Hout RJ, Lamb HJ, van den Aardweg JG et al. Real-time MR imaging of aortic flow: influence of breathing on left ventricular stroke volume in chronic obstructive pulmonary disease. Radiology 2003;229:513-9.
25. Akasaka T, Yoshikawa J, Yoshida K et al. Flow capacity of internal mammary artery grafts: early restriction and later improvement assessed by Doppler guide wire. Comparison with saphenous vein grafts. J Am Coll Cardiol 1995;25:640-7.
26. Stauder NI, Scheule AM, Hahn U et al. Perioperative monitoring of flow and patency in native and grafted internal mammary arteries using a combined MR protocol. Br J Radiol 2005;78:292-8.

27. Galjee MA, van Rossum AC, Doesburg T, van Eenige MJ, Visser CA. Value of magnetic resonance imaging in assessing patency and function of coronary artery bypass grafts. An angiographically controlled study. Circulation 1996;93:660-6.
28. Hoogendoorn LI, Pattynama PM, Buis B, van der Geest RJ, van der Wall EE, de Roos A. Noninvasive evaluation of aortocoronary bypass grafts with magnetic resonance flow mapping. Am J Cardiol 1995;75:845-8.

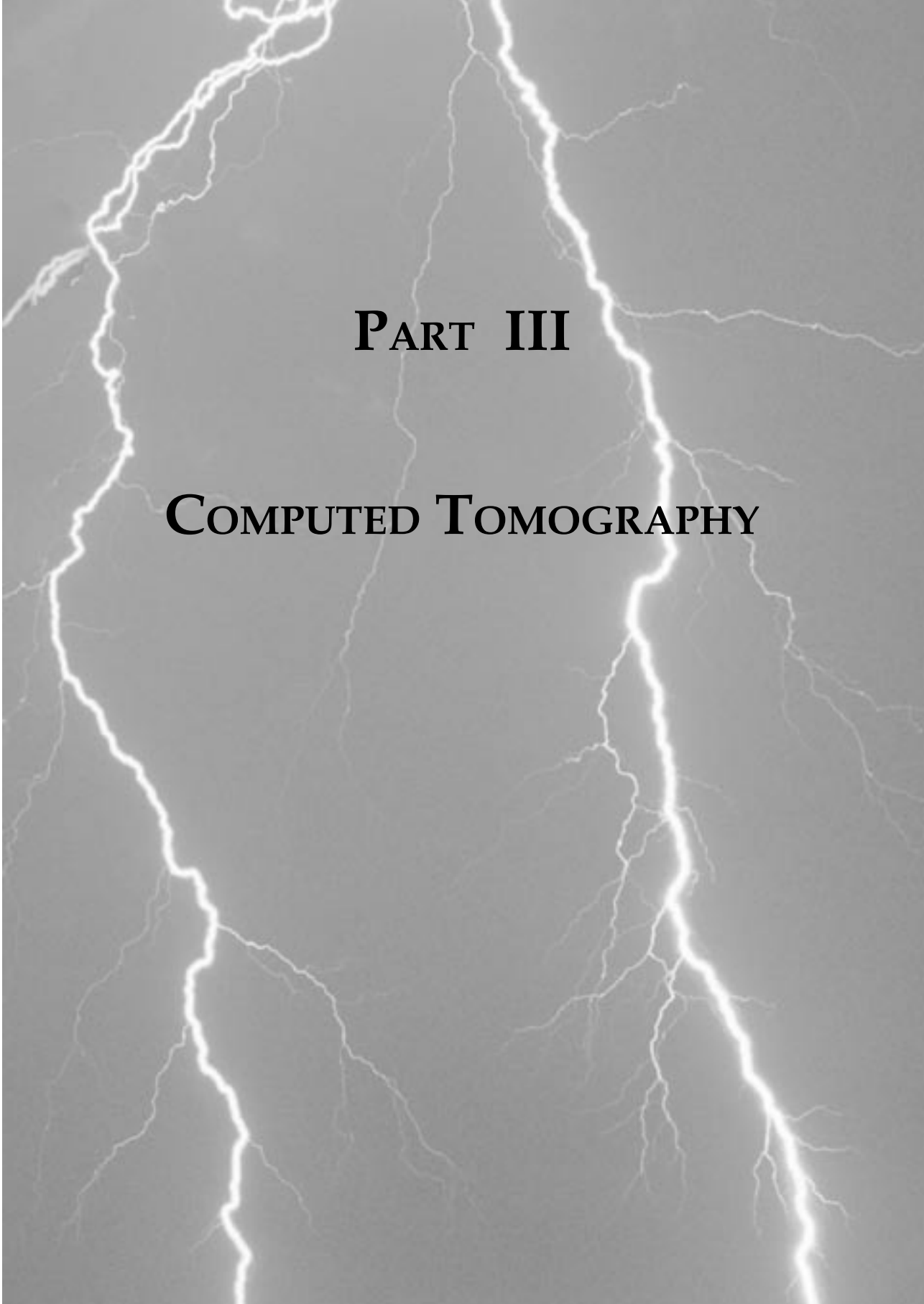

Part III

Computed Tomography

CHAPTER 7

Comprehensive assessment of patients after coronary artery bypass grafting by 16-detector row computed tomography

Liesbeth P. Salm
Jeroen J. Bax
J. Wouter Jukema
Joanne D. Schuijf
Hubert W. Vliegen
Hildo J. Lamb
Ernst E. van der Wall
Albert de Roos

Am Heart J 2005; 150, 4, 775-781

ABSTRACT

Background: Multi-detector row computed tomography (MDCT) is a versatile modality to evaluate stenoses in native coronary arteries and bypass grafts. Acquired MDCT data can additionally be used to assess left ventricular ejection fraction (LVEF). The purpose was to use MDCT for the assessment of bypass graft and coronary artery disease combined with evaluation of LVEF.

Methods: Twenty-five patients underwent 16-detector-row CT examination and coronary angiography. Bypass grafts and nongrafted coronary artery segments at MDCT were evaluated on eligibility, patency and ≥50% stenosis. The MDCT data set was used to calculate LVEF and was divided into patients with no/subendocardial/transmural myocardial infarctions (MIs).

Results: Ninety vessels were evaluated: 14 arterial grafts/53 vein grafts/23 nongrafted vessels. Of 225 segments, 17 were ineligible for evaluation because of metal clips. With MDCT, patency in segments of arterial grafts/vein grafts/nongrafted vessels could be evaluated with high accuracy in 100%/100%/97% of segments. In arterial grafts stenoses ≥50% did not occur at angiography, which was for all eligible segments correctly diagnosed at MDCT. Stenosis ≥50% could be correctly detected by MDCT with a sensitivity/specificity of 100%/94% for vein grafts, and 100%/89% for nongrafted vessels. Negative predictive value was 100% for vein grafts and nongrafted vessels. In patients with transmural MI, MDCT revealed a significant lower LVEF as compared with patients without or with subendocardial MI ($p<0.05$).

Conclusion: Comprehensive assessment of bypass grafts, nongrafted vessels, and LVEF is feasible with MDCT. Owing to the high negative predictive value this noninvasive approach may be used as gatekeeper before coronary angiography.

Introduction

Recently, multidetector-row computed tomography (MDCT) has gained rapid acceptance as a diagnostic cardiac imaging modality, allowing noninvasive visualization of cardiac anatomy, coronary arteries, and coronary artery bypass grafts with high spatial resolution. With the introduction of 16-detector-row CT, significant stenoses (≥50%) in coronary arteries can be detected with high sensitivity and specificity (1;2). Earlier studies showed that 4-detector-row CT technology allows adequate detection of significant stenosis in both arterial and vein grafts, although with lower spatial resolution than the current state-of-the-art 16-detector-row technology (3;4). In addition, 16-detector MDCT technology has been used for bypass grafts visualization, although no direct comparison with coronary angiography was performed and nongrafted coronary arteries were not evaluated at the same time (5;6). As recurrent chest pain after coronary artery bypass graft surgery has a high prevalence and conventional coronary angiography has a small risk of potentially lethal complications, a noninvasive approach to evaluate both grafts and nongrafted coronary arteries in one comprehensive evaluation would be of great clinical benefit.

Furthermore, the acquired MDCT data set can additionally be used to assess global left ventricular (LV) function (7). Left ventricular ejection fraction (LVEF), and stroke volume, obtained with MDCT, have been shown to correlate well with cine magnetic resonance imaging (MRI) (8-10), echocardiography (11), and cine ventriculography (12). For patients with previous myocardial infarction (MI) measurement of LVEF is important for risk stratification, and adjustment of medical therapy in order to prevent congestive heart failure, as underscored in the practice guidelines for both non-ST-segment elevation and ST-segment elevation MI (13;14). In addition, LVEF was identified as an independent predictor of mortality in patients with previous bypass graft surgery (15;16). In patients with prior coronary artery bypass graft surgery presenting with recurrent chest pain, early risk stratification and adjustment of medical therapy based on measurement of LVEF would be important extra advantages of MDCT.

Accordingly, the purpose of the present study is to evaluate the use of 16-detector-row CT for the comprehensive assessment of bypass graft, as well as native coronary artery disease in conjunction with evaluation of global LV function.

Methods

Study Population

Consecutive patients with a history of bypass graft surgery, who were awaiting coronary angiography, were screened for participation in the study. Exclusion criteria were renal failure, allergy to contrast agents, irregular heart rhythm, and pregnancy. Included patients underwent coronary angiography for recurrent chest pain or a prior episode of severe arrhythmia and MDCT examination. No cardiac event occurred between angiography and MDCT. All patients gave written informed consent and the study was approved by the institutional ethical committee.

Coronary angiography was performed according to a standard procedure using the femoral approach. To determine stenosis severity in coronary arteries or bypass grafts objectively, quantitative coronary arteriography was performed by an independent,

experienced researcher. Quantitative coronary arteriography was performed according to standardized methods (17;18).
For all included patients, the presence of a prior MI was assessed, concerning patient history and electrocardiography criteria. Subendocardial infarctions were defined as non-Q-wave infarctions, transmural infarctions as Q-wave infarctions.

Multdetector-row Computed Tomography
Multdetector-row computed tomography examination was performed using a 16-detector-row CT scanner (Aquilion 16, Toshiba, Japan). None of the patients received additional β-blockers to reduce heart rate. A localizer scan was obtained to establish the scanning range, from proximal origin of the arterial graft from the subclavian artery to the heart base. When a patient had only vein grafts the top of the aortic arch was set as proximal boundary. The sure-start feature was used to determine the arrival of contrast agent in the ascending aorta. Data acquisition was initiated after the contrast agent (jobitridol, Guerbet, Aulnay sur Bois, France) appeared in the ascending aorta, and the patient was instructed to hold his breath. Additional scan parameters for arterial grafts were the following: 16 x 1.0-mm detector collimation, 0.4 to 0.5 seconds rotation time and 3.2 to 4.0 pitch dependent on patient's heart rate, 0.8 mm^3 pixel size, 120 kV at 320 mA tube voltage, 200 to 250 mm scanning range, administration of intravenous contrast agent at 4 ml/s to a total of 160 ml, and 25 to 30 seconds breath-hold duration. For vein grafts, because of a shorter scanning range (150-200 mm), 16 x 0.5 mm detector collimation was allowed, with 0.4 mm^3 pixel size. An electrocardiogram was simultaneously recorded, and data were retrospectively reconstructed using a segmental reconstruction algorithm, obviating the use of additional β-blockers to lower the heart rate. Axial images were reconstructed at intervals of 5% throughout the cardiac cycle with 0.8-mm increment for arterial grafts and 0.4 mm for vein grafts.
The reconstructed images were viewed on a Vitrea workstation (Vitrea 2, Vital Images, Plymouth, Minn) using 2D axial, 3D, and multiplanar reformat reconstructions. The cardiac phase with the least motion artifacts (mostly at 75%, 80% or 85%) was used for evaluation of bypass grafts, recipient vessels and nongrafted arteries. An experienced cardiologist and radiologist evaluated the scans in consensus. Bypass grafts were divided into segments. The course of the graft from its origin to the first anastomosis was regarded as one segment (graft body). If one graft had more recipient vessels (sequential grafts), the course of the graft from the first anastomosis to the second anastomosis was regarded as a separate segment (second graft body), and so on. The recipient vessels were regarded as separate segments. Proximal segments of coronary arteries receiving a graft were not assessed. Of nongrafted arteries, left main artery, left anterior descending artery, circumflex artery, and right coronary artery were distinguished as separate segments. All segments were evaluated on eligibility for assessment, and on patency. Eligible, patent segments of graft bodies and nongrafted arteries were further searched for the presence of a significant stenosis (≥50%).
Using the CT data set, a short-axis view of the left ventricle was reconstructed by multiplanar reformat (11). Endocardial contours were manually traced using cardiac analysis software (CT MASS, Medis, Leiden, the Netherlands), and LVEF was calculated.

Statistical Analysis

Computed tomography evaluation of vessel segments was compared with angiographic analysis. Sensitivity, specificity, diagnostic accuracy, positive predictive value (PPV) and negative predictive value (NPV) were based on their standard definitions. Agreements between the diagnostic modalities were assessed using κ statistics, with a κ value <0.4, between 0.4 and 0.75, and >0.75 representing modest, fair to good, and excellent agreement, respectively. Data of LVEF are presented as mean ± SD, and are compared using a Student t test.

RESULTS

Study Population

A total of 30 consecutive patients were screened for inclusion in the study. Of these, 5 were excluded because of (supra)ventricular arrhythmias and/or renal insufficiency. Characteristics of the included 25 patients are shown in Table 7.1. A total of 90 vessels were evaluated; vessel characteristics are summarized in Table 7.2. The vessels were subdivided into 225 segments: in graft bodies 104 segments (22 in arterial, 82 in vein grafts), in recipient vessels 82 segments, in native, nongrafted arteries 39 segments. At coronary angiography, 187 (83%) segments were patent. Of these 187 segments, 17 (9%) were ineligible for evaluation of ≥50% stenosis because of metal clips used in arterial bypass grafting. Of the remaining 170 segments, 91 were segments of grafts bodies and nongrafted arteries and were screened for a stenosis ≥50%. In 14 (15%) segments a significant stenosis was present at coronary angiography.

Number of patients	25
Male/female	24/1
Age (years)	66.7 ± 9.4
Diabetes mellitus	8 (32%)
Currently smoking	3 (12%)
Hypertension	13 (52%)
Hypercholesterolemia	16 (64%)
Prior myocardial infarction	14 (56%)
Pacemaker or ICD	2 (8%)
Time after CABG (years)	9.2 ± 5.3
Medication	
β-blocker	14 (56%)
ACE-inhibitor	12 (48%)
Calcium antagonist	14 (56%)
Nitrate	12 (48%)
Diuretic	7 (28%)
Statin	19 (76%)
Oral anticoagulant	7 (28%)

Table 7.1
Patient Characteristics
ICD = intracardiac defibrillator; CABG = coronary artery bypass grafting; ACE = angiotensin-converting enzyme

Number of vessels	90
Single arterial grafts	7
Sequential arterial grafts	7
Single vein grafts	25
Sequential vein grafts	28
Nongrafted arteries	23
Vascular territory perfused by vessel	
LAD	34
LCX	34
RCA	22

Table 7.2
Vessel Characteristics
LAD = left anterior descending artery; LCX = left circumflex artery; RCA = right coronary artery

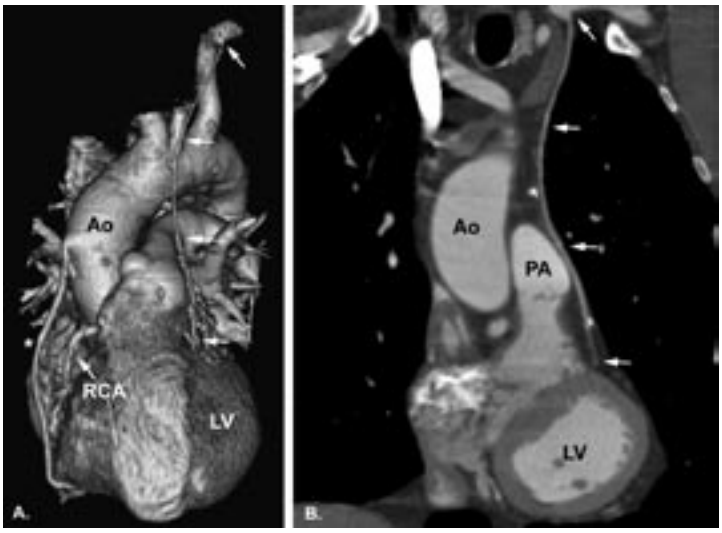

Figure 7.1
Example of an arterial and a vein graft. A, a 3D reconstruction of the heart and vessels. The white arrows highlight a left internal mammary artery graft to the left anterior descending artery from its left subclavian artery origin to the anastomosis. B, after the anastomosis the recipient vessel is occluded, also illustrated as multiplanar reformat reconstruction. The asterisk represents a vein graft to the posterior descending branch (anastomosis not shown). The native RCA is severely diseased. Ao = aorta; RCA = right coronary artery; LV = left ventricle; PA = pulmonary artery. A full colour version of this illustration can be found in the full colour section (page 167).

Comparison of MDCT and Coronary Angiography

Multidetector-row computed tomography examination was successfully accomplished in all patients. Heart rate varied from 53 to 85 beats/min (mean 64 ± 9 beats/min). Figures 7.1 and 7.2 depict typical examples of MDCT reconstructions of arterial and vein grafts. Patency on MDCT was scored in all 225 segments. When metal clips prevented adequate assessment of arterial graft segments, patency was evaluated by the presence or absence of contrast agent in the vessel in between the metal clip artifacts. All grafts were correctly identified as either patent or occluded by MDCT. Neither of the arterial graft segments (n = 22) were occluded. Accordingly, specificity, accuracy, and NPV were 100% for arterial grafts; sensitivity and PPV could not be calculated. Comparison of MDCT with coronary angiography for vein grafts, recipient and nongrafted vessels on vessel patency is illustrated in Table 7.3.

In patent graft bodies and nongrafted arteries the presence of a significant stenosis (≥50%) was evaluated by MDCT. All eligible arterial graft segments (n = 5) were not stenosed, which was correctly recognized by MDCT. Specificity, accuracy, and NPV were 100% for arterial grafts in the detection of a significant stenosis. Shown in Table 7.4 are the results of MDCT compared with angiography in the evaluation of significant stenoses for vein grafts and nongrafted vessels. κ values indicate a good to excellent agreement of MDCT and angiography. Particularly, NPV is high in all vessels when assessing patency or significant stenosis by MDCT.

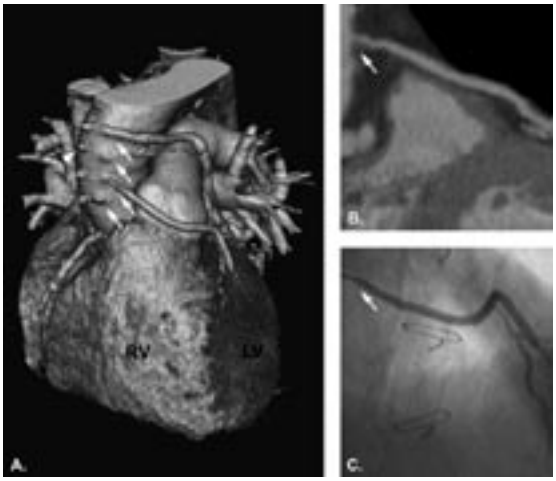

Figure 7.2

Example of a patient with multiple vein grafts. A, a 3D reconstruction of the heart, revealing 4 grafts (white arrows). Two patent grafts supply the obtuse marginal branch and the second diagonal branch, respectively; 2 grafts are totally occluded. Lateral from the graft origins, metal clips have been placed for identifying the graft locations (white arrowhead marks one of the clips). The vein graft to the second diagonal branch has a significant stenosis at its ostium. B and C, the multiplanar reformat reconstruction and coronary angiography of the ostium stenosis (arrow). RV = right ventricle; LV = left ventricle. A full colour version of this illustration can be found in the full colour section (page 168).

Vessel type	Sensitivity	Specificity	Accuracy	PPV	NPV	κ	p
Vein grafts	25/25 (100)	57/57 (100)	82/82 (100)	25/25 (100)	57/57 (100)	1.00	<0.001
Recipient vessels	2/3 (67)	77/79 (97)	79/82 (96)	2/4 (50)	77/78 (99)	0.55	<0.001
Nongrafted vessels	9/10 (90)	29/29 (100)	38/39 (97)	9/9 (100)	29/30 (97)	0.93	<0.001

Table 7.3

Comparison of MDCT and Coronary Angiography on Vessel Segment Patency

Values in parentheses are percentages. All arterial grafts were patent and correctly identified by MDCT. PPV = positive predictive value; NPV = negative predictive value

Vessel type	Sensitivity	Specificity	Accuracy	PPV	NPV	κ	p
Vein grafts	3/3 (100)	51/54 (94)	54/57 (95)	3/6 (50)	51/51 (100)	0.64	<0.001
Nongrafted vessels	11/11 (100)	16/18 (89)	27/29 (93)	11/13 (85)	16/16 (100)	0.86	<0.001

Table 7.4

Comparison of MDCT and Coronary Angiography on ≥50% Stenosis

Values in parentheses are percentages. Only patent vessels, eligible for evaluation, are included. Arterial grafts had no stenoses and were correctly identified by MDCT. Abbreviations as in Table 7.3

Global LV Function

Of the 25 patients, 14 had a prior MI in their medical history. Six patients had a subendocardial MI, 8 a transmural MI. In all patients LVEF could be derived from the MDCT examination. Mean LVEF for patients with no, subendocardial, and transmural infarctions were 51.1% ± 15.7%, 56.0% ± 17.7%, and 39.9% ± 9.1%, respectively (p = NS). Mean LVEF of patients without MI and with subendocardial MI demonstrated a significant difference compared with mean LVEF of transmural MI ($p<0.05$).

Discussion

In the present study a comprehensive 16-detector-row CT assessment of bypass grafts and native coronary arteries together with cardiac function has been shown to be feasible. With MDCT, patency and the presence of a significant stenosis in grafts or coronary arteries could be evaluated with high accuracy. Additional evaluation of LV function can be used in patients with previous MI for risk stratification or adjustment of medical therapy.

Computed Tomographic Angiography in Native Coronary Arteries

Multidetector-row computed tomography examination is a rapidly evolving, versatile technique, gaining acceptance as a diagnostic cardiac imaging tool. Four-detector-row CT already demonstrated promising results, when CT angiography was compared with coronary angiography, showing sensitivities of 81% to 93%, specificities of 76% to 97%, PPV of 57% to 66%, and NPV of 97% to 99% for the detection of ≥50% stenosis in eligible native coronary arteries (19-22). In these studies segments of vessels were excluded from analysis because of image artefacts from metal objects, calcification, coronary motion, or the patients' inability to perform the necessary breath-hold. With the introduction of the 16-detector-row CT technique, detection of significant stenoses in native coronary arteries improved because of higher spatial and temporal resolution, and shorter scanning time (23). Sensitivities of 92% to 95%, specificities of 86% to 95%, PPV of 79% to 80%, and NPV of 97% to 98% were reported for the detection of ≥50% stenosis, when compared with coronary angiography (1;2;24). If the heart rate exceeded 60 beats/min, additional β-blockers were administered in these studies to enhance image quality.

In the current study similar results were demonstrated for native coronary arteries in patients who had undergone bypass grafting. Segments were ineligible for evaluation by MDCT because of metal clip artifacts. All patients were able to sustain the necessary breath-hold, and none of the segments had to be excluded because of coronary motion artifacts or calcification. Vessel calcification was mostly observed in grafted arteries proximal to the first anastomosis and occluded grafts, proposing no difficulty for the eligible segments to be assessed.

Because of segmental reconstruction of the raw data sets, no prescan β-blockers were necessary. Heart rates varied to a maximum of 85 beats/min. Image quality was excellent and did not decline with higher heart rates.

Computed Tomographic Angiography in Bypass Grafts

Both arterial and vein grafts have been investigated with 4-detector-row CT and the results, compared with coronary angiography, showed fair diagnostic accuracies in the detection of ≥50% stenosis (3;4). However, there was a high number of unevaluable grafts in one study (3): only 62% of patent grafts could be assessed for the detection of significant stenoses because of metal and motion artifacts. In the study by Nieman et al. (4), assessability for the evaluation of stenoses was good for vein grafts (95%-100%), whereas for arterial grafts and nongrafted coronary arteries assessability was much lower (58%-73% and 66%-69%, respectively). Major causes of non-assessability were the patients' inability to sustain a long breath-hold (35-45 seconds) and cardiac motion artifacts. Heart rate had a significant influence on the assessment of nongrafted arteries. In patients with a heart rate ≥65 beats/min, assessability was 52% for nongrafted arteries. In both studies the proximal part of arterial grafts could not be included in the scan because of the limited scanning range.

Sixteen-detector-row CT technology has been used to assess the patency of arterial grafts within a short period (1 week to 12 months) after surgery (6). The entire arterial graft could be included in the scan, and graft patency was easily recognized. In addition, both arterial and vein grafts were investigated by 16-detector-row CT in one study, demonstrating the

ability of this technique to reliably depict grafts with fair diagnostic quality (5). However, both studies did not have a head-to-head comparison with coronary angiography, and native, nongrafted coronary arteries were not included in the analysis.
In the current study, arterial and vein grafts, recipient vessels, and native, nongrafted coronary arteries were evaluated by MDCT, compared in a head-to-head fashion with coronary angiography, demonstrating good diagnostic accuracy in the assessment of patency and in the detection of significant stenosis (≥50%). Owing to the high NPV (100% for nongrafted arteries, arterial and vein grafts) this approach may be used as gatekeeper before coronary angiography. For all arterial grafts the entire graft, from origin to the distal recipient vessel, could be assessed. Image quality was excellent for all patients; no motion artifacts were observed. Metal clips still proposed a difficulty in the evaluation of arterial grafts and recipient vessels, causing 9% of segments to be excluded from analysis. Because MDCT is becoming widely available and is gaining acceptance as a cardiac diagnostic tool, MDCT-compatible clips may be preferential to be used in bypass graft surgery.

Global LV Function with MDCT
Using 4-detector-row CT global LV function correlated well with cine MRI (8-10), echocardiography (11), and cine ventriculography (12). In a recent study, infarct volumes assessed by MDCT showed a negative correlation to LVEF measured by contrast ventriculography (25). The present study confirmed these findings by demonstrating that mean LVEF of patients with prior transmural MI was significantly lower than mean LVEF of patients with no or prior subendocardial MI. Both practice guidelines for non-ST-segment elevation and ST-segment elevation MI emphasize the need to determine LVEF for risk stratification and to adjust medical therapy to prevent congestive heart failure (13;14). Because an entire scan of the heart is required for the detection of significant stenoses in grafts or coronary arteries, determination of LVEF may be performed using the same CT data set, obviating the use of an additional diagnostic test. As cardiac CT software is still under development, more diagnostic potential of MDCT may be expected (7).

Comparison of MDCT with Established Noninvasive Modalities
Besides MDCT, the number of noninvasive modalities available for simultaneous assessment of stenoses in bypass grafts, nongrafted arteries, and LV function is limited. Currently, only cardiovascular magnetic resonance may suit this description. Accurate assessment of global and regional LV function with cine MRI has been described (26;27). However, magnetic resonance angiography still lacks the ability to evaluate stenoses in native coronary arteries and bypass grafts with high accuracy (28-30).
Other noninvasive modalities, such as gated single photon emission computed tomography and stress echocardiography (31;32), allow assessment of LV function and myocardial perfusion, which is an indirect marker of coronary artery disease; however direct visualization of bypass grafts and nongrafted arteries is impossible.

Limitations

Radiation exposure remains high for cardiac MDCT examinations, which is reported to be between 6.7 and 13.0 mSv (33;34). Because cardiac MDCT is becoming a robust diagnostic tool, future developments should focus on reducing radiation exposure.

The sample size of the current study is small. The results must be confirmed in a larger study before MDCT can be used as a gatekeeper in patients with prior bypass surgery.

No gold standard for the 16-detector-row CT LVEF measurements is available. Because LVEF measurements performed with a 4-detector row CT were proven to be very accurate in previous studies (8-12), differences from LVEF derived from 16-detector-row CT images are expected to be low. A study, which validates the 16-detector-row CT LV function by head-to-head comparison with an established modality, would be fitting.

Conclusion

Comprehensive assessment of bypass grafts, nongrafted vessels and global cardiac function is feasible with 16-detector-row CT. Good diagnostic accuracy in the detection of significant stenosis (≥50%) in comparison with coronary angiography was demonstrated. Owing to the high NPV, this noninvasive approach may be used as gatekeeper before conventional coronary angiography.

REFERENCES

1. Nieman K, Cademartiri F, Lemos PA, Raaijmakers R, Pattynama PM, de Feyter PJ. Reliable noninvasive coronary angiography with fast submillimeter multislice spiral computed tomography. Circulation 2002;106:2051-4.
2. Ropers D, Baum U, Pohle K et al. Detection of coronary artery stenoses with thin-slice multi-detector row spiral computed tomography and multiplanar reconstruction. Circulation 2003;107:664-6.
3. Ropers D, Ulzheimer S, Wenkel E et al. Investigation of aortocoronary artery bypass grafts by multislice spiral computed tomography with electrocardiographic-gated image reconstruction. Am J Cardiol 2001;88:792-5.
4. Nieman K, Pattynama PM, Rensing BJ, van Geuns RJ, de Feyter PJ. Evaluation of patients after coronary artery bypass surgery: CT angiographic assessment of grafts and coronary arteries. Radiology 2003;229:749-56.
5. Dewey M, Lembcke A, Enzweiler C, Hamm B, Rogalla P. Isotropic half-millimeter angiography of coronary artery bypass grafts with 16-slice computed tomography. Ann Thorac Surg 2004;77:800-4.
6. Gurevitch J, Gaspar T, Orlov B et al. Noninvasive evaluation of arterial grafts with newly released multidetector computed tomography. Ann Thorac Surg 2003;76:1523-7.
7. Saito K, Saito M, Komatu S, Ohtomo K. Real-time four-dimensional imaging of the heart with multi-detector row CT. Radiographics 2003;23:e8.
8. Juergens KU, Grude M, Maintz D et al. Multi-detector row CT of left ventricular function with dedicated analysis software versus MR imaging: initial experience. Radiology 2004;230:403-10.
9. Grude M, Juergens KU, Wichter T et al. Evaluation of global left ventricular myocardial function with electrocardiogram-gated multidetector computed tomography: comparison with magnetic resonance imaging. Invest Radiol 2003;38:653-61.
10. Halliburton SS, Petersilka M, Schvartzman PR, Obuchowski N, White RD. Evaluation of left ventricular dysfunction using multiphasic reconstructions of coronary multi-slice computed tomography data in patients with chronic ischemic heart disease: validation against cine magnetic resonance imaging. Int J Cardiovasc Imaging 2003;19:73-83.
11. Dirksen MS, Bax JJ, de Roos A et al. Usefulness of dynamic multislice computed tomography of left ventricular function in unstable angina pectoris and comparison with echocardiography. Am J Cardiol 2002;90:1157-60.
12. Juergens KU, Grude M, Fallenberg EM et al. Using ECG-gated multidetector CT to evaluate global left ventricular myocardial function in patients with coronary artery disease. AJR Am J Roentgenol 2002;179:1545-50.
13. Braunwald E, Antman EM, Beasley JW et al. ACC/AHA 2002 guideline update for the management of patients with unstable angina and non-ST-segment elevation myocardial infarction--summary article: a report of the American College of Cardiology/American Heart Association task force on practice guidelines (Committee on the Management of Patients With Unstable Angina). J Am Coll Cardiol 2002;40:1366-74.
14. Ryan TJ, Antman EM, Brooks NH et al. 1999 update: ACC/AHA guidelines for the management of patients with acute myocardial infarction. A report of the American College of Cardiology/American Heart Association Task Force on Practice Guidelines (Committee on Management of Acute Myocardial Infarction). J Am Coll Cardiol 1999;34:890-911.
15. Veldkamp RF, Valk SD, van Domburg RT, van Herwerden LA, Meeter K. Mortality and repeat interventions up until 20 years after aorto-coronary bypass surgery with saphenous vein grafts. A follow-up study of 1041 patients. Eur Heart J 2000;21:747-53.
16. Herlitz J, Wognsen GB, Karlson BW et al. Mortality, mode of death and risk indicators for death during 5 years after coronary artery bypass grafting among patients with and without a history of diabetes mellitus. Coron Artery Dis 2000;11:339-46.
17. Reiber JH, van der Zwet PM, Koning G et al. Accuracy and precision of quantitative digital coronary arteriography: observer-, short-, and medium-term variabilities. Cathet Cardiovasc Diagn 1993;28:187-98.
18. Reiber JH, Jukema W, van Boven A, van Houdt RM, Lie KI, Bruschke AV. Catheter sizes for quantitative coronary arteriography. Cathet Cardiovasc Diagn 1994;33:153-5.
19. Achenbach S, Giesler T, Ropers D et al. Detection of coronary artery stenoses by contrast-enhanced, retrospectively electrocardiographically-gated, multislice spiral computed tomography. Circulation 2001;103:2535-8.
20. Becker CR, Knez A, Leber A et al. Detection of coronary artery stenoses with multislice helical CT angiography. J Comput Assist Tomogr 2002;26:750-5.
21. Kopp AF, Schroeder S, Kuettner A et al. Non-invasive coronary angiography with high resolution multidetector-row computed tomography. Results in 102 patients. Eur Heart J 2002;23:1714-25.
22. Nieman K, Rensing BJ, van Geuns RJ et al. Usefulness of multislice computed tomography for detecting obstructive coronary artery disease. Am J Cardiol 2002;89:913-8.

23. Flohr TG, Schoepf UJ, Kuettner A et al. Advances in cardiac imaging with 16-section CT systems. Acad Radiol 2003;10:386-401.
24. Mollet NR, Cademartiri F, Nieman K et al. Multislice spiral computed tomography coronary angiography in patients with stable angina pectoris. J Am Coll Cardiol 2004;43:2265-70.
25. Nikolaou K, Knez A, Sagmeister S et al. Assessment of myocardial infarctions using multidetector-row computed tomography. J Comput Assist Tomogr 2004;28:286-92.
26. Pujadas S, Reddy GP, Weber O, Lee JJ, Higgins CB. MR imaging assessment of cardiac function. J Magn Reson Imaging 2004;19:789-99.
27. Ichikawa Y, Sakuma H, Kitagawa K et al. Evaluation of left ventricular volumes and ejection fraction using fast steady-state cine MR imaging: comparison with left ventricular angiography. J Cardiovasc Magn Reson 2003;5:333-42.
28. Flamm SD, Muthupillai R. Coronary artery magnetic resonance angiography. J Magn Reson Imaging 2004;19:686-709.
29. Jahnke C, Paetsch I, Schnackenburg B et al. Coronary MR angiography with steady-state free precession: individually adapted breath-hold technique versus free-breathing technique. Radiology 2004;232:669-76.
30. Langerak SE, Vliegen HW, de Roos A et al. Detection of Vein Graft Disease using High-resolution Magnetic Resonance Angiography. Circulation 2002;105:328-33.
31. Lakkis NM, Mahmarian JJ, Verani MS. Exercise thallium-201 single photon emission computed tomography for evaluation of coronary artery bypass graft patency. Am J Cardiol 1995;76:107-11.
32. Chirillo F, Bruni A, De Leo A et al. Usefulness of dipyridamole stress echocardiography for predicting graft patency after coronary artery bypass grafting. Am J Cardiol 2004;93:24-30.
33. Morin RL, Gerber TC, McCollough CH. Radiation dose in computed tomography of the heart. Circulation 2003;107:917-22.
34. Hunold P, Vogt FM, Schmermund A et al. Radiation exposure during cardiac CT: effective doses at multi-detector row CT and electron-beam CT. Radiology 2003;226:145-52.

CHAPTER 8

Global and regional left ventricular function assessment with 16-detector row CT: comparison with echocardiography and cardiovascular magnetic resonance

Liesbeth P. Salm
Joanne D. Schuijf
Albert de Roos
Hildo J. Lamb
Hubert W. Vliegen
J. Wouter Jukema
Raoul Joemai
Ernst E. van der Wall
Jeroen J. Bax

Eur J Echocardiogr 2006; 7, 4, 308-314

ABSTRACT

Aims: To compare multidetector row computed tomography (MDCT) global and regional left ventricular (LV) function assessment with echocardiography and cardiovascular magnetic resonance (CMR).

Methods and Results: In 25 patients, who were referred for noninvasive angiography with 16-detector row CT, LV function assessment was also performed. A subsequent echocardiogram was performed, and in a subgroup of patients, CMR examination was completed to evaluate LV function. For global function assessment, the LV ejection fraction (LVEF) was calculated. Regional LV function was scored using a 17-segment model and a 4–point scoring system.

MDCT agreed well with echocardiography for the assessment of LVEF ($r = 0.96$; bias 0.54%; $p<0.0001$), and regional LV function ($\kappa = 0.78$). Eight patients had no contra-indications and gave informed consent for CMR examination. A fair correlation between MDCT and CMR was demonstrated in the assessment of LVEF ($r = 0.86$; bias –1.5%; $p<0.01$). Regional LV function agreement between MDCT and CMR was good ($\kappa = 0.86$).

Conclusion: MDCT agreed well with both echocardiography and CMR in the assessment of global and regional LV function. Global and regional LV function may accurately be evaluated by 16-detector row CT, and can be added to a routine CT image analysis protocol without need for additional contrast or imaging time.

Introduction

Global and regional left ventricular (LV) function are well-known indicators of cardiac disease. For patients with heart failure LV function assessment is often used to identify systolic and diastolic LV dysfunction, and to monitor the progression of the disease (1). Moreover, after myocardial infarction, left ventricular ejection fraction (LVEF) is an important prognostic marker (2-4).

Noninvasive modalities to measure global and regional LV function include echocardiography, cardiovascular magnetic resonance (CMR), and single photon emission computed tomography (SPECT). These techniques have been shown to agree well with invasively acquired LV function assessment by angiography (5-7). Multidetector row computed tomography (MDCT) is a relatively new technique used for noninvasive angiography, but does also allow evaluation of LV function. Several studies showed that 4-detector row CT allowed accurate assessment of global and regional LV function (8-10). The first study using the next-generation 16-detector row CT has shown to evaluate LV function with similar accuracy (11). However, no validation of global and regional LV function assessment with 16-detector row CT has yet been conducted. Accordingly, the purpose of the present study is to compare global and regional LV function assessment by 16-detector row CT with echocardiography and CMR.

Methods

Patients

In patients who were referred for noninvasive coronary angiography by MDCT for evaluation of coronary artery disease, LV function assessment was also performed. A subsequent echocardiogram was scheduled. If no contra-indications for CMR existed, patients were also asked for a CMR examination to assess LV function. Contra-indications for CMR were metal implants, irregular heart rhythm, and claustrophobia. The examinations were performed within three months after the first examination. No cardiac events occurred between examinations. All patients gave informed consent and the study was approved by the institutional ethical committee.

MDCT

MDCT examination was performed using a 16-detector row CT scanner (Aquilion 16, Toshiba, Japan). Patients did not receive additional β-blockers to reduce heart rate. A localizer scan was obtained to establish the scanning range. The sure-start feature was used to determine the arrival of contrast agent in the ascending aorta. Data acquisition was initiated after the contrast agent (jobitridol, Guerbet, Aulnay sur Bois, France) appeared in the ascending aorta, and the patient was instructed to hold his breath. Additional scan parameters were: 16 x 0.5 mm detector collimation, 0.4-0.5 s rotation time, 3.2-4.0 pitch and 97-200 ms temporal resolution dependent on patient's heart rate, 0.4 mm^3 pixel size, 120 kV at 320 mA tube voltage, 150-200 mm scanning range, administration of intravenous contrast agent at 4 ml/s to a total of 160 ml, and 25-30 s breathhold duration. An electrocardiogram (ECG) was simultaneously recorded, and data were retrospectively reconstructed using a multisegmental reconstruction algorithm, obviating the use of additional β-blockers to lower heart rate. Axial images were reconstructed at intervals

of 5% throughout the cardiac cycle with 0.4 mm increment. A short axis view of the left ventricle was reconstructed by multiplanar reformat (10) by an experienced observer. Endocardial contours were manually traced using cardiac analysis software (CT MASS, Medis, Leiden, the Netherlands), and LVEF was calculated. An independent, second observer additionally performed manual tracing of endocardial contours, blinded to the results of the first observer, in order to establish interobserver agreement. For assessment of regional LV function, a 17-segment model was used (12). Each segment was assigned a wall motion score (WMS), with 1) normal wall motion; 2) hypokinesia; 3) akinesia; and 4) dyskinesia. Short axis views at 0% to 95% were presented in cine on a Linux workstation and regional LV function was evaluated by an experienced cardiologist.

Echocardiography

Patients were imaged in the left lateral decubitus position using a commercially available system (Vingmed system Seven, General Electric-Vingmed, Milwaukee, Wisconsin, USA). Images were obtained using a 3.5-MHz transducer, at a depth of 16 cm in the parasternal and apical views (standard parasternal long- and short-axis, apical 2- and 4-chamber images). The images were saved in cine loop format (triggered to the ECG). The LVEF was calculated from the conventional apical 2- and 4-chamber images, using the biplane Simpson's technique and commercially available software (Echopac 6.1, General Electric - Vingmed) (13;14). For the evaluation of regional LV function, the same 17-segment model was used as with MDCT, with a similar scoring system (scores 1 to 4, from normokinesia to dyskinesia). The echocardiography LV function assessment was performed by an experienced cardiologist, who was blinded to the results of MDCT.

CMR

For CMR imaging a 1.5 T Gyroscan ACS-NT MR scanner (Philips Medical Systems, Best, the Netherlands), equipped with Powertrak 6000 gradients, a cardiac research software patch, and 5-element cardiac synergy coil was used. Gross cardiac anatomy was visualized by means of a scout scan. A SENSE reference scan was performed in order to use this application in the subsequent scans. A 2-chamber view was planned on the transversal scout and scanned by means of a breathhold, ECG-triggered, balanced fast field echo sequence. A 4-chamber view was then scanned using the 2-chamber view for planning. The short-axis view was scanned in 3 breathholds using the 2-chamber and 4-chamber views in end-systole and end-diastole for reference. MR parameters for the 2-chamber, 4-chamber, and short axis views were: TR/TE 3.6/1.8 ms, flip angle of 50°, temporal resolution of 32 ms, field of view of 400 x 400 mm, data acquisition matrix of 256 x 256 mm, section thickness of 10 mm, scan duration of 26 heart beats. At short axis, 12 slices were acquired at 10 mm slice thickness. Image data were transferred to a personal computer and viewed using MASS Suite 6.0.6 (Medis, Leiden, the Netherlands). For global LV function analysis endocardial contours were manually traced, and LVEF was calculated by an experienced observer, who was blinded to the results of MDCT and echocardiography. For regional LV function analysis short axis views in cine were evaluated by an experienced cardiologist, who was blinded to the results of MDCT and echocardiography, using the 17-segment model identically as for the MDCT images.

Statistical Analysis
Data is presented as mean ± standard deviation. Agreement between the imaging methods and observers was calculated as Pearson correlation and by means of Bland-Altman analysis (15). The 95% limits of agreement were defined as the range of values ± 2 SD from the mean difference. Agreement between methods on regional function was expressed as percentage and κ-value, in which κ-values <0.4, between 0.4 and 0.75, and >0.75 represented modest, fair to good, and excellent agreement, respectively. A p-value <0.05 was considered significant.

RESULTS

MDCT
A total of 25 patients were enrolled in the study. Patient characteristics are summarized in Table 8.1. Heart rate at MDCT scanning varied from 53 to 85 beats per minute (mean 64 ± 9 bpm). For all patients global and regional function could be assessed by MDCT. Mean LVEF was 48.9 ± 15.2% (range 15.4 to 73.5%). Interobserver agreement was excellent with a correlation coefficient (r) of 0.96, p<0.0001. At Bland-Altman analysis, the bias was 1.8%, and 95% limits of agreement ranged between -6.7 and 10.3%. For regional function assessment, 425 segments were analyzed. A normal WMS was assigned to 325 segments, 58 segments were hypokinetic, 30 segments akinetic, and 12 dyskinetic.

Echocardiography
All patients underwent 2-dimensional echocardiography. At echocardiography, the mean LVEF was 48.3 ± 15.1% (range 19 to 75%). All 425 segments could be analyzed; 325 segments had normal wall motion, 50 were hypokinetic, 42 akinetic and 8 dyskinetic.

CMR
Eight of 25 patients gave informed consent for the CMR examination. Contra-indications for CMR existed for 9 patients, 8 patients refused to give informed consent. Mean LVEF derived from MR images was 56.7 ± 16.7% (range 28.4 to 77.6%). A total of 136 segments were analyzed for regional LV function assessment. Normal WMS was allocated to 104 segments, 25 segments were hypokinetic, and 7 akinetic; none were dyskinetic.

Number of patients	25
Gender (M/F)	24/1
Age (years)	66.7 ± 9.4
Diabetes mellitus	8 (32%)
Currently smoking	3 (12%)
Hypertension	13 (52%)
Hypercholesterolemia	16 (64%)
Prior myocardial infarction	14 (56%)
Pacemaker or ICD	2 (8%)

Table 8.1
Patient Characteristics
ICD = intracardiac defibrillator

MDCT versus Echocardiography

For global LV function evaluation, the LVEF correlated well for MDCT and echocardiography. The trendline equalled y = 0.97x + 1.83, r = 0.96, p<0.0001 (Figure 8.1). At Bland-Altman analysis a bias of 0.54% was demonstrated, and 95% limits of agreement ranged from -7.7% to 8.8%. All data points stayed within 2 SD of the mean difference. For regional LV function assessment, MDCT agreed well with echocardiography in 91% of segments (κ = 0.78; Table 8.2).

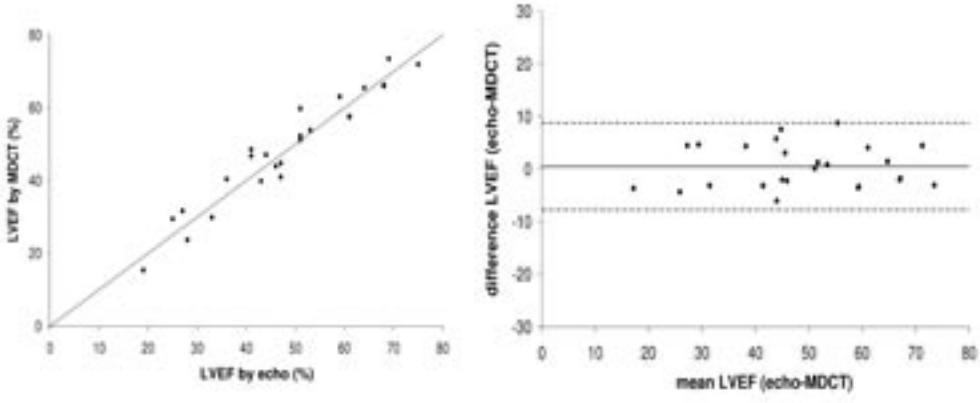

Figure 8.1

Correlation and Bland-Altman plot of LVEF by echocardiography and MDCT. Identity line (y = x) is shown in the correlation plot in gray.

		Echocardiography				
	WMS	1	2	3	4	Total
	1	314	9	2	0	325
	2	10	39	9	0	58
MDCT	3	1	2	27	0	30
	4	0	0	4	8	12
	Total	325	50	42	8	425

Table 8.2

Agreement between MDCT and Echocardiography in Wall Motion Score

Wall motion scores of 1 to 4 were assigned to the different segments: 1 = normal wall motion; 2 = hypokinesia; 3 = akinesia; 4 = dyskinesia. WMS = wall motion score; MDCT = multidetector row computed tomography

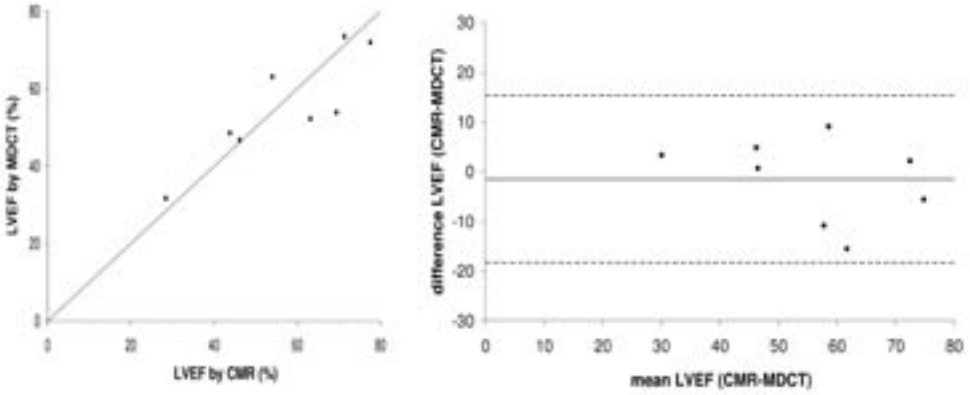

Figure 8.2

Correlation and Bland-Altman plot of LVEF by CMR and MDCT. Identity line (y = x) is shown in the correlation plot in gray.

		CMR				
	WMS	1	2	3	4	Total
MDCT	1	102	4	0	0	106
	2	2	21	1	0	24
	3	0	0	6	0	6
	4	0	0	0	0	0
	Total	104	25	7	0	136

Table 8.3

Agreement between MDCT and CMR in Wall Motion Score
Wall motion scores of 1 to 4 were assigned to the different segments: 1 = normal wall motion; 2 = hypokinesia; 3 = akinesia; 4 = dyskinesia. CMR = cardiovascular magnetic resonance; WMS = wall motion score; MDCT = multidetector row computed tomography

MDCT versus CMR

A fair correlation of MDCT and CMR on LVEF calculation was shown, $y = 0.72x + 14.3$, $r = 0.86$, $p<0.01$. At Bland-Altman analysis, the bias for MDCT was -1.5%, with 95% limits of agreement ranging from -18.3% to 15.3% (Figure 8.2). At regional LV function assessment, MDCT agreed well with CMR in 95% of segments ($\kappa = 0.86$; Table 8.3).

Discussion

In the present study, LV function measurements by 16-detector row CT were compared with echocardiography and CMR. The results demonstrate a good agreement between MDCT and echocardiography/CMR for the evaluation of LVEF and regional wall motion abnormalities. Moreover, interobserver agreement for LVEF assessment by MDCT was excellent.

LV Ejection Fraction with MDCT

Four-detector row CT has been shown to assess LVEF accurately. A comparison with echocardiography was performed in patients with unstable angina pectoris, demonstrating a good correlation (r = 0.93) and agreement (bias 1.3%) with MDCT for assessment of LVEF (10). Also, in comparison with cineventriculography, MDCT showed a fair correlation (r = 0.8) in the measurement of LVEF (8). In addition, Juergens et al. reported LVEF derived by MDCT to correlate and agree well (r = 0.89; bias 0.25%) with LVEF derived by CMR in patients with known or suspected coronary artery disease (9). In another direct comparison with CMR however, a significant underestimation in LVEF by MDCT (bias -8.5%) was shown (16). This underestimation may be related to the use of a standard image reconstruction algorithm, resulting in limited temporal resolution of MDCT (125-250 ms, heart rate dependent). Superior resolution can be obtained using multisegmental resolution (temporal resolution 75-130 ms), resulting in a better agreement between CMR and MDCT for assessment of LVEF (17).

In the present study, LVEF assessment by 16-detector row CT agreed well with both LVEF assessment by echocardiography (r = 0.96; bias 0.54%), and by CMR (r = 0.86; bias –1.5%). Moreover, for LVEF assessment by MDCT, the interobserver agreement was excellent (r = 0.96; bias 1.8%).

LV Wall Motion Analysis with MDCT

An early study compared single-detector row, ECG-gated CT with echocardiography and left ventriculography for assessment of regional wall motion (18). A good correlation with both echocardiography (86%), and left ventriculography (82%) was shown. Similarly, wall motion assessment by 4-detector row CT has been demonstrated to agree well with echocardiography (88%; $\kappa = 0.84$) (10). Also, good agreement between CMR and 4-detector row CT for assessment of wall motion was shown (agreement 84% [$\kappa = 0.56$] when standard image reconstruction was used, and 93% [$\kappa = 0.82$] when multisegmental reconstruction was used) (17). The results of the current study show that 16-detector row MDCT agreed well with both echocardiography (91%; $\kappa = 0.78$) and CMR (95%; $\kappa = 0.86$) for assessment of regional wall motion.

Why Another Modality for Assessment of LV Function?

Currently, several noninvasive imaging techniques are available for the assessment of LV function. The most frequently used technique in daily routine is 2D echocardiography, which is fast, easily accessible, and contains no radiation exposure (5;19). For patients with obesity, chronic obstructive pulmonary disease (COPD), or prior cardiothoracic surgery, echocardiography may be less optimal, due to poor acoustic windows (20). The current gold standard to evaluate LV function noninvasively is CMR (6;21). This technique is fast, and without radiation exposure. However, CMR is often not readily available, and comprises certain contra-indications, such as metal implants, irregular heart rhythm, and claustrophobia. SPECT imaging, traditionally used for assessment of perfusion, is yet another technique that (with the introduction of ECG gating) allows accurate assessment of global and regional LV function, but it exposes patients to radiation (7;22).

Similar to SPECT imaging, MDCT also requires exposure to radiation (7-8 mSv per cardiac

study), but allows examination of patients with a pacemaker or other metal implants, obesity, COPD, or prior cardiac surgery. With the growing interest in noninvasive angiography by MDCT (in particular with the 16-detector and higher detector row technology) (23;24), evaluation of function by MDCT is of value, since it can be obtained in the same session for noninvasive angiography, without the need for additional contrast or prolonged data acquisition.

Limitations

A limited number of patients underwent CMR imaging, due to contra-indications or refusal of informed consent. Therefore, a larger direct comparison of 16-detector row CT and CMR in the evaluation of LV function is required to confirm the current findings.

Conclusion

MDCT agreed well with both echocardiography and CMR in the assessment of global and regional LV function. Global and regional LV function may accurately be evaluated by 16-detector row CT (in the same session, without need for additional contrast), and can be added when noninvasive angiography with MDCT is performed.

REFERENCES

1. Hunt SA, Baker DW, Chin MH et al. ACC/AHA guidelines for the evaluation and management of chronic heart failure in the adult: executive summary. J Heart Lung Transplant 2002;21:189-203.
2. Schwammenthal E, Adler Y, Amichai K et al. Prognostic value of global myocardial performance indices in acute myocardial infarction: comparison to measures of systolic and diastolic left ventricular function. Chest 2003;124:1645-51.
3. Braunwald E, Antman EM, Beasley JW et al. ACC/AHA 2002 guideline update for the management of patients with unstable angina and non-ST-segment elevation myocardial infarction--summary article: a report of the American College of Cardiology/American Heart Association task force on practice guidelines (Committee on the Management of Patients With Unstable Angina). J Am Coll Cardiol 2002;40:1366-74.
4. Ryan TJ, Antman EM, Brooks NH et al. 1999 update: ACC/AHA guidelines for the management of patients with acute myocardial infarction. A report of the American College of Cardiology/American Heart Association Task Force on Practice Guidelines (Committee on Management of Acute Myocardial Infarction). J Am Coll Cardiol 1999;34:890-911.
5. Folland ED, Parisi AF, Moynihan PF, Jones DR, Feldman CL, Tow DE. Assessment of left ventricular ejection fraction and volumes by real-time, two-dimensional echocardiography. A comparison of cineangiographic and radionuclide techniques. Circulation 1979;60:760-6.
6. Ichikawa Y, Sakuma H, Kitagawa K et al. Evaluation of left ventricular volumes and ejection fraction using fast steady-state cine MR imaging: comparison with left ventricular angiography. J Cardiovasc Magn Reson 2003;5:333-42.
7. Iskandrian AE, Germano G, Vandecker W et al. Validation of left ventricular volume measurements by gated SPECT 99mTc-labeled sestamibi imaging. J Nucl Cardiol 1998;5:574-8.
8. Juergens KU, Grude M, Fallenberg EM et al. Using ECG-gated multidetector CT to evaluate global left ventricular myocardial function in patients with coronary artery disease. AJR Am J Roentgenol 2002;179:1545-50.
9. Juergens KU, Grude M, Maintz D et al. Multi-detector row CT of left ventricular function with dedicated analysis software versus MR imaging: initial experience. Radiology 2004;230:403-10.
10. Dirksen MS, Bax JJ, de Roos A et al. Usefulness of dynamic multislice computed tomography of left ventricular function in unstable angina pectoris and comparison with echocardiography. Am J Cardiol 2002;90:1157-60.
11. Schuijf JD, Bax JJ, Salm LP et al. Assessment of left ventricular function using 16-slice computed tomography. Am J Cardiol 2005;95:571-4.
12. Cerqueira MD, Weissman NJ, Dilsizian V et al. Standardized myocardial segmentation and nomenclature for tomographic imaging of the heart: a statement for healthcare professionals from the Cardiac Imaging Committee of the Council on Clinical Cardiology of the American Heart Association. Circulation 2002;105:539-42.
13. Schiller NB, Acquatella H, Ports TA et al. Left ventricular volume from paired biplane two-dimensional echocardiography. Circulation 1979;60:547-55.
14. Otterstad JE, Froeland G, St John SM, Holme I. Accuracy and reproducibility of biplane two-dimensional echocardiographic measurements of left ventricular dimensions and function. Eur Heart J 1997;18:507-13.
15. Bland JM, Altman DG. Statistical methods for assessing agreement between two methods of clinical measurement. Lancet 1986;1:307-10.
16. Grude M, Juergens KU, Wichter T et al. Evaluation of global left ventricular myocardial function with electrocardiogram-gated multidetector computed tomography: comparison with magnetic resonance imaging. Invest Radiol 2003;38:653-61.
17. Mahnken AH, Spuentrup E, Niethammer M et al. Quantitative and qualitative assessment of left ventricular volume with ECG-gated multislice spiral CT: value of different image reconstruction algorithms in comparison to MRI. Acta Radiol 2003;44:604-11.
18. Bouchard A, Lipton MJ, Farmer DW et al. Evaluation of regional ventricular wall motion by ECG-gated CT. J Comput Assist Tomogr 1987;11:969-74.
19. Parisi AF, Moynihan PF, Folland ED, Feldman CL. Quantitative detection of regional left ventricular contraction abnormalities by two-dimensional echocardiography. II. Accuracy in coronary artery disease. Circulation 1981;63:761-7.
20. Geleijnse ML, Fioretti PM, Roelandt JR. Methodology, feasibility, safety and diagnostic accuracy of dobutamine stress echocardiography. J Am Coll Cardiol 1997;30:595-606.
21. Pattynama PM, Lamb HJ, van der Velde EA, van der Wall EE, de Roos A. Left ventricular measurements with cine and spin-echo MR imaging: a study of reproducibility with variance component analysis. Radiology 1993;187:261-8.

22. Vaduganathan P, He ZX, Vick GW, III, Mahmarian JJ, Verani MS. Evaluation of left ventricular wall motion, volumes, and ejection fraction by gated myocardial tomography with technetium 99m-labeled tetrofosmin: a comparison with cine magnetic resonance imaging. J Nucl Cardiol 1999;6:3-10.
23. Nieman K, Cademartiri F, Lemos PA, Raaijmakers R, Pattynama PM, de Feyter PJ. Reliable noninvasive coronary angiography with fast submillimeter multislice spiral computed tomography. Circulation 2002;106:2051-4.
24. Schlosser T, Konorza T, Hunold P, Kuhl H, Schmermund A, Barkhausen J. Noninvasive visualization of coronary artery bypass grafts using 16-detector row computed tomography. J Am Coll Cardiol 2004;44:1224-9.

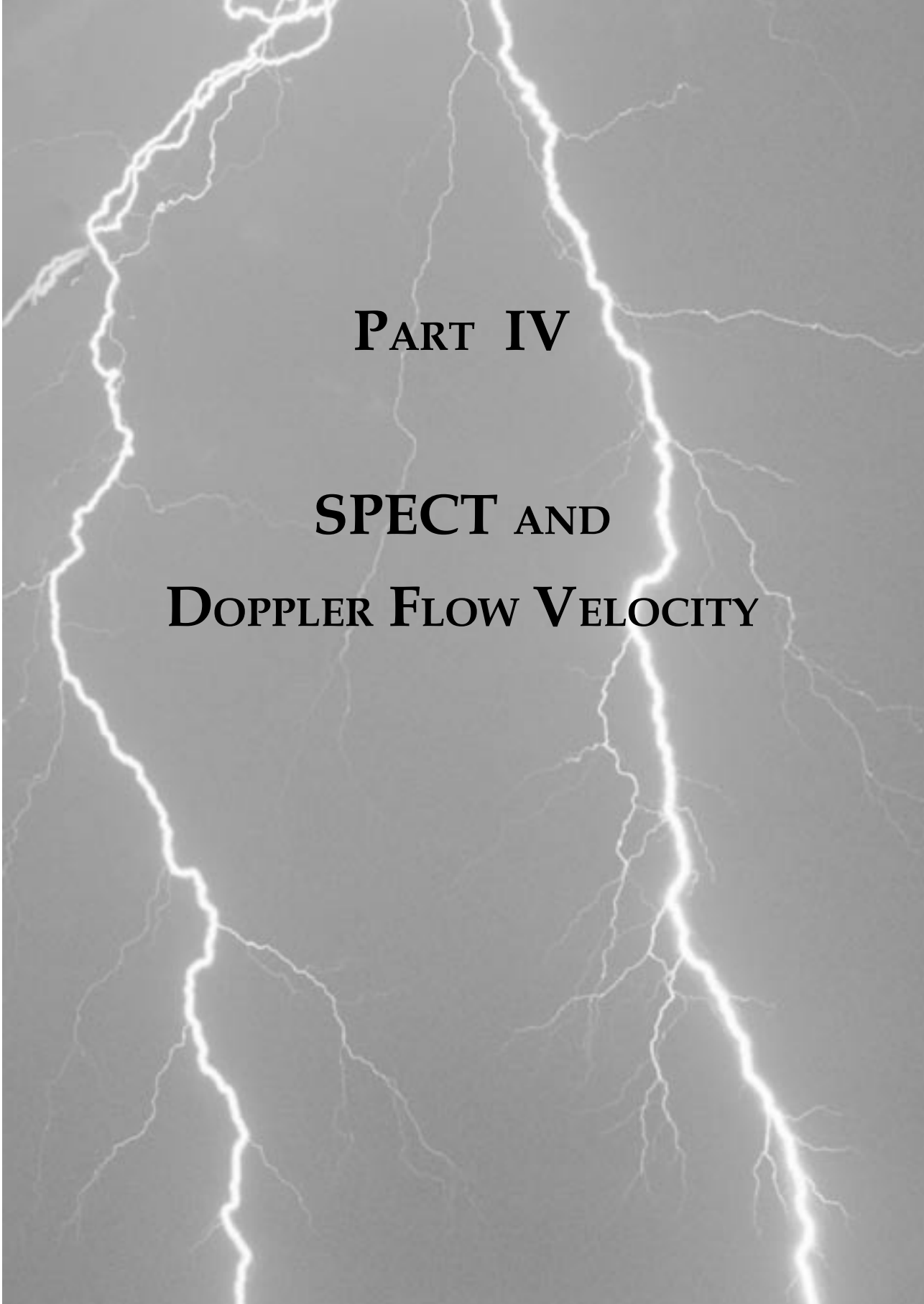

Part IV

SPECT and Doppler Flow Velocity

CHAPTER 9

Hemodynamic evaluation of saphenous vein coronary artery bypass grafts: relative merits of Doppler flow velocity and SPECT perfusion imaging

Liesbeth P. Salm
Jeroen J. Bax
J. Wouter Jukema
Susan E. Langerak
Hubert W. Vliegen
Paul Steendijk
Hildo J. Lamb
Albert de Roos
Ernst E. van der Wall

J Nucl Cardiol 2005; 12, 5, 545-552

ABSTRACT

Background: Coronary angiography is considered the gold standard in evaluating vein graft disease; however, angiography does not allow assessment of hemodynamic consequences of lesions. In this study, hemodynamic consequences of significant stenoses in vein grafts were evaluated by Doppler velocity assessment, and results were compared with single-photon emission computed tomography (SPECT) perfusion imaging.

Methods and Results: Angiography was performed in 58 patients after coronary artery bypass grafting because of recurrent chest pain. During the procedure, Doppler velocity measurements were acquired before and after administration of adenosine. Of 58 patients (with 78 vein grafts), 20 patients (with 24 vein grafts) underwent SPECT perfusion imaging.

Grafts were divided into those with non-significant percent diameter stenosis (<50%, n = 49), and those with significant percent diameter stenosis (≥50%, n = 29). When a cut-off value for coronary flow velocity reserve (CFVR) of 1.8 was applied, modest agreement (69%, $\kappa = 0.25$, $p<0.05$) between CFVR and angiography was shown. Agreement between SPECT and angiography was also modest (63%, $\kappa = 0.28$, p = NS). SPECT and CFVR provided comparable information in 20 of 24 grafts with available SPECT, illustrating good agreement (83%, $\kappa = 0.61$, $p = 0.001$).

Conclusions: Significant stenoses in vein grafts require further exploration to assess their hemodynamic significance. The Doppler velocity results agreed better with SPECT perfusion imaging than with percent diameter stenosis in the evaluation of vein graft function.

Introduction

Determination of stenosis severity by coronary angiography is considered the gold standard for the assessment of obstructive coronary artery disease, but the hemodynamic significance of a stenosis cannot be derived from the coronary angiogram (1;2), and additional diagnostic testing is required. Invasively, the hemodynamic consequences can be determined by flow velocity measurements by use of the Doppler flow wire at rest and during hyperemia, as well as calculation of the coronary flow velocity reserve (CFVR) (3;4). This technique has been extensively explored in native coronary arteries (5-8), but studies in bypass grafts are limited. In vein grafts in particular, discordance between the angiographic severity of the stenosis and the hemodynamic consequences occurs (4).

Myocardial perfusion imaging with single-photon emission computed tomography (SPECT) is a noninvasive imaging technique that also allows evaluation of the hemodynamic significance of stenotic lesions in coronary arteries or bypass grafts (9;10). For clinical routine use, noninvasive testing may be preferred. However, direct comparisons between the invasive flow wire measurements and noninvasive SPECT imaging for assessment of the hemodynamic significance of lesions in patients with vein grafts are lacking. Accordingly, the aim of this study was to evaluate the relationship between angiographic stenosis severity and CFVR in a large number of vein grafts, as well as to perform a comparison between the Doppler flow wire and SPECT perfusion imaging to evaluate the hemodynamic consequences of stenoses in vein grafts.

Methods

Study Population

A total of 58 patients with a history of coronary artery bypass grafting (CABG) underwent coronary angiography because of recurrent chest pain. All underwent Doppler flow velocity measurements, and in 20 patients SPECT perfusion imaging was performed. The protocol was approved by the local medical ethics committee and informed consent was obtained from all patients.

Coronary Angiography and Doppler Flow Velocity Measurements

Routine coronary angiography procedures were performed; vascular access was obtained via the femoral approach. Doppler flow velocity measurements were performed in vein grafts only. A 0.014-inch Doppler guide wire (FloWire, Cardiometrics, Mountain View, CA) was advanced proximal into the graft and adjusted until a stable blood flow velocity signal was acquired (3;4). After the bolus injection of 18 µg adenosine directly into the graft, hyperemic velocity was measured (11). When velocity returned to baseline, measurements were repeated. When two baseline measurements differed by more than 10%, a third measurement was obtained and values were averaged. Doppler flow velocity measurements were previously validated by comparison with flow meters (12;13) and good reproducibility of measurements was demonstrated (14).

Subsequently, angiography of the graft was performed according to the standard protocol. All percent diameter stenoses and percent area stenoses in either bypass graft or distal coronary arteries supplied by the graft were analyzed objectively by use of

quantitative coronary arteriography (QCA) by an independent core laboratory (Heart Core, Leiden, the Netherlands). If two or more stenoses were present in either graft or recipient vessels, the most severe lesion was considered the most flow limiting stenosis. Coronary bypass graft flow velocity was digitized offline by use of a computer with a custom-made software program. Digitized peak flow velocity from at least three cardiac cycles was averaged to calculate the average peak velocity (APV; cm/s), systolic peak velocity (SPV; cm/s), and diastolic peak velocity (DPV; cm/s) at baseline and during hyperemia by use of adenosine. CFVR was computed as the ratio of hyperemic to baseline APV, and diastolic-to-systolic velocity ratio (DSVR) as the ratio of DPV and SPV.

Gated SPECT Perfusion Imaging

For the gated SPECT examination, a 2-day stress-rest protocol was used (15). The stress protocol included a symptom-limited treadmill exercise test. Test endpoints were physical exhaustion, dyspnea, angina pectoris, significant decrease in blood pressure (>10 mmHg), or achievement of the maximum age-related heart rate. Technetium 99m tetrofosmin (500 MBq) was injected intravenously at peak exercise, which was continued for 1 minute after tracer injection. In patients unable to exercise (n = 10), adenosine stress was used. On the second day, resting images were obtained by use of 500 MBq Tc-99m tetrofosmin. The resting studies were acquired by use of electrocardiography gating, allowing assessment of left ventricular ejection fraction (LVEF) and left ventricular volumes (16).

Imaging was performed with a triple-head SPECT camera system (GCA 9300/HG, Toshiba Corporation, Tokyo, Japan) equipped with low-energy, high-resolution collimators. A 20% window was used around the 140-keV energy-peak of Tc-99m tetrofosmin. A total of 90 projections (step-and-shoot mode, 35 s/projection, total imaging time of 23 min) were obtained over a 360˚ circular orbit. Data were stored in a 64 x 64 matrix. The raw scintigraphic data were reconstructed by filtered backprojection via a Butterworth filter (cutoff frequency at 0.26 cycle/pixel; order 9). No attenuation correction was used. Reconstruction of the images yielded standard long- and short-axis projections perpendicular to the heart axis. Reconstructed slices were 6.4 mm in all projections. The short-axis slices were displayed in polar map format, adjusted for peak myocardial activity (100%). The myocardium was divided into 17 segments, as recently proposed (17). Segmental tracer activity was expressed as percentage of maximum. Perfusion defects on stress images were considered to be present when tracer activity was <75% of maximum tracer uptake. Mild to moderate defects were defined as having 50% to 75% of normalized tracer uptake and severe defects as having <50% of normalized tracer uptake. When significant fill-in (>10% increase of normalized tracer activity) of perfusion defects was observed on the resting images, segments were classified as reversible (ischemic); defects without fill-in were classified as irreversible (scar) (18). The individual segments on the SPECT images were assigned to the distinct native coronary arteries, according to recently published guidelines (17). The anastomoses of the bypass graft on the different native coronary arteries then defined the vascular territory that the graft perfused.

Statistical Analysis

Data are presented as mean ± SD. On the basis of QCA analysis, grafts were divided into two categories: those with nonsignificant percent diameter stenosis (<50%; n = 49), and those with significant percent diameter stenosis (≥50%; n = 29) in either graft or recipient vessel. Grafts were also divided into those with nonsignificant percent area stenosis (<80%; n = 52), and those with significant percent area stenosis (≥80%; n = 26).

Mean Doppler parameters were compared by Student t-test. A previously reported cut-off value for CFVR of 1.8 was used to distinguish between normal and diseased grafts (19). Agreements between the diagnostic modalities were assessed by use of κ statistics, with a κ value <0.4, between 0.4 and 0.75, and >0.75 representing modest, fair to good, and excellent agreement, respectively. The association between CFVR and percent diameter stenosis, and between CFVR and percent area stenosis on angiography was also assessed by use of Pearson correlation. A p-value <0.05 was considered statistically significant.

RESULTS

Study Population

A total of 58 patients were included in the study. Patient characteristics are presented in Table 9.1. Coronary angiography and Doppler velocity assessment was performed in 78 vein grafts. Mean time after CABG was 10.2 ± 5.2 years, ranging from 1 to 23 years. Bypass graft characteristics are shown in Table 9.2. The characteristics of the 20 patients who underwent SPECT imaging resembled those of the overall patient group. With regard to these 20 patients, the mean time after CABG was 10.3 ± 5.0 years, 30% of them had diabetes, and 60% were treated for hypertension. The time interval between the coronary angiography and SPECT imaging was 3.4 ± 2.8 months. No events happened between the examinations.

Number of patients	58
Male/female	48/10
Age (years)	66.4 ± 8.7
Diabetes mellitus	13 (22%)
Currently smoking	5 (9%)
Hypertension	30 (52%)
Hypercholesterolemia	45 (78%)
Prior myocardial infarction in bypass graft region	22 (38%)
Time after CABG (years)	10.2 ± 5.2

Table 9.1
Patient Characteristics
CABG = coronary artery bypass grafting

Number of bypass grafts	78
Single/sequential grafts	47/31
Vascular territory perfused by graft	
LAD	26 (33%)
LCX	29 (37%)
RCA	23 (30%)
Percentage diameter stenosis (QCA)	40 ± 33%
<50%	49
≥50%	29
Percent area stenosis (QCA)	52 ± 39%
<80%	52
≥80%	26

Table 9.2
Bypass Graft Characteristics
LAD = left anterior descending artery; LCX = left circumflex artery; RCA = right coronary artery

Coronary Angiography and Doppler Flow Velocity Measurements
In all 78 vein grafts coronary angiography was successfully performed. Stenosis severity, as measured by QCA, ranged from 0% to 100%, with a mean percent diameter stenosis of 40 ± 33% and a mean percent area stenosis of 52 ± 39%. On the basis of the QCA results, grafts were divided into those with angiographically nonsignificant percent diameter and area stenoses and those with significant percent diameter and area stenosis (Table 9.2).
Successful flow velocity signals were acquired in all bypass grafts. A biphasic flow velocity pattern, typical for vein grafts, was demonstrated in all 78 grafts. During Doppler velocity assessment, the heart rate and mean aortic pressure at baseline were 67 ± 12 beats/min and 97 ± 15 mm Hg, respectively. After adenosine injection, heart rate and mean aortic pressure did not change significantly. Mean Doppler velocity parameters per category are displayed in Table 9.3. Baseline peak velocities did not show a statistically significant difference between the significantly and nonsignificantly stenosed vessels, except for DPV. Doppler peak velocities with adenosine stress demonstrated significantly decreased values at ≥50% diameter stenosis, and ≥80% area stenosis. Accordingly, CFVR was significantly decreased in ≥50% diameter stenosis, and ≥80% area stenosis in vein grafts. These results are in concordance with those in previously reported studies on Doppler flow velocity in native coronary arteries (3;4).

Agreement between Coronary Angiography and Doppler Velocity
Percent diameter stenosis on angiography versus Doppler velocity
The individual data (except for 8 grafts with a total occlusion in the graft or recipient vessel) for CFVR as compared with percent diameter stenosis on angiography are shown in Figure 9.1 A. In all 70 grafts, CFVR ranged from 0.98 to 5.8. A moderate, inverse

correlation between percent diameter stenosis and CFVR existed (y = -0.0085x + 2.53; r = 0.30; p<0.05). In 49 grafts with <50% diameter stenosis, CFVR ranged from 1.4 to 5.8. In grafts with ≥50% stenosis, CFVR ranged from 0.98 to 3.4, demonstrating that percentage diameter stenosis on the coronary angiogram does not reliably reflect hemodynamic consequences of vein graft lesions. When the cut-off value for CFVR of 1.8 was applied, a modest agreement of 69% (κ = 0.25; p<0.05) between CFVR and percent diameter stenosis at coronary angiography was shown (Table 9.4). Disagreement between the two parameters was observed in 11 of 49 (22%) grafts with a stenosis <50%, and in 11 of 21 (52%) grafts with a stenosis ≥50%. The distribution of CFVR in categories with increasing percent diameter stenosis is shown in Figure 9.2 A.

	<50% DS	**≥50% DS**	**<80% AS**	**≥80% AS**
APV baseline (cm/s)	17.6 ± 9.2	14.4 ± 7.9	17.4 ± 9.3	14.6 ± 7.7
APV stress (cm/s)	38.6 ± 14.2	26.9 ± 12.8 †	37.8 ± 14.7	27.1 ± 12.4 §
CFVR	2.40 ± 0.79	1.99 ± 0.65 *	2.38 ± 0.77	1.97 ± 0.68 ‡
SPV baseline (cm/s)	13.7 ± 7.3	11.6 ± 7.3	13.4 ± 7.4	11.9 ± 7.2
SPV stress (cm/s)	29.9 ± 12.9	21.4 ± 10.1 †	29.3 ± 13.3	21.7 ± 9.2 §
DPV baseline (cm/s)	22.0 ± 12.4	16.5 ± 9.5 *	21.7 ± 12.4	16.6 ± 9.4 ‡
DPV stress (cm/s)	46.5 ± 17.0	30.9 ± 16.0 †	45.5 ± 17.4	31.1 ± 16.0 §
DSVR baseline	1.76 ± 0.77	1.76 ± 1.07	1.77 ± 0.75	1.73 ± 1.12
DSVR stress	1.67 ± 0.48	1.50 ± 0.57	1.68 ± 0.48	1.46 ± 0.56

Table 9.3

Mean Values of Flow Velocity Parameters

** p<0.05; † p<0.01 versus <50% diameter stenosis; ‡ p<0.05; § p<0.01 versus <80% area stenosis; DS = diameter stenosis; AS = area stenosis; APV = average peak velocity; SPV = systolic peak velocity; DPV = diastolic peak velocity; CFVR = coronary flow velocity reserve; DSVR = diastolic-to-systolic velocity ratio*

Doppler velocity	Coronary angiography			
	%DS <50%	%DS ≥50%	%AS <80%	%AS ≥80%
CFVR ≥1.8	38	11	41	8
CFVR <1.8	11	10	11	10
Total	49	21	52	18

Table 9.4

Agreement between CFVR and Percent Diameter and Area Stenoses on Coronary Angiography Only patent grafts were included (n = 70). %DS = percent diameter stenosis; %AS = percent area stenosis; CFVR = coronary flow velocity reserve

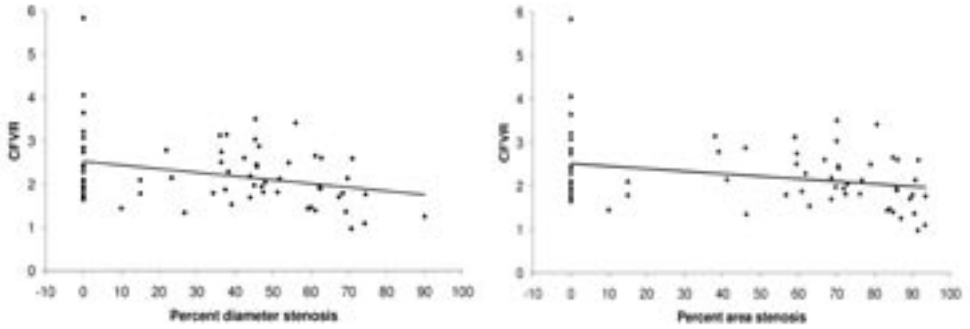

Figure 9.1

Scatterplot of CFVR versus percent diameter stenosis (A), and versus percent area stenosis (B). Grafts without a total occlusion are included (n = 70). Regression line for CFVR versus percent diameter stenosis represents the following: y = -0.0085x + 2.53, pearson regression coefficient r = 0.30, p<0.05. CFVR versus percent area stenosis yielded the following: y = -0.0085x + 2.52, r = 0.28, p<0.05.

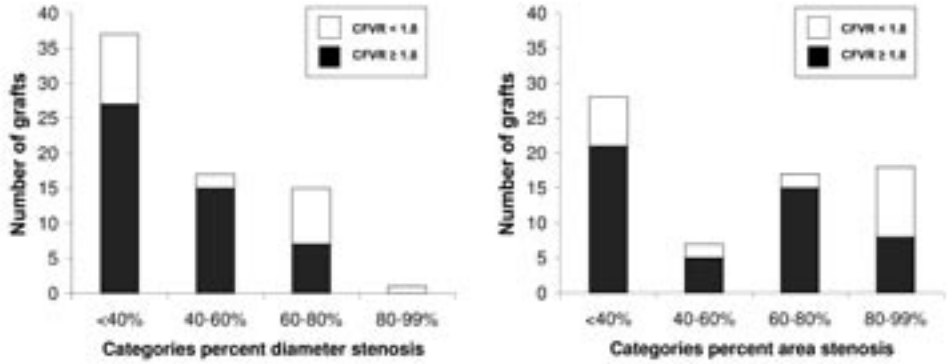

Figure 9.2

Distribution of CFVR (<1.8 versus ≥1.8) in grafts according to percent diameter stenosis (A), and percent area stenosis (B).

Percent area stenosis on angiography versus Doppler velocity

A moderate correlation was also demonstrated between percent area stenosis and CFVR (y = -0.0058x + 2.52; r = 0.28; p<0.05, Figure 9.1 B). When the cut-off value for CFVR of 1.8 for percent area stenosis of 80% were applied, a modestly improved agreement of 73% (κ = 0.33; p<0.01) as compared with percent diameter stenosis was shown. CFVR and percent area stenosis disagreed in 11 of 52 grafts (21%) with an area stenosis <80%, and in 8 of 18 grafts (44%) with an area stenosis ≥80%. In categories with an increasing percent area stenosis, allocation of CFVR is depicted in Figure 9.2 B.

Gated SPECT Perfusion Imaging

Gated SPECT in 20 patients demonstrated a mean LVEF of 54 ± 18% (range 24-85%). Mean left ventricular end-systolic and end-diastolic volumes were 66 ± 56 ml and 123 ± 70 ml, respectively. In the vascular territories supplied by 24 grafts, stress myocardial perfusion was normal in the territories allocated to 15 grafts, mildly to moderately reduced in territories of 4 grafts, and severely reduced in territories of 5 grafts. Rest perfusion was normal in 19 grafts, mildly to moderately reduced in 3 grafts, and severely reduced in 2 grafts. Accordingly, perfusion was normal in the vascular territory of 15 grafts, ischemia was present in the territory of 6 grafts, while irreversible defects (indicating scar tissue) were present in the territory of 3 grafts.

Agreement between Coronary Angiography and SPECT

Percent diameter stenosis on angiography versus SPECT

A modest agreement of 63% (15 of 24 grafts; $\kappa = 0.28$; $p = 0.13$) was demonstrated between SPECT and percent diameter stenoses on coronary angiography (Table 9.5). SPECT perfusion and percent diameter stenosis did not agree in 2 of 10 grafts (20%) with nonsignificant stenosis, and in 7 of 14 grafts (50%) with significant stenosis.

	Coronary angiography			
SPECT	%DS <50%	%DS ≥50%	%AS <80%	%AS ≥80%
Normal perfusion	8	7	10	5
Abnormal perfusion	2	7	2	7
Total	10	14	12	12

Table 9.5

Agreement between SPECT Perfusion and Coronary Angiography

Only grafts with available SPECT (n = 24) were included. %DS = percent diameter stenosis; %AS = percent area stenosis; SPECT = single-photon emission computed tomography

	Doppler velocity		
SPECT	CFVR ≥1.8	CFVR <1.8	Total
Normal perfusion	15	0	15
Abnormal perfusion	4	5	9
Total	19	5	24

Table 9.6

Agreement between CFVR and SPECT Perfusion

Only grafts with available SPECT (n = 24) were included. SPECT = single-photon emission computed tomography; CFVR = coronary flow velocity reserve

Percent area stenosis on angiography versus SPECT
SPECT and percent area stenoses showed fair agreement (17 of 24 grafts; 71%), when area stenoses <80% and ≥80% were considered nonsignificant or significant ($\kappa = 0.42$; $p<0.05$). Disagreement between SPECT and percent area stenosis occurred in 2 of 12 (17%) grafts with an area stenosis <80%, and in 5 of 12 grafts (42%) with an area stenosis ≥80%.

Agreement between Doppler Velocity and SPECT
In 15 of the 15 grafts (100%) with normal perfusion on SPECT, CFVR was ≥1.8 (Table 9.6). Conversely, in 5 of 9 grafts (56%) with abnormal perfusion on SPECT, CFVR showed a value <1.8. SPECT and Doppler velocity provided similar information in 20 of 24 grafts (83%; $\kappa = 0.61$), illustrating good agreement between SPECT and CFVR ($p = 0.001$).
Because the influence of scar tissue on CFVR is unpredictable, agreement between SPECT and CFVR was also established after exclusion of 3 grafts showing an irreversible perfusion defect. Of these 3 grafts, one had a CFVR <1.8, and 2 grafts had a CFVR >1.8. Agreement then improved to 90% (19 of 21 grafts; $\kappa = 0.74$).

Discussion
In this study the hemodynamic consequences of angiographically significant stenoses in vein grafts were explored by Doppler flow velocity assessment and SPECT perfusion imaging. The nonsignificant percent diameter stenoses on angiography showed a reduced CFVR in 22% and an abnormal SPECT study in 20%, indicating that these stenoses were hemodynamically significant. Alternatively, the angiographically significant percent diameter stenoses exhibited a normal CFVR in 52% and a normal SPECT in 50%, indicating that these stenoses were hemodynamically nonsignificant. In addition, agreements between angiography and CFVR or SPECT were only modest. Accordingly, the results demonstrate that the angiographic stenosis severity did not correctly reflect the presence or absence of hemodynamic consequences in vein grafts, indicating the need for additional testing to assess the hemodynamic significance of the angiographic findings. CFVR agreed better with SPECT perfusion imaging than with percent diameter stenosis, suggesting that CFVR may also be used to assess the hemodynamic significance of a vein graft lesion.

Doppler Flow Velocity Assessment in Vein Grafts
In early studies the coronary flow reserve (CFR) was introduced in order to evaluate the physiology of coronary artery stenoses, visualized at angiography (20;21). At that time, absolute coronary blood flow could only be measured by perivascular flow transducers in "open chest" procedures. CFR was therefore validated in animal models and patients undergoing open heart surgery (1;20;22), though clinical use remained limited. When the diameter of intravascular catheter-based Doppler ultrasound devices could be reduced to 0.018 inch, measurement of flow velocity and CFVR in coronary arteries in patients during catheterization was realized. Absolute blood flow correlated well with Doppler-derived flow velocity both in vitro and in vivo (12;13;23). Thereafter the value of Doppler CFVR was extensively researched in native coronary arteries (4;8;24;25). However, studies focusing on the use of Doppler measurements in vein grafts are limited. In our

study, the mean resting flow (APV) was not different in the grafts with ≥50% diameter stenosis (or ≥80% area stenosis) or without a significant stenosis on angiography, confirming that resting flow frequently remains normal despite the presence of stenoses, as demonstrated previously for native coronary arteries (3;20). However, the mean CFVR was significantly lower in the grafts with a significant stenosis on angiography (Table 9.3). Still, only a moderate inverse correlation was demonstrated for CFVR and quantitative analysis of the coronary angiogram (r = 0.30 for percent diameter stenosis; r = 0.28 for percent area stenosis) with a wide range for CFVR in both nonsignificant and significant stenoses. Indeed, when individual data were analyzed, many grafts with an angiographically significant stenosis had preserved CFVR and some grafts without a significant stenosis had reduced CFVR indicating the relative inability to determine the hemodynamic significance from angiography alone.

Value of SPECT Perfusion Imaging

SPECT perfusion imaging is a well-established technique by which to detect obstructive coronary artery disease by evaluating regional myocardial perfusion at rest and during stress. Excellent sensitivities and specificities of SPECT to detect stenoses in native coronary arteries were demonstrated (9;18;26). In addition, studies evaluating patients after CABG with SPECT showed good results for the assessment of graft disease. In 50 patients with 119 bypass grafts a sensitivity of 80% with a specificity of 87% for the detection of >50% stenosis have been reported (10). In another study 88 grafts were studied late after surgery (4.0 ± 1.2 years) by SPECT, and a comparable sensitivity and specificity (83% and 88%, respectively) for the detection of >50% stenosis were shown (27).

However, the agreement between SPECT and angiography is not perfect (5). In this study SPECT perfusion imaging agreed moderately with percent diameter stenosis (63%; $\kappa = 0.28$; p = NS). In particular, 20% of nonsignificant stenoses on angiography had abnormal SPECT perfusion results, and 50% of the angiographically significant stenoses had normal SPECT results.

Agreement between Doppler CFVR and SPECT

More recently, for SPECT imaging the emphasis has shifted from detection of coronary artery disease to hemodynamic evaluation of stenoses. Comparative studies between SPECT imaging and Doppler assessment have been performed, demonstrating a good agreement (ranging from 72% to 96%) between these two techniques for the assessment of the hemodynamic consequence of an intermediate native coronary artery stenosis (5;19;28-30). In these studies, the cut-off value for CFVR to predict an abnormal SPECT study varied from 1.7 to 2.0. The best concordance (96%) between between Doppler assessment and SPECT imaging was obtained when a cut-off value for CFVR of 1.8 was used (19).

Studies evaluating the hemodynamic consequences of bypass graft lesions are lacking. In this study, good agreement between Doppler assessment (with the use of the cut-off value of 1.8 for CFVR) and SPECT imaging was demonstrated in vein grafts (83%; $\kappa = 0.61$; p = 0.001), suggesting that both SPECT imaging and CFVR assessment may be used

to characterize the hemodynamic consequences of vein graft stenoses. The agreement increased to 90% ($\kappa = 0.74$) when grafts subtending an area with infarcted tissue were excluded. In these regions SPECT findings are abnormal (irreversible defects), whereas CFVR may be preserved, if an intact graft subtends a partially infarcted region.

Clinical Implications

Vein graft disease occurs frequently after CABG, affecting 48% of grafts at 5 years and 81% at ≥15 years (31). Still, revascularization after initial CABG is required in 19% of patients by 10 years (32). Our study shows that coronary angiography alone, currently widely used as gold standard, does not reliably reflect the hemodynamic consequences of stenoses in vein grafts. Thus further assessment of stenoses in vein grafts or recipient vessels is required. This study suggests that either SPECT perfusion imaging or CFVR assessment may be used to characterize the hemodynamic consequence of a vein graft lesion.

Limitations

SPECT perfusion imaging was not available in all patients who underwent coronary angiography with Doppler velocity measurements. For logistical reasons, this was only performed in 20 patients; in particular, the number of graft-related region with ischemia was small. However, the characteristics of the patients who underwent SPECT imaging resembled those of the entire population.

No attenuation correction was performed with SPECT imaging, and therefore, some SPECT perfusion defects with normal CFVR may have been caused by attenuation.

Pressure measurements were not performed. The fractional flow reserve can be calculated as the ratio of distal coronary and aortic pressure during maximal hyperemia (33). Large studies investigating the fractional flow reserve in vein or arterial grafts are lacking.

Conclusion

Significant stenoses in vein grafts require further exploration to assess their hemodynamic significance. The Doppler velocity results agreed better with SPECT perfusion imaging than with percent diameter stenosis in the evaluation of vein graft function.

REFERENCES

1. White CW, Wright CB, Doty DB et al. Does visual interpretation of the coronary arteriogram predict the physiologic importance of a coronary stenosis? N Engl J Med 1984;310:819-24.
2. Topol EJ, Nissen SE. Our preoccupation with coronary luminology. The dissociation between clinical and angiographic findings in ischemic heart disease. Circulation 1995;92:2333-42.
3. Ofili EO, Labovitz AJ, Kern MJ. Coronary flow velocity dynamics in normal and diseased arteries. Am J Cardiol 1993;71:3d-9d.
4. White CW. Clinical applications of Doppler coronary flow reserve measurements. Am J Cardiol 1993;71:10d-6d.
5. Heller LI, Cates C, Popma J et al. Intracoronary Doppler assessment of moderate coronary artery disease: comparison with 201Tl imaging and coronary angiography. FACTS Study Group. Circulation 1997;96:484-90.
6. Ferrari M, Schnell B, Werner GS, Figulla HR. Safety of deferring angioplasty in patients with normal coronary flow velocity reserve. J Am Coll Cardiol 1999;33:82-7.
7. Piek JJ, Boersma E, Di Mario C et al. Angiographical and Doppler flow-derived parameters for assessment of coronary lesion severity and its relation to the result of exercise electrocardiography. DEBATE study group. Doppler Endpoints Balloon Angioplasty Trial Europe. Eur Heart J 2000;21:466-74.
8. Chamuleau SA, Tio RA, de Cock CC et al. Prognostic value of coronary blood flow velocity and myocardial perfusion in intermediate coronary narrowings and multivessel disease. J Am Coll Cardiol 2002;39:852-8.
9. Mahmarian JJ, Boyce TM, Goldberg RK, Cocanougher MK, Roberts R, Verani MS. Quantitative exercise thallium-201 single photon emission computed tomography for the enhanced diagnosis of ischemic heart disease. J Am Coll Cardiol 1990;15:318-29.
10. Lakkis NM, Mahmarian JJ, Verani MS. Exercise thallium-201 single photon emission computed tomography for evaluation of coronary artery bypass graft patency. Am J Cardiol 1995;76:107-11.
11. Wilson RF, Wyche K, Christensen BV, Zimmer S, Laxson DD. Effects of adenosine on human coronary arterial circulation [see comments]. Circulation 1990;82:1595-606.
12. Doucette JW, Corl PD, Payne HM et al. Validation of a Doppler guide wire for intravascular measurement of coronary artery flow velocity. Circulation 1992;85:1899-911.
13. Sudhir K, Hargrave VK, Johnson EL et al. Measurement of volumetric coronary blood flow with a Doppler catheter: validation in an animal model. Am Heart J 1992;124:870-5.
14. Di Mario C, Gil R, Serruys PW. Long-term reproducibility of coronary flow velocity measurements in patients with coronary artery disease. Am J Cardiol 1995;75:1177-80.
15. Berman DS, Kiat HS, Van Train KF, Germano G, Maddahi J, Friedman JD. Myocardial perfusion imaging with technetium-99m-sestamibi: comparative analysis of available imaging protocols. J Nucl Med 1994;35:681-8.
16. Germano G, Berman DS. Quantitative gated SPECT. J Nucl Med 2001;42:528-9.
17. Cerqueira MD, Weissman NJ, Dilsizian V et al. Standardized myocardial segmentation and nomenclature for tomographic imaging of the heart: a statement for healthcare professionals from the Cardiac Imaging Committee of the Council on Clinical Cardiology of the American Heart Association. Circulation 2002;105:539-42.
18. Elhendy A, Bax JJ, Poldermans D. Dobutamine stress myocardial perfusion imaging in coronary artery disease. J Nucl Med 2002;43:1634-46.
19. Deychak YA, Segal J, Reiner JS et al. Doppler guide wire flow-velocity indexes measured distal to coronary stenoses associated with reversible thallium perfusion defects. Am Heart J 1995;129:219-27.
20. Gould KL, Lipscomb K, Hamilton GW. Physiologic basis for assessing critical coronary stenosis. Instantaneous flow response and regional distribution during coronary hyperemia as measures of coronary flow reserve. Am J Cardiol 1974;33:87-94.
21. Gould KL, Lipscomb K. Effects of coronary stenoses on coronary flow reserve and resistance. Am J Cardiol 1974;34:48-55.
22. Gould KL, Kirkeeide RL, Buchi M. Coronary flow reserve as a physiologic measure of stenosis severity. J Am Coll Cardiol 1990;15:459-74.
23. Labovitz AJ, Anthonis DM, Cravens TL, Kern MJ. Validation of volumetric flow measurements by means of a Doppler-tipped coronary angioplasty guide wire. Am Heart J 1993;126:1456-61.
24. Serruys PW, De Bruyne B, Carlier S et al. Randomized comparison of primary stenting and provisional balloon angioplasty guided by flow velocity measurement. Doppler Endpoints Balloon Angioplasty Trial Europe (DEBATE) II Study Group. Circulation 2000;102:2930-7.
25. Albertal M, Regar E, Van Langenhove G et al. Value of coronary stenotic flow velocity acceleration in prediction of angiographic restenosis following balloon angioplasty. Eur Heart J 2002;23:1849-53.
26. Maddahi J, Kiat H, Van Train KF et al. Myocardial perfusion imaging with technetium-99m sestamibi SPECT in the evaluation of coronary artery disease. Am J Cardiol 1990;66:55E-62E.

27. Pinarli AE, Gursurer M, Aksoy M, Yavuz A, Ersek B. Assessment of Graft Patency Rate After Coronary Artery Bypass Surgery by Exercise TL-201 Single Photon Emission Computed Tomography. Int J Angiol 1998;7:313-6.
28. Miller DD, Donohue TJ, Younis LT et al. Correlation of pharmacological 99mTc-sestamibi myocardial perfusion imaging with poststenotic coronary flow reserve in patients with angiographically intermediate coronary artery stenoses. Circulation 1994;89:2150-60.
29. Joye JD, Schulman DS, Lasorda D, Farah T, Donohue BC, Reichek N. Intracoronary Doppler guide wire versus stress single-photon emission computed tomographic thallium-201 imaging in assessment of intermediate coronary stenoses. J Am Coll Cardiol 1994;24:940-7.
30. Verberne HJ, Piek JJ, van Liebergen RA, Koch KT, Schroeder-Tanka JM, van Royen EA. Functional assessment of coronary artery stenosis by doppler derived absolute and relative coronary blood flow velocity reserve in comparison with (99m)Tc MIBI SPECT. Heart 1999;82:509-14.
31. Fitzgibbon GM, Kafka HP, Leach AJ, Keon WJ, Hooper GD, Burton JR. Coronary bypass graft fate and patient outcome: angiographic follow-up of 5,065 grafts related to survival and reoperation in 1,388 patients during 25 years [see comments]. J Am Coll Cardiol 1996;28:616-26.
32. Weintraub WS, Jones EL, Craver JM, Guyton RA. Frequency of repeat coronary bypass or coronary angioplasty after coronary artery bypass surgery using saphenous venous grafts. Am J Cardiol 1994;73:103-12.
33. Kern MJ. Coronary physiology revisited : practical insights from the cardiac catheterization laboratory. Circulation 2000;101:1344-51.

EDITORIAL

Defining the "gold standard": A changing paradigm

Ami E. Iskandrian

J Nucl Cardiol 2005; 12, 5, 520-522

At the inception of nuclear cardiology, the accuracy of perfusion (planar and single-photon emission computed tomography [SPECT]) and function (first-pass and gated equilibrium radionuclide angiography) was assessed against percent diameter stenosis (DS) by coronary angiography, a tradition that has changed very little over the past three decades and has spilled over to other imaging methods such as stress two-dimensional echocardiography and magnetic resonance (1). The foundation for such an approach was deeply rooted on the elegant work by Gould et al (2;3) showing a decline in the hyperemic coronary blood flow at approximately 50% DS of a coronary vessel in the animal model. Scores of articles using this threshold have not only shown that imaging works but, in the process, have reinforced the validity of DS as a measure of stenosis severity (1).

Then came the revelations that DS did not agree well with physiologic severity of stenosis when the latter was assessed by catheter-based techniques or by positron emission tomography. The pioneer work of many groups, notably those from the same institution as the authors of the current article in the Journal (4), showed a significant scatter between measures of physiologic severity (flow velocity reserve ratio, fractional flow reserve, and stenosis resistance) with DS, even when measured quantitatively by state-of-the-art methods (4-10).

These results, as important as they are, are not unexpected, as coronary atherosclerosis in humans differs from ligature-induced stenosis in animal models in multiple ways. These include the presence of diffuse disease and differences in diameter of the vessel, length of stenosis, entrance and exit stenosis angles, location, serial lesions, endothelial dysfunction, microvascular dysfunction, vasomotion, and collaterals. It is intuitive to conclude that, if there is discordance between catheter-based physiologic measures of coronary stenosis and DS, then there must also be discordance between DS and imaging methods that reflect the physiologic relevance of stenosis severity, such as gated SPECT perfusion imaging. Such a confirmation has been previously reached in native coronary vessels and in the current study in bypass grafts after coronary artery bypass graft surgery (CABG).

Obviously, with SPECT perfusion imaging, several factors affect regional myocardial tracer concentration in addition to myocardial blood flow (MBF) or, more precisely, myocardial blood volume. These include the changes in first-pass extraction fraction in relation to flow (which is tracer-dependent and has considerable species and individual differences), type of stress, type of imaging protocol, relative changes in MBF in relation to changes in cardiac output, myocardial viability, tracer kinetics, metabolic alterations, attenuation, scatter, and depth resolution (1). The differences in regional tracer concentration reflect relative flow differences rather than absolute or hyperemic MBF (relative flow reserve ratio [peak/resting flow] in culprit lesion compared with a normal zone). Given this complexity in the interrelationship between MBF and tracer concentration, it is not unexpected that imaging could not identify all coronary lesions or all patients with coronary lesions by coronary angiography. Experience has taught us another valuable lesson: interventions (such as statin therapy or conventional antianginal medications) that have little effect on DS could remarkably alter the perfusion results.

One final point worth mentioning is that catheter-based methods for assessing stenosis severity do not provide information on the area of myocardium at risk. Studies during stress, during rest, or with temporary balloon occlusion at the time of angioplasty have consistently shown a wide variability between coronary angiography and the area of ischemic myocardium or size of myocardial infarction (1). It would seem that those who try hard to show a perfect correlation between DS and imaging are indeed missing the point that a perfect correlation is neither logical nor expected and the beauty of imaging is the fact that it provides independent and complementary information to coronary angiography. And thank goodness for that; otherwise, it would have merely provided redundant information (11). These features of perfusion imaging explain very well why and how SPECT imaging works so well in risk assessment. Our challenges are to better understand the mechanisms of why few patients with left-main or three-vessel disease show no reversible perfusion abnormalities, to determine how to define ischemia in regions with prior partial-thickness infarcts, and to keep the pressure on industry about our needs for perfusion tracers with improved physical and biologic kinetics.

With regard to patients with prior coronary revascularization, both percutaneous coronary interventions and CABG have witnessed major changes in the past decade. The number of percutaneous coronary intervention procedures now exceeds those with CABG, and those patients referred to CABG are likely to be sicker, with more advanced disease and poorer target vessels. This shift is important to keep in mind, as American College of Cardiology/American Heart Association guidelines cite studies from a much earlier time with a different patient mix. It is not unusual now to see patients with recurrent symptoms at one year or earlier after CABG, and the five-year honeymoon period cited in these guidelines may apply to fewer patients (12-14).

In this issue of the *Journal*, Salm et al (4) examined the correlation between DS, Doppler flow velocity (78 grafts in 58 patients), and SPECT results (24 grafts in 20 patients) in patients after CABG. On the basis of 50% DS and a flow velocity reserve ratio of 1.8,

there was only a modest correlation between DS and reserve ratio or between SPECT and DS (4). However, SPECT and reserve ratios provided comparable data in 20 of 24 grafts (83%). This study therefore extends the concepts gained in patients with native coronary stenosis to those with graft lesions. There are a few features of the study worth mentioning. First, this must have been an unusual group of patients who had CABG because there were only 1.2 grafts per patient among those who had SPECT imaging. Second, the use of 50% DS by the group who defamed this measurement appears to be interesting especially in vein grafts, which are known to be of larger diameter than native vessels. Third, we do not know from this study how to interpret the data in patients with more grafts and more severe disease such as stenosis in a graft to one branch of the left circumflex artery but no disease in a second branch, or vice versa (or any similar scenario in a different vascular bed). Fourth, we have no information on flow velocity reserve ratio in a control vessel for reasons discussed previously (perfusion pattern reflects relative rather than absolute flow reserve ratio). Finally, we do not know whether the adenosine dose was optimal in all grafts in all locations to produce a maximal response.

Nevertheless, the importance of this study rests on the need for a constant reminder that DS should be abandoned as a gold standard and future studies should use physiologic measures of coronary stenosis, which unfortunately are invasive and not that easy to perform by less expert individuals than those in the current study. This should not, however, be a green light signal that any discordance between SPECT and coronary angiography, which is still the most widely available method, should be explained by limitations of coronary angiography in every patient. The truth is probably that no single method has a monopoly on how to define the "gold standard" of ischemia, but at least there has been a shift in the paradigm and SPECT results are not always made the scapegoat (false positive or false negative). This observation did not go unnoticed by the Food and Drug Administration, which now does not insist on using coronary angiography as the "gold standard" for approving new products of interest to our field.

REFERENCES

1. Iskandrian AE, Verani MS. Nuclear cardiac imaging principles and applications (3rd ed), Oxford University Press, New York 2003.
2. Gould KL, Lipscomb K, Hamilton GW. Physiologic basis for assessing critical coronary stenosis. Instantaneous flow response and regional distribution during coronary hyperemia as measures of coronary flow reserve. Am J Cardiol 1974;33:87–94.
3. Gould KL, Kirkeeide RL, Buchi M. Coronary flow reserve as a physiologic measure of stenosis severity. J Am Coll Cardiol 1990;15:459–474.
4. Salm LP, Bax JJ, Jukema JW, et al. Hemodynamic evaluation of saphenous vein coronary artery bypass grafts relative merits of Doppler flow velocity and SPECT perfusion imaging. J Nucl Cardiol 2005;12:545–552.
5. Serruys PW, De Bruyne B, Carlier S, et al. Randomized comparison of primary stenting and provisional balloon angioplasty guided by flow velocity measurement. Doppler Endpoints Balloon Angioplasty Trial Europe (DEBATE) II Study Group. Circulation 2000;102:2930–2937.
6. Albertal M, Regar E, Van Langenhove G, et al. Value of coronary stenotic flow velocity acceleration in prediction of angiographic restenosis following balloon angioplasty. Eur Heart J 2002;23:1849–1853.
7. Kern MJ. Coronary physiology revisited practical insights from the cardiac catheterization laboratory. Circulation 2000;101:1344–1351.
8. Pijls NHJ, Van Son JAM, Kirkeeide RL, De Bruyne B, Gould KL. Experimental basis of determining maximum coronary, myocardial and collateral blood flow by pressure measurements for assessing functional stenosis severity before and after PTCA. Circulation 1993;87:1354–1367.
9. Piek JJ, Van Liebergen RAM, Koch KT, Peters RJ, David GK. Clinical, angiographic and hemodynamic predictors of recruitable collateral flow assessed during balloon angioplasty coronary occlusion. J Am Coll Cardiol 1997;29:275–282.
10. Heller LI, Cates C, Popma J, et al. Intracoronary Doppler assessment of moderate coronary artery disease: comparison with 201Tl imaging and coronary angiography. FACTS Study Group, Circulation 1997;96:484–490.
11. Shaw LJ, Iskandrian AE. Prognostic value of gated myocardial perfusion SPECT. J Nucl Cardiol 2004;11:171–185.
12. Gibbons RJ, Abrams J, Chatterjee K, et al. ACC/AHA 2002 guideline update for the management of patients with chronic stable angina—summary article a report of the American College of Cardiology/American Heart Association Task Force on practice guidelines (Committee on the Management of Patients With Chronic Stable Angina). J Am Coll Cardiol 2003;41:159–168.
13. Gibbons RJ, Balady GJ, Bricker JT, et al. ACC/AHA 2002 guideline update for exercise testing: summary article: a report of the American College of Cardiology/American Heart Association Task Force on Practice Guidelines (Committee to Update the 1997 Exercise Testing Guidelines). Circulation 2002;106:1883–1892.
14. Cardiac radionuclide imaging. ACC/AHA/ASNC 2003 guideline update for the clinical use. Available from: URL www.acc.org. Accessed June 28, 2005.

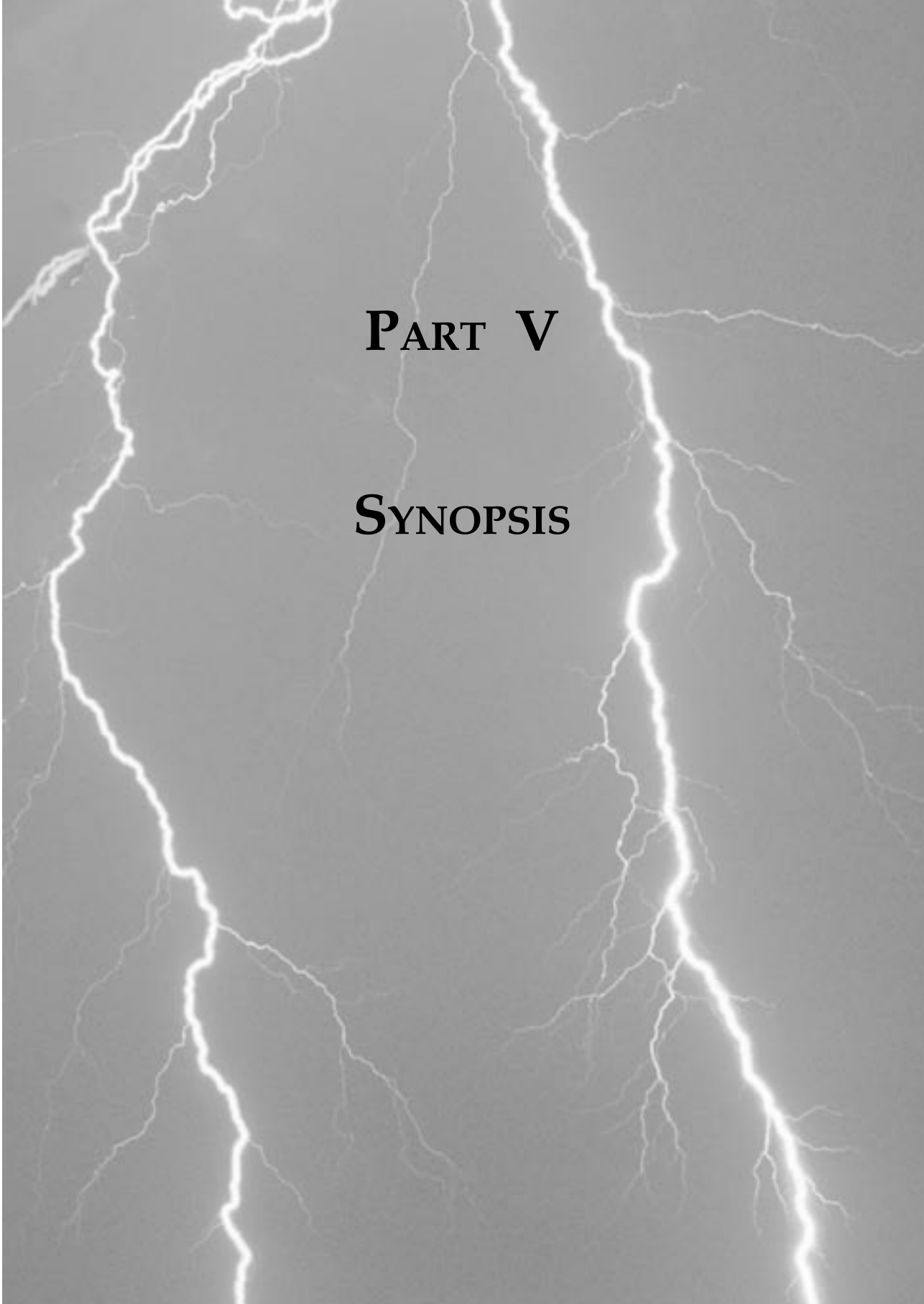

Part V

Synopsis

Chapter 10

Summary and future perspectives

Introduction

Coronary artery bypass grafting (CABG) is a commonly performed surgical procedure for alleviation of symptoms and prolonging survival for patients with coronary heart disease (CHD). Bypass graft disease is a common consequence, requiring coronary angiography for diagnosis. Coronary angiography is an invasive procedure that includes arterial puncture, x-ray exposition, and hospitalization. Complications include ventricular arrhythmias, myocardial infarction, cardiac perforation, necessary emergency CABG, and death, even though the risks are small. A noninvasive diagnostic method for the assessment of bypass graft anatomy and function is of great benefit. The aim of the thesis is to describe multiple modalities to examine coronary artery bypass grafts, and to further develop noninvasive imaging techniques to detect stenoses in native coronary arteries and bypass grafts in patients who experienced recurrent chest pain after CABG. **Part I** of this thesis **(Chapters 1 and 2)** reviews the research that has been performed in evaluating bypass grafts noninvasively using cardiovascular magnetic resonance (CMR) and computed tomography in earlier studies.

Part II Cardiovascular magnetic resonance

This part of the thesis focuses on CMR flow velocity imaging in vein and arterial grafts. The aim of the study, described in **Chapter 3**, was to retrospectively test two previously described analysis methods of CMR flow measurements, and to compare their diagnostic accuracy in detecting diseased vein grafts. In 125 vein grafts of 68 patients volume flow parameters (volume flow, systolic and diastolic peak flow, diastolic-to-systolic flow ratio at rest and during adenosine stress, and flow reserve) were derived from the CMR velocity maps. Method 1 implemented basal flow <20 ml/min or flow reserve <2, yielding a sensitivity and specificity of 70% and 38% in the detection of a diseased graft or recipient vessel. Method 2 used receiver operating characteristic (ROC) curve analysis and implemented all significant volume flow parameters in a logistic regression model, yielding a sensitivity of 74% with a specificity of 68% in the detection of a diseased graft or recipient vessel. Evaluating single and sequential grafts separately, this method yielded a sensitivity and specificity of 79% and 87% for single grafts, and 62% and 94% for sequential grafts in the detection of ≥50% stenosis in grafts or recipient vessels. Using ROC curve analysis with logistic regression the specificity of the analysis method improved considerably. Best results were acquired when single and sequential grafts were separately analyzed.

In **Chapter 4**, two analysis methods for the CMR flow velocity maps, i.e. velocity and volumetric flow, are compared using flow velocity maps of vein grafts. Forty-nine patients with previous bypass surgery underwent coronary angiography and CMR with flow velocity measurements of single vein bypass grafts. Volume flow and velocity analysis of the CMR velocity maps was performed and compared. Bland-Altman analysis showed close agreement between both analyses. Comparison of ROC areas-under-the-curve of both analyses revealed no significant differences for detection of stenoses ≥70%. Diagnostic accuracy for volume flow and velocity parameters was 92% and 93%, respectively. Velocity analysis appears to be the method of preference, because this approach is less time-consuming and has a similar diagnostic accuracy as volume flow analysis.

The hemodynamic significance of a bypass graft stenosis may not always accurately be determined from a coronary angiogram. A variety of diagnostic tests (invasive or noninvasive) are available to further characterize the hemodynamic consequence of a lesion. The objective of the study, presented in **Chapter 5**, was to perform a head-to-head comparison between single photon emission computed tomography (SPECT) perfusion imaging and CMR to evaluate hemodynamic significance of angiographic findings in bypass grafts. Fifty-seven arterial and vein grafts in 25 patients were evaluated by angiography, SPECT perfusion imaging, and coronary flow velocity reserve determination by CMR. Based on angiography and SPECT, 4 different groups could be identified: 1) no significant stenosis (<50%), normal perfusion; 2) significant stenosis (≥50%), abnormal perfusion; 3) significant stenosis, normal perfusion (no hemodynamic significance); and 4) no significant stenosis, abnormal perfusion (suggesting microvascular disease). Complete evaluation was obtained in 46 grafts. SPECT and CMR provided similar information in 37 of 46 (80%) grafts, illustrating good agreement ($\kappa = 0.61$, $p<0.001$). Eight grafts perfused a territory with scar tissue. When agreement between SPECT and CMR was restricted to grafts without scar tissue, it improved to 84% ($\kappa = 0.68$). Integration of angiography with SPECT categorized 14 lesions in group 1; 23 in group 2; 6 in group 3; and 3 in group 4. SPECT and CMR agreement per group was 86%, 78%, 100% and 33%, respectively. Head-to-head comparison showed good agreement between SPECT and CMR for functional evaluation of bypass grafts. CMR may offer an alternative method to SPECT for functional characterization of angiographic lesions.

In **Chapter 6**, a novel CMR phase-contrast sequence to measure flow velocity in arterial and vein grafts is introduced. The purpose of the study was to validate a CMR high-resolution, phase-contrast sequence for quantifying flow in small and large vessels, and to demonstrate its feasibility to measure flow in bypass grafts. A breathhold, echo planar imaging (EPI) sequence was developed and validated in a flow phantom using a fast field echo (FFE) sequence as reference. In 17 healthy volunteers aortic flow was measured using both sequences. In 5 patients flow in the left internal mammary artery (LIMA) graft and aorta was measured at rest and during adenosine stress, and coronary flow reserve (CFR) was calculated; in 7 patients vein graft flow velocity was measured. When using the flow pump, the EPI sequence yielded an excellent correlation with the FFE sequence ($r = 0.99$; $p<0.001$ for all parameters). In healthy volunteers, aortic volume flow correlated well ($r = 0.88$; $p<0.01$). In patients, mean LIMA CFR was 2.70 ± 0.88 for nonstenosed grafts. Percentage LIMA flow of cardiac output was $0.71 \pm 0.17\%$ at rest, and $1.56 \pm 0.52\%$ during adenosine stress ($p<0.01$). For nonstenosed single vein grafts, mean average peak velocity was 11.6 ± 2.4 cm/s. The high-resolution, breathhold CMR velocity-encoded sequence correlated well with a free-breathing, FFE sequence. Using the EPI sequence, it is feasible to measure flow velocity in both LIMA and vein grafts, and in the aorta.

PART III COMPUTED TOMOGRAPHY

Part III of the thesis concentrates on multidetector row computed tomography (MDCT) imaging of coronary artery bypass grafts. In **Chapter 7**, a comprehensive assessment by 16-detector row CT of patients after CABG is investigated. MDCT is a versatile modality to

evaluate stenoses in native coronary arteries and bypass grafts. Acquired MDCT data can additionally be used to assess left ventricular ejection fraction (LVEF). The purpose was to use MDCT for the assessment of bypass graft and coronary artery disease combined with evaluation of LVEF. Twenty-five patients underwent 16-detector-row CT examination and coronary angiography. Bypass grafts and nongrafted coronary artery segments at MDCT were evaluated on eligibility, patency and ≥50% stenosis. The MDCT data set was used to calculate LVEF and was divided into patients with no/subendocardial/transmural myocardial infarctions. Ninety vessels were evaluated: 14 arterial grafts, 53 vein grafts, and 23 nongrafted vessels. Of 225 segments, 17 were ineligible for evaluation because of metal clips. With MDCT, patency in segments of arterial grafts/vein grafts/nongrafted vessels could be evaluated with high accuracy in 100%/100%/97% of segments. In arterial grafts stenoses ≥50% did not occur at angiography, which was for all eligible segments correctly diagnosed with MDCT. Stenosis ≥50% could be correctly detected by MDCT with a sensitivity/specificity of 100%/94% for vein grafts, and 100%/89% for nongrafted vessels. Negative predictive value (NPV) was 100% for vein grafts and nongrafted vessels. In patients with transmural myocardial infarction, MDCT revealed a significant lower LVEF as compared with patients without or with subendocardial myocardial infarction ($p<0.05$). Comprehensive assessment of bypass grafts, nongrafted vessels, and LVEF is feasible with MDCT. Owing to the high NPV, this noninvasive approach may be used as gatekeeper before coronary angiography.

In order to evaluate MDCT accuracy, the aim of the study portrayed in **Chapter 8**, was to compare MDCT global and regional left ventricular (LV) function assessment with echocardiography and CMR. In 25 patients, who were referred for noninvasive angiography with 16-detector row CT, LV function assessment was also performed. A subsequent echocardiogram was performed, and in a subgroup of patients, CMR examination was completed to evaluate LV function. For global function assessment, LVEF was calculated. Regional LV function was scored using a 17-segment model and a 4–point scoring system. MDCT agreed well with echocardiography for the assessment of LVEF ($r = 0.96$; bias 0.54%; $p<0.0001$), and regional LV function ($\kappa = 0.78$). Eight patients had no contra-indications and gave informed consent for CMR examination. A fair correlation between MDCT and CMR was demonstrated in the assessment of LVEF ($r = 0.86$; bias –1.5%; $p<0.01$). Regional LV function agreement between MDCT and CMR was good ($\kappa = 0.86$). MDCT agreed well with both echocardiography and CMR in the assessment of global and regional LV function. Global and regional LV function may accurately be evaluated by 16-detector row CT, and can be added to a routine CT image analysis protocol without need for additional contrast or imaging time.

PART IV SPECT AND DOPPLER FLOW VELOCITY

Part IV focuses on the hemodynamic consequences of vein graft lesions. Coronary angiography is considered the gold standard in evaluating vein graft disease. However, angiography does not allow assessment of hemodynamic consequences of lesions. In the study presented in **Chapter 9**, hemodynamic consequences of significant stenoses in vein grafts were evaluated by Doppler velocity assessment, and results were compared with SPECT perfusion imaging. Coronary angiography was performed in 58

patients after CABG because of recurrent chest pain. During the procedure, Doppler velocity measurements were acquired before and after administration of adenosine. Of 58 patients (with 78 vein grafts), 20 patients (with 24 vein grafts) underwent SPECT perfusion imaging. Grafts were divided into those with nonsignificant percent diameter stenosis (<50%, n = 49), and those with significant percent diameter stenosis (≥50%, n = 29). When a cut-off value for coronary flow velocity reserve (CFVR) of 1.8 was applied, modest agreement (69%, $\kappa = 0.25$, $p<0.05$) between CFVR and angiography was shown. Agreement between SPECT and angiography was also modest (63%, $\kappa = 0.28$, p = NS). SPECT and CFVR provided comparable information in 20 of 24 grafts with available SPECT, illustrating good agreement (83%, $\kappa = 0.61$, $p = 0.001$). Significant stenoses in vein grafts require further exploration to assess their hemodynamic significance. The Doppler velocity results agreed better with SPECT perfusion imaging than with percent diameter stenosis in the evaluation of vein graft function.

Considerations and future perspectives

This thesis aimed to describe multiple modalities to examine coronary artery bypass grafts, and to further develop noninvasive imaging techniques to detect stenoses in native coronary arteries and bypass grafts in patients who experienced recurrent chest pain after CABG.

Several considerations must be regarded when examining patients after CABG by (non)invasive imaging modalities. To image bypass grafts is technically demanding for the different imaging modalities. Small vessels around the heart are constantly moving throughout the cardiac cycle. The temporal resolution of an imaging technique must be sufficient to avoid blurring in the acquired image.

The course of arterial grafts, inserting at the subclavian artery, is extensive and requires a large acquisition window for a single scan in e.g. CMR or CT angiography.

Spatial resolution must be adequate to depict narrowings in the small vessels. The diameter of bypass grafts is generally slightly larger than the diameter of native coronary arteries. However, for clinical use in diagnosing coronary heart disease a full examination of bypass grafts, recipient vessels and native coronary arteries is required in order to identify a target lesion for revascularization. Studies only focusing on bypass grafts are merely a first step in shaping the modality for eventual clinical use.

The physiologic consequences of CABG on the heart's vascularization are complex. In addition, when a stenosis in a bypass graft is visualized by any imaging modality, it may not have hemodynamic consequences. Due to e.g. competitive flow from a native coronary artery, a collateral circulation or a sufficient blood flow passing the stenosis, the myocardial region supplied by the graft may still function adequately. Conversely, absence of a stenosis does not necessarily imply that the graft performs well. Diffuse atherosclerosis in a graft may not show a focal lesion, but can still impair graft function. This emphasizes the importance of analyzing myocardial function in addition to bypass graft angiography.

X-ray coronary angiography is still widely used to diagnose bypass graft disease. Despite its disadvantages, it is a rapid test and most centers have experienced operating physicians. Noninvasive imaging should focus on further developing a gatekeeper function prior to x-ray coronary angiography. Future studies may focus on safely deferring patients that show no abnormalities. Conversely, patients diagnosed with progressive CHD may directly be referred for percutaneous intervention or (re-)CABG. At present, this is not common clinical practice since noninvasive tests lack a 100% specificity and NPV. Ideally, a noninvasive test should match the following criteria: a full anatomical examination of native coronary arteries, bypass grafts and recipient vessels, and analysis of myocardial function in one single test with 100% specificity and NPV, not being too time-consuming or a large burden for the patient, holding only minor complications, lacking the necessity for radiation exposure, and bearing low costs. Such a test does not exist, but different imaging modalities show great potential and are constantly being improved.

Recently, developments in CMR angiography showed an improvement in diagnostic accuracy in detecting CHD using 3D whole-heart angiography with volume rendering in comparison with x-ray coronary angiography (1). Sensitivity, specificity, positive predictive value (PPV) and NPV in the detection of CHD were 82%, 91%, 78%, and 93%, respectively. Visualized length of the major coronary arteries held up to 12.8 ± 3.4 cm. Time to perform the total examination was shortened to less than 30 minutes. With the introduction of next-generation 3 Tesla MR scanners an significant advancement in signal-to-noise and contrast-to-noise ratio was established in comparison with 1.5 Tesla MR scanners (2). However, image quality and diagnostic accuracy in detecting stenoses in coronary arteries were similar. Future studies should focus on analyzing bypass grafts in addition to native coronary arteries using the latest CMR angiography techniques.

CMR angiography may also be added to a functional MR study. A recent feasibility study presented a CMR protocol which included first-pass myocardial perfusion at rest, a myocardial viability analysis using delayed enhancement, and angiography of the proximal and middle coronary artery segments, with a total imaging time of 30-45 minutes (3). CMR first-pass myocardial perfusion in a rest-stress protocol was shown to accurately detect CHD in comparison with SPECT myocardial perfusion imaging (4). These studies did not explicitly include patients with bypass grafts. Specifically in this patient group it is important to demonstrate that functional CMR examinations are feasible and yield similar diagnostic accuracies, as patients tend to be older, often present with more extensive heart disease or are unable to sustain an obligatory breathhold. High-dose dobutamine-atropine stress CMR with wall motion analysis was shown to provide a reliable examination after percutaneous intervention or CABG for patients suspected of having CHD (5). No CMR angiography was added to this protocol.

Flow velocity measurements by CMR at rest and during stress are feasible for both vein and arterial grafts, and yield a good diagnostic accuracy in detecting vein graft disease, as described in this thesis. In earlier studies was demonstrated that CMR flow velocity measurements were also feasible in native coronary arteries (6-8). However, no one has succeeded in providing a complete flow velocity examination of all native coronary arteries and bypass grafts by CMR, thereby limiting its clinical use.

MDCT is another robust noninvasive modality in detecting or excluding stenoses in coronary arteries and bypass grafts, and combining a limited functional study of the myocardium in one scan is feasible. A comparative study between state-of-the-art CMR and CT angiography showed that both techniques yielded a similar high diagnostic accuracy (77% versus 80%, p = NS) in identification of coronary artery disease (9). The next-generation CT scanners contain 64 detectors for image acquisition, which is a factor 4 higher than the last generation. Initial results demonstrate an excellent image quality, and display a high overall sensitivity, specificity, PPV, and NPV of 94%, 97%, 87%, and 99%, respectively (10). Bypass grafts have not yet been investigated by 64-detector row CT. Functional examinations with MDCT are restricted to global LV function assessment and wall motion analysis at rest. Since patients' radiation exposure is high using MDCT imaging, a second scan under pharmacological stress is impracticable.
Gated SPECT myocardial perfusion imaging is the most established noninvasive imaging technique that is used as a gatekeeper prior to x-ray coronary angiography (11). Still, diagnostic accuracy in detecting or excluding coronary artery or bypass graft disease by this technique is not powerful enough, especially in obese patients, patients with poor LV function, or women. Furthermore, SPECT perfusion imaging does not provide data on coronary artery or bypass graft anatomy. Myocardial positron emission tomography (PET) imaging allows perfusion and viability imaging with low radiation exposure and high efficiency (12). Latest developments in PET-hardware include hybrid PET/CT-scanners which have the power to provide a functional examination of the myocardium, and an anatomical delineation of native coronary arteries. Preliminary results promise great clinical potential in the detection of CHD (13). A rest/adenosine-stress protocol for PET/CT scanning was performed. Reported sensitivity, specificity, PPV, and NPV of PET/CT were 90%, 98%, 82%, and 99%, respectively, versus PET in combination with x-ray coronary angiography for clinical decision-making. Estimated radiation exposure using this technique was 10-12 mSv, whereas MDCT scanning alone holds a similar 8-12 mSv, and a rest/stress SPECT imaging protocol 7 mSv (14). Using this technique it may become achievable to refer patients directly for percutaneous intervention or CABG without the mandatory diagnostic x-ray coronary angiography (15). Patients with bypass grafts have not yet been evaluated using this modality. Future studies will further specify the clinical capabilities of this technique.

In conclusion, noninvasive imaging modalities have shown great potential in detecting or excluding CHD in patients who experienced recurrent chest pain after CABG. New developments in the field of cardiovascular MR, MDCT and nuclear imaging are promising. Extended scientific effort may result in integrating diagnostic noninvasive imaging further in daily clinical practice.

REFERENCES

1. Sakuma H, Ichikawa Y, Suzawa N et al. Assessment of coronary arteries with total study time of less than 30 minutes by using whole-heart coronary MR angiography. Radiology 2005;237:316-21.
2. Sommer T, Hackenbroch M, Hofer U et al. Coronary MR angiography at 3.0 T versus that at 1.5 T: initial results in patients suspected of having coronary artery disease. Radiology 2005;234:718-25.
3. Foo TK, Ho VB, Saranathan M et al. Feasibility of integrating high-spatial-resolution 3D breath-hold coronary MR angiography with myocardial perfusion and viability examinations. Radiology 2005;235:1025-30.
4. Sakuma H, Suzawa N, Ichikawa Y et al. Diagnostic accuracy of stress first-pass contrast-enhanced myocardial perfusion MRI compared with stress myocardial perfusion scintigraphy. AJR Am J Roentgenol 2005;185:95-102.
5. Wahl A, Paetsch I, Roethemeyer S, Klein C, Fleck E, Nagel E. High-dose dobutamine-atropine stress cardiovascular MR imaging after coronary revascularization in patients with wall motion abnormalities at rest. Radiology 2004;233:210-6.
6. Hundley WG, Hamilton CA, Clarke GD et al. Visualization and functional assessment of proximal and middle left anterior descending coronary stenoses in humans with magnetic resonance imaging. Circulation 1999;99:3248-54.
7. Hundley WG, Hillis LD, Hamilton CA et al. Assessment of coronary arterial restenosis with phase-contrast magnetic resonance imaging measurements of coronary flow reserve. Circulation 2000;101:2375-81.
8. Nagel E, Thouet T, Klein C et al. Noninvasive determination of coronary blood flow velocity with cardiovascular magnetic resonance in patients after stent deployment. Circulation 2003;107:1738-43.
9. Kefer J, Coche E, Legros G et al. Head-to-head comparison of three-dimensional navigator-gated magnetic resonance imaging and 16-slice computed tomography to detect coronary artery stenosis in patients. J Am Coll Cardiol 2005;46:92-100.
10. Leschka S, Alkadhi H, Plass A et al. Accuracy of MSCT coronary angiography with 64-slice technology: first experience. Eur Heart J 2005;26:1482-7.
11. Sciagra R, Leoncini M. Gated single-photon emission computed tomography. The present-day "one-stop-shop" for cardiac imaging. Q J Nucl Med 2005;49:19-29.
12. Machac J. Cardiac positron emission tomography imaging. Semin Nucl Med 2005;35:17-36.
13. Namdar M, Hany TF, Koepfli P et al. Integrated PET/CT for the assessment of coronary artery disease: a feasibility study. J Nucl Med 2005;46:930-5.
14. Geleijns J, Kroft LJM, Bax JJ, Lamb HJ, de Roos A. Techniques for cardiovascular computed tomography. In: MRI and CT of the cardiovascular system. Lippincott, Williams & Wilkins, 2005:37-52.
15. Wijns W. The diagnosis of coronary artery disease: in search of a "one-stop shop"? J Nucl Med 2005;46:904-5.

Samenvatting en toekomstperspectieven

Introductie

Omleiding- of bypasschirurgie is een vaak uitgevoerde operatie voor het verlichten van ziekteverschijnselen en het verbeteren van overleving voor patiënten met angina pectoris. Atherosclerose van de coronaire omleidingen is een vaak voorkomend gevolg, dat middels hartcatheterisatie moet worden gediagnosticeerd. Hartcatheterisatie is echter een invasieve procedure, waarvoor het aanprikken van een slagader, blootstelling aan röntgenstraling en dagopname in het ziekenhuis nodig is. Complicaties houden in kamerritmestoornissen, hartinfarct, perforatie van het hart, noodbypassoperatie en cardiale dood, hoewel de risico's hierop klein zijn. Een niet-invasieve diagnostische procedure voor het analyseren van anatomie en functie van de coronaire omleidingen zou een groot voordeel bieden. Het doel van dit proefschrift is het beschrijven van verschillende modaliteiten om coronaire omleidingen te analyseren en het verder ontwikkelen van niet-invasieve beeldvormingtechnieken om vernauwingen in natieve coronaire arteriën en omleidingen te detecteren in patiënten met terugkerende pijn op de borst na een bypassoperatie. **Deel I** van dit proefschrift **(Hoofdstukken 1 en 2)** geeft een overzicht van het onderzoek dat eerder is verricht naar het niet-invasief evalueren van coronaire omleidingen middels cardiovasculaire magnetische resonantie (CMR) en computertomografie.

Deel II Cardiovasculaire magnetische resonantie

Dit deel van het proefschrift concentreert zich op bloedstroomsnelheidmetingen van veneuze en arteriële omleidingen middels CMR. Het doel van het onderzoek, beschreven in **Hoofdstuk 3**, was het retrospectief testen van twee eerder beschreven analyse methoden van bloedstroommetingen via CMR en het vergelijken van hun diagnostische nauwkeurigheid in het aantonen van zieke veneuze omleidingen. In 125 veneuze omleidingen van 68 patiënten werden bloedstroommetingparameters (totale volume flow, systolische en diastolische piekstroom, diastolisch-naar-systolische flow ratio in rust en gedurende adenosine stress, en flow reserve) afgeleid van de CMR stro omsnelheidafbeeldingen. Methode 1 implementeerde een basale volume flow <20 ml/ min of een flow reserve <2, welke een sensitiviteit van 70% en een specificiteit 38% in het aantonen van een zieke omleiding of ontvangend vat inhield. Methode 2 gebruikte "receiver operating characteristic" (ROC) curve analyse en implementeerde alle significante bloedstroommetingparameters in een logistisch regressie model, welke een sensitiviteit van 74% en een specificiteit van 68% in het aantonen van een zieke omleiding of ontvangend vat inhield. Wanneer enkelvoudige en meervoudige omleidingen apart werden geanalyseerd, had deze methode een sensitiviteit en specificiteit van 79% en 87% voor enkelvoudige omleidingen en 62% en 94% voor meervoudige omleidingen in het aantonen van ≥50% stenose in omleidingen of ontvangend vaten. Wanneer ROC curve analyse met logistische regressie werd gebruikt, verbeterde de specificiteit van de methode aanzienlijk. Als enkelvoudige en meervoudige omleidingen apart werden geanalyseerd, werden de beste resultaten bereikt.

In **Hoofdstuk 4** werden twee verschillende analyse methoden voor de stroomsnelheid afbeeldingen verkregen via CMR, namelijk volume flow en stroomsnelheidmetingen, vergeleken. Stroomsnelheidafbeeldingen van veneuze omleidingen werden hiervoor gebruikt. Negenenveertig patiënten met een bypassoperatie in hun voorgeschiedenis ondergingen hartcatheterisatie en CMR met het afbeelden van de bloedstroomsnelheid van enkelvoudige veneuze omleidingen. Volume flow en snelheidsmetingen van de afbeeldingen werden uitgevoerd en vergeleken. Bland-Altman analyse liet een goede overeenkomst tussen de analyses zien. Vergelijking van ROC oppervlakten-onder-de-curve van de beide analyses toonde geen significante verschillen voor het detecteren van ≥70% stenose aan. Diagnostische nauwkeurigheid van de volume flow en snelheidsparameters was respectievelijk 92% en 93%. De stroomsnelheidanalyse lijkt de methode van voorkeur, want deze aanpak kost minder tijd en heeft een vergelijkbare diagnostische nauwkeurigheid als de volume flow analyse.
De hemodynamische significantie van een vernauwing in een omleiding kan niet altijd nauwkeurig middels hartcatheterisatie worden bepaald. Een keur aan diagnostische onderzoeken (invasief danwel niet-invasief) zijn beschikbaar om de hemodynamische consequentie van een laesie te karakteriseren. De opzet van het onderzoek, gepresenteerd in **Hoofdstuk 5**, was het uitvoeren van een directe vergelijking tussen "single-photon emissie computertomografie" (SPECT) perfusie afbeeldingen en CMR in het evalueren van de hemodynamische significantie van angiografische bevindingen in omleidingen. Zevenenvijftig arteriële en veneuze omleidingen in 25 patiënten werden middels coronaire angiografie, SPECT perfusiemeting van het myocard, en CMR flow reserve bepaling geëvalueerd. Gebaseerd op coronaire angiografie en SPECT konden 4 groepen worden onderscheiden: 1) geen significante stenose (<50%), normale perfusie; 2) significante stenose (≥50%), abnormale perfusie; 3) significante stenose, normale perfusie (geen hemodynamische significantie); en 4) geen significante stenose, abnormale perfusie (microvasculaire aandoening van het myocard suggererend). Een volledige evaluatie werd in 46 omleidingen verkregen. SPECT en CMR verschaften vergelijkbare informatie in 37 van de 46 (80%) omleidingen, wat een goede overeenkomst ($\kappa = 0.61$, $p<0.001$) aanduidde. Acht omleidingen perfundeerden een myocardgebied met littekenweefsel. Wanneer de overeenkomst tussen SPECT en CMR tot omleidingen zonder littekenweefsel in hun perfusiegebied werd beperkt, verbeterde het tot 84% ($\kappa = 0.68$). Integratie van coronaire angiografie met SPECT deelde 14 laesies in groep 1 in, 23 in groep 2, 6 in groep 3 en 3 in groep 4. De overeenkomst tussen SPECT en CMR per groep was respectievelijk 86%, 78%, 100% en 33%. Directe vergelijking toonde goede overeenstemming aan tussen SPECT en CMR voor de functionele evaluatie van omleidingen. CMR zou een alternatief voor SPECT voor de functionele karakterisering van angiografische laesies kunnen bieden.
In **Hoofdstuk 6** wordt een nieuwe CMR sequentie om de doorstroming in arteriële en veneuze omleidingen te meten geïntroduceerd. Het doel van de studie was om een hoog resolutie, fasecontrast CMR sequentie te valideren in het meten van doorstroming in grote en kleine vaten en om aan te tonen dat deze sequentie tevens geschikt is om doorstroming in omleidingen te meten. Een "echo planar imaging" (EPI) sequentie werd ontwikkeld en middels een fantoom gevalideerd tegen een "fast field echo" (FFE)

sequentie. In 17 gezonde vrijwilligers werd de doorstroming van de aorta gemeten middels beide sequenties. In 5 patiënten werd de doorstroming in de linker arteriële omleiding en aorta gemeten in rust en gedurende adenosine stress en werd de flow reserve berekend; in 7 patiënten werd de doorstromingssnelheid in veneuze omleidingen gemeten. Voor het fantoom had de EPI sequentie een uitstekende correlatie met de FFE sequentie ($r = 0.99$; $p<0.001$ voor alle parameters). Voor de gezonde vrijwilligers was er een goede correlatie voor de aortadoorstroming ($r = 0.88$; $p<0.01$). Voor de patiënten was de gemiddelde flow reserve van de arteriële omleidingen zonder stenosen 2.70 ± 0.88. Percentage doorstroming van de arteriële omleidingen van het hartdebiet was 0.71 ± 0.17% in rust en 1.56 ± 0.52% gedurende adenosine stress ($p<0.01$). Voor enkelvoudige veneuze omleidingen zonder vernauwingen was de gemiddelde pieksnelheid 11.6 ± 2.4 cm/s. De hoog resolutie CMR snelheidsgeëncodeerde sequentie correleerde goed met de referentie sequentie. De EPI sequentie is geschikt om doorstroming te meten in arteriële en veneuze omleidingen en de aorta.

Deel III Computertomografie

Deel III van het proefschrift richt zich op multidetector computertomografie (MDCT) van omleidingen. In **Hoofdstuk 7** wordt een uitgebreide 16-detector MDCT evaluatie van patiënten na een omleidingoperatie onderzocht. MDCT is een veelzijdige modaliteit om vernauwingen in natieve coronaire arteriën en omleidingen te beoordelen. Met de verworven MDCT data kan tevens de linker kamer ejectiefractie (LVEF) worden bepaald. Het doel was om MDCT te gebruiken voor de evaluatie van omleidingen en natieve coronaire arteriën, gecombineerd met de bepaling van de LVEF. Vijfentwintig patiënten ondergingen een 16-detector CT onderzoek en coronaire angiografie. Op de CT-afbeeldingen werden omleidingen en niet-gegrafte coronaire segmenten op geschiktheid voor evaluatie, doorgankelijkheid en ≥50% stenose onderzocht. De LVEF werd bepaald uit de MDCT data sets en de resultaten werden in patiënten met geen/subendocardiale/transmurale myocardinfarcten opgesplitst. Negentig vaten zijn onderzocht: 14 arteriële omleidingen, 53 veneuze omleidingen en 23 niet-gegrafte arteriën. Van de 225 segmenten waren 17 segmenten niet geschikt voor evaluatie vanwege metalen clips. Met MDCT kon de doorgankelijkheid van de segmenten van arteriële omleidingen/veneuze omleidingen/niet-gegrafte arteriën met hoge nauwkeurigheid worden geëvalueerd, in respectievelijk 100%/100%/97% van de segmenten. In de arteriële omleidingen werden geen stenosen van ≥50% gezien bij angiografie, wat voor alle geschikte segmenten correct met MDCT werd gediagnosticeerd. Vernauwingen ≥50% konden correct met MDCT worden gedetecteerd met een sensitiviteit/specificiteit van 100%/94% voor veneuze omleidingen en 100%/89% voor niet-gegrafte arteriën. Negatief voorspellende waarde was 100% voor veneuze omleidingen en niet-gegrafte arteriën. Bij patiënten met een transmuraal myocardinfarct werd een significant lagere LVEF waargenomen in vergelijking tot patiënten zonder infarct of met een subendocardiaal infarct ($p<0.05$). Een uitgebreide evaluatie van omleidingen, niet-gegrafte arteriën en LVEF is mogelijk met MDCT. Vanwege de hoge negatief voorspellende waarde zou deze niet-invasieve benadering als een poortwachter voor de coronaire angiografie kunnen dienen.

Om de nauwkeurigheid van MDCT te evalueren was het doel van de studie, beschreven in **Hoofdstuk 8**, het vergelijken van een MDCT onderzoek van globale en regionale linker ventrikel (LV) functie met echocardiografie en CMR. In 25 patiënten, die voor een niet-invasieve 16-detector CT angiografie waren verwezen, werd tevens een LV functie reconstructie vervaardigd. Vervolgens werd een echocardiogram gemaakt en in een subgroep patiënten een CMR onderzoek om de LV functie te bepalen. Voor de globale functie evaluatie werd de LVEF berekend. Regionale LV functie werd middels een 17-segmentmodel en een 4-puntscoringsysteem gescoord. MDCT vertoonde goede overeenstemming met echocardiografie in de bepaling van LVEF ($r = 0.96$; bias 0.54%; $p<0.0001$) en regionale LV functie ($\kappa = 0.78$). Acht patiënten hadden geen contra-indicaties en gaven toestemming voor een CMR onderzoek. Een redelijk goede correlatie tussen MDCT en CMR in de evaluatie van LVEF werd aangetoond ($r = 0.86$; bias –1.5%; $p<0.01$). Voor regionale LV functie liet MDCT een goede overeenstemming met CMR zien ($\kappa = 0.86$). MDCT kwam goed overeen met zowel echocardiografie als CMR in de evaluatie van globale en regionale LV functie. Globale en regionale LV functie kunnen nauwkeurig met 16-detector CT worden bepaald en kunnen aan een routine CT analyse protocol worden toegevoegd zonder dat extra contrast of onderzoekstijd nodig is.

DEEL IV SPECT EN DOPPLER STROOMSNELHEID

Deel IV richt zich op de hemodynamische consequenties van vernauwingen in veneuze omleidingen. Hartcatheterisatie wordt beschouwd als de gouden standaard in het evalueren van vernauwingen in veneuze omleidingen. De hartcatheterisatie geeft echter geen uitsluitsel over de hemodynamische consequenties van de vernauwingen. In de studie gepresenteerd in **Hoofdstuk 9** werden de hemodynamische consequenties van significante stenosen in veneuze omleidingen met Doppler stroomsnelheidmetingen geëvalueerd en de resultaten vergeleken met SPECT perfusie beeldvorming. Hartcatheterisatie werd in 58 patiënten na bypassoperatie uitgevoerd vanwege terugkerende pijn op de borst. Gedurende de procedure werden Doppler stroomsnelheidmetingen voor en na toediening van adenosine verkregen. Van de 58 patiënten (met 78 veneuze omleidingen) ondergingen 20 patiënten (met 24 omleidingen) SPECT perfusie beeldvorming. Omleidingen werden ingedeeld in diegenen met een niet-significant percentage diameter stenose (<50%, n = 49) en diegenen met een significant percentage diameter stenose (≥50%, n = 29). Wanneer voor coronaire flow velocity reserve (CFVR) een afbreekpunt van 1.8 werd toegepast, werd een matige overeenstemming (69%, $\kappa = 0.25$, $p<0.05$) tussen CFVR en angiografie gezien. Overeenstemming tussen SPECT en angiografie was tevens matig (63%, $\kappa = 0.28$, p = NS). SPECT en CFVR verschaften vergelijkbare informatie in 20 van de 24 omleidingen met een beschikbare SPECT, wat een goede overeenkomst aangaf (83%, $\kappa = 0.61$, $p = 0.001$). Significante vernauwingen in veneuze omleidingen vereisen verdere exploratie naar hun hemodynamische significantie. Het resultaat van Doppler stroomsnelheidmetingen kwam beter overeen met SPECT perfusie beeldvorming dan met percentage diameter stenose bepaling in de evaluatie van de functie van veneuze omleidingen.

Overwegingen en toekomstperspectieven

Dit proefschrift had tot doel het beschrijven van verschillende modaliteiten in het onderzoeken van omleidingen en het ontwikkelen van niet-invasieve technieken om vernauwingen in natieve coronaire arteriën en omleidingen te detecteren bij patiënten met terugkerende pijn op de borst na bypasschirurgie.
Een aantal overwegingen moeten worden genoemd als patiënten na bypasschirurgie met (niet-)invasieve modaliteiten worden onderzocht. Het afbeelden van omleidingen vraagt veel van de techniek van de verschillende afbeeldingmodaliteiten. Kleine vaten rond het hart zijn gedurende de hartcyclus constant aan het bewegen. De temporele resolutie van een afbeeldingtechniek moet toereikend genoeg zijn om vaagheid van het verkregen beeld te vermijden.
Het verloop van arteriële omleidingen met hun insertie in de arteria subclavia is langgerekt en heeft een groot "acquisition window" voor een enkele scan nodig in bijvoorbeeld CMR of CT angiografie.
Spatiële resolutie moet adequaat zijn om vernauwingen in de kleine vaten af te beelden. De diameter van omleidingen is over het algemeen iets wijder dan de diameter van natieve coronaire arteriën. Voor gebruik in de kliniek bij het diagnosticeren van ischemische hartziekten is echter een volledig onderzoek van omleidingen, ontvangende vaten en natieve coronaire arteriën nodig om een target laesie voor revascularisatie te identificeren. Studies die zich alleen op omleidingen richten zijn slechts een eerste stap in het vormen van de modaliteit voor zijn uiteindelijke gebruik in de kliniek.
De fysiologische consequenties van een bypassoperatie op de doorbloeding van het hart zijn complex. Als bovendien een stenose in een omleiding middels een afbeeldingmodaliteit wordt gevisualiseerd, hoeft het geen hemodynamische consequenties te hebben. Door bijvoorbeeld competitieve doorstroming van een natieve coronaire arterie, een collaterale circulatie of voldoende stroming langs een stenose kan het gedeelte van het myocard, dat door de omleiding van bloed wordt voorzien, nog steeds adequaat functioneren. Tegengesteld hieraan hoeft afwezigheid van een stenose niet te impliceren dat een omleiding goed werkt. Diffuse atherosclerose in een omleiding hoeft geen focale laesie te laten zien, maar kan wel de functie van de omleiding aantasten. Dit benadrukt het belang om hartfunctie naast angiografie van de omleidingen te analyseren.

Hartcatheterisatie met coronairangiografie wordt nog veelvuldig gebruikt om zieke omleidingen te diagnosticeren. Ondanks de nadelen is het een snel onderzoek en de meeste centra hebben ervaren specialisten in dienst. Niet-invasieve beeldvorming zou zich moeten richten op het verder ontwikkelen van een poortwachterfunctie vóór de hartcatheterisatie. Vervolgstudies zouden zich kunnen richten op het veilig verwijzen van patiënten die geen afwijkingen laten zien. Tegengesteld hieraan zouden patiënten waarbij progressieve ischemische hartziekte wordt vastgesteld meteen voor percutane interventie of (re)bypasschirurgie kunnen worden doorverwezen. Nu is dit niet gewoonlijk in de klinische praktijk, omdat niet-invasieve onderzoeken een 100% specificiteit en negatief voorspellende waarde missen. Idealiter zou een niet-invasieve test aan de volgende criteria moeten voldoen: een volledig anatomisch onderzoek van natieve coronaire arteriën, omleidingen en ontvangende vaten én analyse van hartfunctie in één enkele

test met 100% specificiteit en negatief voorspellende waarde, niet te tijdrovend of een te grote belasting voor de patiënt, slechts kleine complicaties met zich meebrengend, geen blootstelling aan straling nodig en niet te duur. Zo'n onderzoek bestaat niet, maar de verschillende afbeeldingmodaliteiten zijn veelbelovend en worden constant verbeterd.
Recent hebben ontwikkelingen in CMR angiografie een verbetering in de diagnostische nauwkeurigheid in het aantonen van ischemische hartziekten laten zien, gebruikmakend van 3D "whole-heart" angiografie met volume rendering in vergelijking met hartcatheterisatie (1). Sensitiviteit, specificiteit, positief en negatief voorspellende waarde in het aantonen van ischemische hartziekte waren respectievelijk 82%, 91%, 78%, en 93%. Gevisualiseerde lengte van de hoofdkransslagaders was 12.8 ± 3.4 cm. Tijdsduur van het totale onderzoek was ingekort tot minder dan 30 minuten. Met de introductie van de volgende generatie 3 Tesla MR scanners werden significante verbeteringen in signaal-ruis en contrast-ruis ratio in vergelijking tot 1.5 Tesla MR scanners bereikt (2). Beeldkwaliteit en diagnostische nauwkeurigheid in het aantonen van stenosen in coronaire arteriën waren echter gelijk. Studies zouden zich verder moeten richten op het analyseren van omleidingen naast natieve coronaire arteriën, gebruikmakend van de laatste CMR angiografie technieken.
CMR angiografie kan ook aan een functioneel MR-onderzoek worden toegevoegd. Een recente studie presenteerde een uitvoerbaar CMR protocol, dat bestond uit een myocardperfusie en -viability analyse middels "delayed enhancement" én angiografie van de proximale en middelste segmenten van de hoofdkransslagaders met een totale onderzoeksduur van 30-45 minuten (3). CMR myocardperfusie in een rust-stress protocol kon nauwkeurig een ischemische hartziekte aantonen in vergelijking tot SPECT myocardperfusie beeldvorming (4). Deze studies hadden niet expliciet patiënten met omleidingen geïncludeerd. Specifiek in deze patiëntengroep is het belangrijk aan te tonen dat functionele CMR onderzoeken uitvoerbaar zijn en dezelfde diagnostische nauwkeurigheid omvatten, omdat patiënten vaak ouder zijn, met meer uitgebreide hartziekte zich presenteren of de noodzakelijke ademinhouding niet kunnen volhouden. Hooggedoseerde dobutamine-atropine stress CMR met wandbeweginganalyse verschafte een betrouwbaar onderzoek na percutane interventie of bypasschirurgie bij patiënten die werden verdacht een ischemische hartziekte te hebben (5). Geen CMR angiografie was aan dit protocol toegevoegd.
Doorstromingsmetingen middels CMR in rust en gedurende stress zijn uitvoerbaar voor zowel veneuze als arteriële omleidingen en hebben een goede diagnostische nauwkeurigheid in het aantonen van zieke veneuze omleidingen, zoals in dit proefschrift wordt beschreven. In eerdere studies is aangetoond dat CMR doorstromingsmetingen ook uitvoerbaar zijn in natieve coronaire arteriën (6-8). Niemand is het echter gelukt een compleet doorstromingsonderzoek van alle natieve coronaire arteriën en omleidingen middels CMR uit te voeren, daarmee zijn klinische toepassing beperkend.
MDCT is een andere robuuste, niet-invasieve modaliteit in het aantonen of uitsluiten van stenosen in coronaire arteriën en omleidingen en het combineren van een beperkt functieonderzoek van het myocard is mogelijk in één scan. Een vergelijkende studie tussen hoogstaande CMR en CT angiografie liet zien dat beide technieken een zelfde hoge diagnostische nauwkeurigheid (77% versus 80%, p = NS) in het aanwijzen van

een ischemische hartziekte bezitten (9). De volgende generatie CT-scanners hebben 64 detectoren voor het construeren van een afbeelding, wat een factor 4 hoger is dan de vorige generatie. Initiële resultaten geven een uitstekende beeldkwaliteit weer en laten algeheel een hoge sensitiviteit, specificiteit, positief en negatief voorspellende waarde van respectievelijk 94%, 97%, 87% en 99% zien (10). Omleidingen zijn nog niet met 64-detector CT onderzocht. Functioneel onderzoek middels MDCT is beperkt tot globale LV functie evaluatie en wandbewegingsstoornissen in rust. Aangezien de röntgenstrali ngsbelasting van de patiënt hoog is met MDCT beeldvorming, is een tweede scan onder farmacologische stress onuitvoerbaar.
Gated SPECT myocardperfusie beeldvorming is de meest gevestigde niet-invasieve techniek, die als poortwachter voor de hartcatheterisatie wordt gebruikt (11). Toch is de diagnostische nauwkeurigheid in het aantonen of uitsluiten van een ischemische hartziekte middels deze techniek niet krachtig genoeg, specifiek bij obese patiënten, patiënten met een slechte LV functie of vrouwen. Voorts verschaft SPECT perfusie beeldvorming geen data over de anatomie van coronaire arteriën of omleidingen. Met myocard positron emissie tomografie (PET) beeldvorming kunnen perfusie- en viability-afbeeldingen met een lage stralingsbelasting en een hoge efficiëntie worden verkregen (12). De laatste ontwikkeling in PET-apparatuur omvat hybride PET/CT-scanners, die een functioneel onderzoek van het myocard en een anatomische uitlijning van de natieve coronaire arteriën kunnen combineren. De eerste resultaten zijn veelbelovend in het aantonen van een ischemische hartziekte (13). Een rust/adenosine-stress protocol voor PET/CT werd uitgevoerd. Gemelde sensitiviteit, specificiteit, positief en negatief voorspellende waarde van PET/CT waren respectievelijk 90%, 98%, 82% en 99%, versus PET in combinatie met hartcatheterisatie voor klinische besluitvorming. Geschatte stralingsbelasting middels deze techniek was 10-12 mSv, terwijl alleen MDCT een vergelijkbare 8-12 mSv inhield en een rust/stress SPECT beeldvormingprotocol 7 mSv (14). Met deze techniek zou het haalbaar kunnen worden om patiënten direct voor percutane interventie of bypasschirurgie te verwijzen zonder de noodzakelijke diagnostische hartcatheterisatie (15). Patiënten met omleidingen zijn nog niet onderzocht middels deze modaliteit. Toekomstige studies zullen de klinische capaciteiten van deze techniek verder specificeren.

Concluderend hebben niet-invasieve beeldvormingmodaliteiten veelbelovende resultaten laten zien in het aantonen of uitsluiten van een ischemische hartziekte in patiënten met terugkerende pijn op de borst na bypasschirurgie. Nieuwe ontwikkelingen op het terrein van de cardiovasculaire MR, MDCT en nucleaire beeldvorming zijn hoopvol. Voortgaande wetenschappelijke inspanning kan resulteren in het nader integreren van diagnostische, niet-invasieve beeldvorming in de dagelijkse, klinische praktijk.

Full colour images section

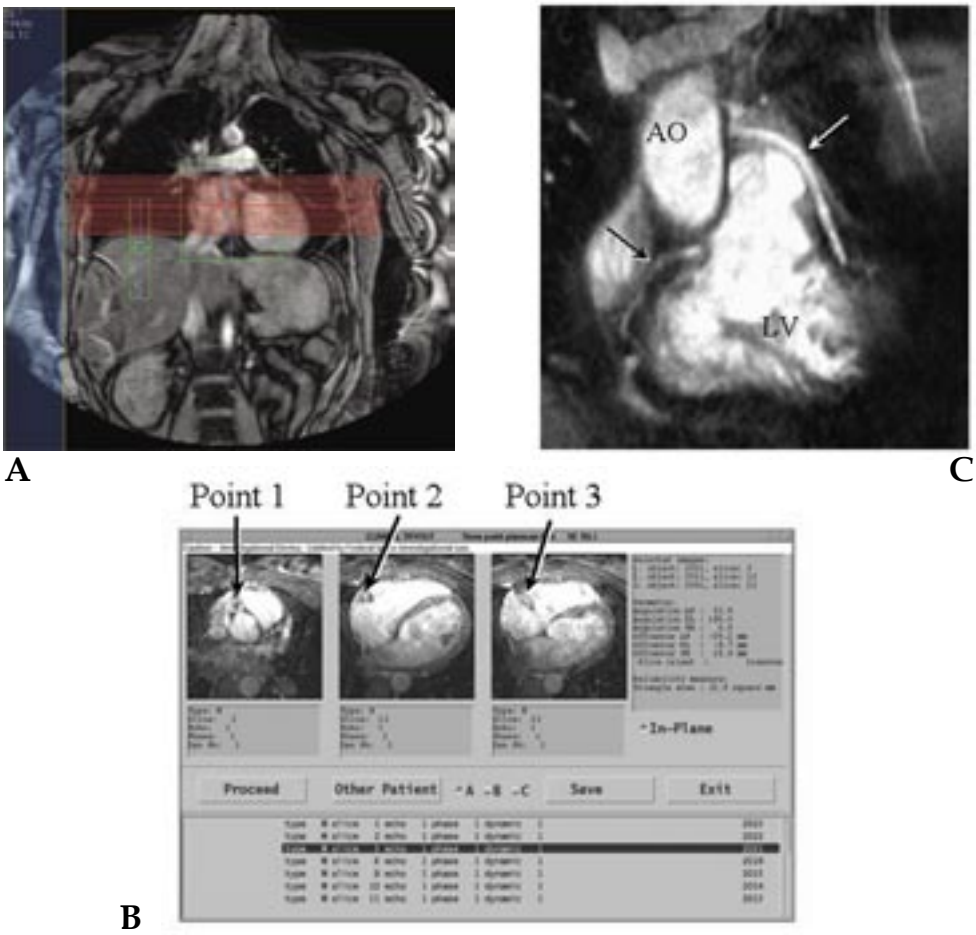

Figure 2.1, Chapter 2, Page 20

Typical magnetic resonance (MR) acquisition protocol. (A) Typical plan-scan for cardiovascular magnetic resonance (CMR) angiography. Axial imaging volume (horizontal lines); volume used for localized shimming (large box); position in the right hemidiaphragm of the respiratory navigator (rectangular box); position of a saturation band for suppression of image artifacts (left box). (B) With the use of axial scout images, the three-point plan-scan is used to select three points in space, one at the origin of the coronary artery or bypass graft, one at the most distal point, and one in the middle of the first two points. From this information, an imaging plane is automatically calculated in plane with the coronary artery or bypass graft of interest. (C) CMR angiography of a patient with a bypass of the left coronary system (white arrow) and a visible native right coronary artery (black arrow). This imaging approach can be used clinically to assess bypass graft patency. AO = aorta; LV = left ventricle. (Courtesy of H.J. Lamb)

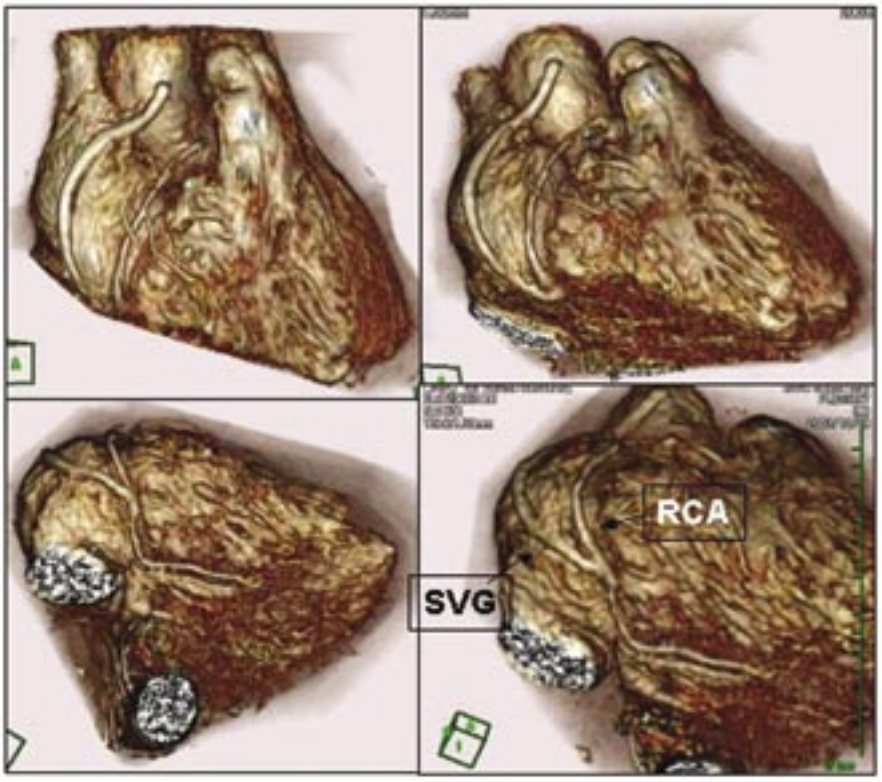

Figure 2.2, Chapter 2, Page 21
Whole-heart CMR angiography of a vein bypass graft to the right coronary artery at different rotation angles. (Courtesy of Dr. H. Sakuma)

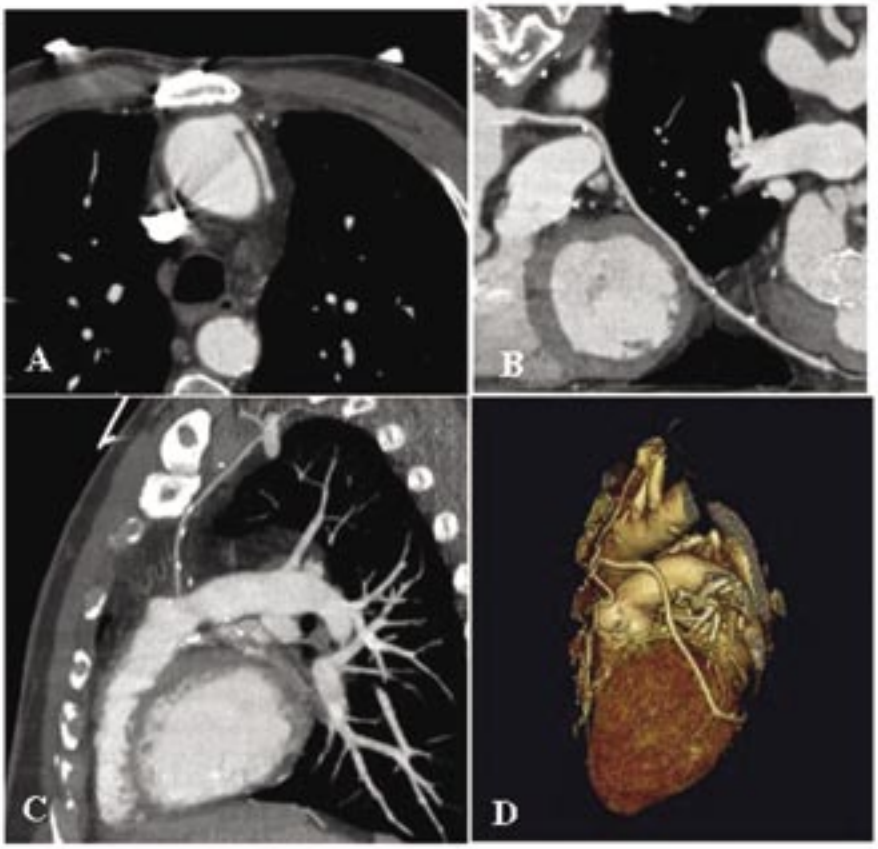

Figure 2.8, Chapter 2, Page 31

For the evaluation of MSCT angiograms, several imaging displays can be used. (A) Original axial slice. (B) Curved multiplanar reconstruction of a vein graft. (C) Maximum intensity projection of an arterial graft. (D) For an overview of the coronary arteries and bypass grafts, 3D volume-rendered reconstructions can be useful.

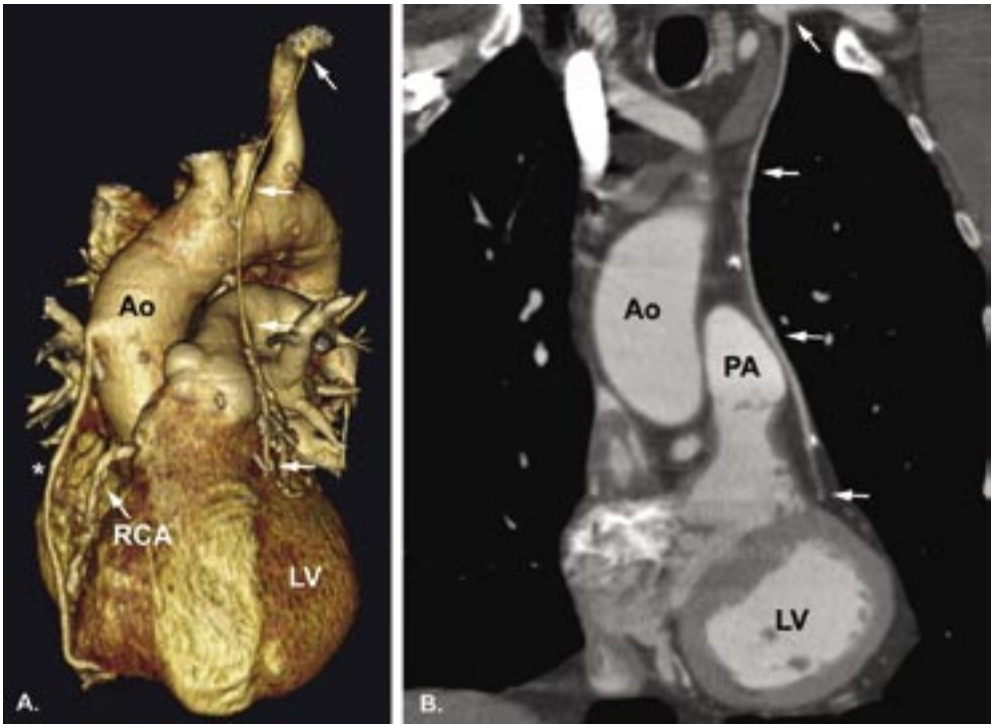

Figure 7.1, Chapter 7, Page 104

Example of an arterial and a vein graft. A, a 3D reconstruction of the heart and vessels. The white arrows highlight a left internal mammary artery graft to the left anterior descending artery from its left subclavian artery origin to the anastomosis. B, after the anastomosis the recipient vessel is occluded, also illustrated as multiplanar reformat reconstruction. The asterisk represents a vein graft to the posterior descending branch (anastomosis not shown). The native RCA is severely diseased. Ao = aorta; RCA = right coronary artery; LV = left ventricle; PA = pulmonary artery

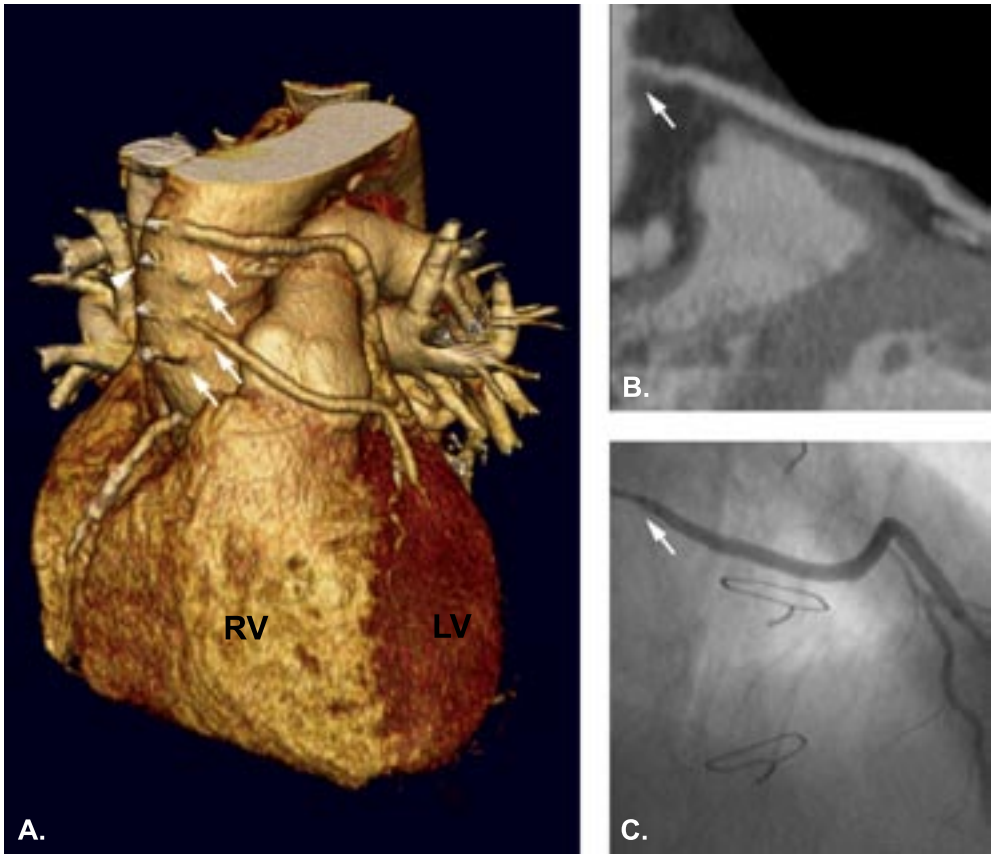

Figure 7.2, Chapter 7, Page 105

Example of a patient with multiple vein grafts. A, a 3D reconstruction of the heart, revealing 4 grafts (white arrows). Two patent grafts supply the obtuse marginal branch and the second diagonal branch, respectively; 2 grafts are totally occluded. Lateral from the graft origins, metal clips have been placed for identifying the graft locations (white arrowhead marks one of the clips). The vein graft to the second diagonal branch has a significant stenosis at its ostium. B and C, the multiplanar reformat reconstruction and coronary angiography of the ostium stenosis (arrow). RV = right ventricle; LV = left ventricle

Dankwoord

Eindelijk, na jaren van gestaag doorwerken en doorzetten, is het volbracht. Jaren waarin mij de mogelijkheid is gegeven veel te leren, zowel op wetenschappelijk gebied als in persoonlijke ontwikkeling. Mijn dank is groot aan iedereen die mij daarin heeft bijgestaan!

Mijn wetenschappelijke queeste begon bij de afdeling Cardiologie van het Leids Universitair Medisch Centrum (LUMC) bij Prof. Dr. A. van der Laarse. In het cardiobiochemielabora torium zou het onderzoek over hypertriglyceridemie mijn onderwerp worden. Door een samenloop van externe omstandigheden kwam hieraan voortijdig een eind. Beste Arnoud, ik wil je bedanken voor je vertrouwen in mij. Ik heb onze (helaas korte) samenwerking als prettig ervaren.
Gelukkig vond ik een voortzetting bij de cardiale beeldvorming, een samenwerking tussen de afdelingen Cardiologie (onder leiding van Prof. Dr. E.E. van der Wall) en Radiologie (onder leiding van Prof. Dr. A. de Roos) van het LUMC, waar de in dit proefschrift beschreven onderzoeken zijn uitgevoerd. Financieel werd het onderzoek door het Interuniversitair Cardiologisch Instituut Nederland (ICIN) ondersteund.
Graag wil ik de cardiologen bedanken die mij tijdens de opzet en uitvoering van de studies, het analyseren van de data en het schrijven van de artikelen hebben begeleid. Mede dankzij jullie zijn mijn artikelen als zodanig tot stand gekomen en in vooraanstaande tijdschriften gepubliceerd.
Alle (ex-)inwoners van de Cardiologie "tuin" (Susan, Eva, Mascha, Fleur, Natasja, Sander, Sweder, Astrid, Maartje, Monique, Philippine, Joanne, Pascalle, Miriam, Bart, Gabe, Sven, Bas, Su San, Saskia, Marleen) wil ik bedanken voor steun, medeleven en vooral voor veel gezelligheid. Susan, bedankt dat je me in de opstartfase geduldig hebt ingewerkt in het MRI-onderzoek. Joanne, bedankt voor je hulp bij de CT- en MRI-onderzoeken en bij de beeldanalyse. Voor de ICT ondersteuning wil ik Tom en Hylke bedanken.
Van de afdeling Radiologie wil ik de MRI technici, onder wie Hildo Lamb, graag bedanken voor het ontwerpen van de MRI flow sequentie, de uitleg over MRI techniek en de nuttige commentaren op mijn artikelen. Dankzij jullie heb ik mijn weg binnen de Radiologie kunnen vinden. Voor de revisie van het flow-fantoom bedank ik Nico Binnendijk van de Medische Instrumentatie.
Tevens de onderzoekers op het gebied van de cardiovasculaire MRI, Alexander en Dirk, bedankt voor uitleg over praktische MRI aangelegenheden en gezelligheid tijdens radiologiecongressen! Martijn, ondanks dat onze samenwerking helaas verre van optimaal was, bedankt voor je uitleg en hulp bij de cardiale CT en beeldverwerking. Ik wens jullie allen veel succes bij de opleiding tot radioloog.
Alle radiologie-medewerkers wil ik bedanken voor assistentie en samenwerking bij de CT-onderzoeken.
Iedereen die vrijwillig (minimaal) twee uur voor mij in de MRI-scanner wilde liggen, heel hartelijk bedankt! En vooral aan de patiënten die bereid waren voor mij een keer extra naar het ziekenhuis te komen voor een scan ben ik veel dank verschuldigd.

De medewerkers van de secretariaten bij de Cardiologie en Radiologie, met name Lya Verlinde en Natascha Meewisse-Schuitemaker, wil ik bedanken voor administratieve ondersteuning.
Van het Laboratorium voor Klinische en Experimentele Beeldverwerking (onder leiding van Prof. Dr. J.H. Reiber) wil ik Rob van der Geest en Jos Westenberg graag bedanken. Fijn dat ik bij jullie altijd terecht kon met vragen over de beeldanalyse-software.
Voor deskundig advies op het gebied van de statistiek is Koos Zwinderman onmisbaar geweest voor mij!

Aan mijn lieve vrienden, bedankt voor de vele uurtjes ontspanning! Onze weekendjes/ weekjes-weg zijn altijd fantastisch leuk. Sandra, Stefan, Yuri, Ard, Jo, Jeroen, Bert, Wybrand, Nick, Martin, Alonzo, Wendy, Pascal, ik hoop dat we samen nog veel avonturen zullen beleven, ook IRL! Lieve Sandra, dat er nog maar veel gezellige avonden samen mogen volgen. Tof dat je tijdens mijn promotie naast me komt zitten. Wendy, bedankt voor je inspanningen voor de mooie omslag en lay-out van dit boekje.
Olaf en Judith, Dénes en Marcsi, er is sinds de barcommissietijd veel gebeurd. Afstuderen, verhuizingen, emigratie, trouwerijen, gezinsuitbreiding, promotie, fijn dat we het nog steeds met jullie mogen meemaken!
Harry en Anneke, bedankt voor de hartelijke manier waarop jullie me in het gezin hebben opgenomen. Ik waardeer jullie steun ontzettend. Ilja en Lars, jullie ook bedankt voor de support!
Pappa en mamma, bedankt voor alles.
Loes, lieve zus, ik bewonder je kracht en expressiviteit. Grotere tegenpolen dan wij bestaan bijna niet. Ik vind het heel fijn dat onze band steeds hechter wordt.
En lieve Hugo… je hebt met me moeten afzien de afgelopen jaren. Uit diepe dalen heb je me getrokken, maar ook hebben we hoge bergen bewandeld. Bedankt voor je geduld, steun en liefde. Dat we de Reis nog maar lang mogen vervolgen.

List of publications

ORIGINAL PEER-REVIEWED ARTICLES

Huitinga I, Van der Cammen M, Salm L, Erkut Z, Van Dam A, Tilders F, Swaab D. IL-1ß immunoreactive neurons in the human hypothalamus: reduced numbers in multiple sclerosis. J Neuroimmunol 2000; 107, 8-20.

Salm LP, Bax JJ, Dirksen MS, Vliegen HW, Jukema JW, Schalij MJ, Van der Wall EE, Lamb HJ. Comparison of MSCT and MRA in the evaluation of an anomalous right coronary artery. J Cardiovasc Magn Reson 2003; 5 (2), 403-5.

Salm LP, Bax JJ, Lamb HJ, Hazekamp MG, De Roos A,Van der Wall EE, Vliegen HW. Evaluation of re-routing surgery of a coronary artery anomaly by magnetic resonance angiography. Ann Thor Surg 2003; 76, 1748.

Salm LP, Langerak SE, Vliegen HW, Jukema JW, Bax JJ, Zwinderman AH, Van der Wall EE, De Roos A, Lamb HJ. Blood flow in coronary artery bypass vein grafts: volume versus velocity at cardiovascular MR imaging. Radiology 2004; 232 (3), 915-20.

Salm LP, Bax JJ, Vliegen HW, Langerak SE, Dibbets P, Jukema JW, Lamb HJ, Pauwels EKJ, De Roos A, Van der Wall EE. Functional significance of stenoses in coronary artery bypass grafts. Evaluation by single-photon emission computed tomography perfusion imaging, cardiovascular magnetic resonance, and angiography. J Am Coll Cardiol 2004; 44 (9), 1877-82.

Schuijf JD, Bax JJ, Jukema JW, Lamb HJ, Vliegen HW, Salm LP, de Roos A, van der Wall EE. Noninvasive angiography and assessment of left ventricular function using multislice computed tomography in patients with type 2 diabetes. Diabetes Care 2004; 27 (12), 2905-10.

Salm LP, Vliegen HW, Langerak SE, Bax JJ, Jukema JW, Zwinderman AH, Lamb HJ, De Roos A, Van der Wall EE. Evaluation of saphenous vein coronary artery bypass graft flow by cardiovascular magnetic resonance. J Cardiovasc Magn Reson 2005; 7(4), 631-37.

Salm LP, Bax JJ, Jukema JW, Schuijf JD, Vliegen HW, Lamb HJ, Van der Wall EE, De Roos A. Comprehensive assessment of patients after coronary artery bypass grafting by 16-detector row computed tomography. Am Heart J 2005; 150 (4), 775-81.

Salm LP, Bax JJ, Jukema JW, Langerak SE, Vliegen HW, Steendijk P, Lamb HJ, De Roos A, Van der Wall EE. Hemodynamic evaluation of saphenous vein coronary artery bypass grafts: relative merits of Doppler flow velocity and SPECT perfusion imaging. J Nucl Cardiol 2005; 12 (5), 545-52.

Schuijf JD, Bax JJ, Salm LP, Jukema JW, Lamb HJ, van der Wall EE, de Roos A. Noninvasive coronary imaging and assessment of left ventricular function using 16-slice computed tomography. Am J Cardiol 2005; 95 (5), 571-4.

Salm LP, Schuijf JD, De Roos A, Lamb HJ, Vliegen HW, Jukema JW, Joemai R, Van der Wall EE, Bax JJ. Global and regional left ventricular function assessment with 16-detector row CT: comparison with echocardiography and cardiovascular magnetic resonance. Eur J Echocardiogr 2006; 7(4), 308-14.

Salm LP, Schuijf JD, Lamb HJ, Bax JJ, Vliegen HW, Jukema JW, Van der Wall EE, De Roos A, Doornbos J. Validation of a high-resolution, phase contrast cardiovascular magnetic resonance sequence for evaluation of flow in coronary artery bypass grafts. Accepted for publication in J Cardiovasc Magn Reson.

Schuijf JD, Bax JJ, Jukema JW, Lamb HJ, Salm LP, de Roos A, van der Wall EE. Assessment of left ventricular volumes and ejection fraction with 16-slice multi-slice computed tomography; comparison with 2D-echocardiography. Accepted for publication in Int J Cardiol.

OTHER ARTICLES

Salm LP. Acute coronary syndromes: from practice to implementation of guidelines. Neth Heart J 2002; 10 (suppl 2), 26-7.

Salm LP. Treatment strategies to reduce ischaemic events: long-term management of atherothrombosis. Neth Heart J 2002; 10 (suppl 2), 48-9.

Salm LP. New perspectives on clopidogrel in the acute and long-term management of atherothrombosis. Neth Heart J 2002; 10 (6), 298-9.

Salm LP. Get with the guidelines: hypertension. Neth Heart J 2003; 11 (suppl 2), 12-3.

Salm LP. Stent trek: the next generation. Neth Heart J 2003; 11 (suppl 2), 26-7.

Salm LP. Fast reperfusion therapy in acute myocardial infarction. Neth Heart J 2003; 11 (suppl 2), 54-5.

Salm LP. MRI is beter dan echocardiografie voor de visualisatie van intracardiale trombi. Ned Tijdschr Geneeskd 2003; 147 (19), 941.

Swijnenburg RJ, Lange CPE, Salm LP. Niet-invasieve evaluatie van coronairarteriële stenosen; ontwikkeling van 'coronary magnetic resonance angiography'. Ned Tijdschr Geneeskd Studenten-editie 2004; 7 (1), 14-6.

BOOK CHAPTER

Salm LP, Bax JJ, Schuijf JD, Lamb HJ, Jukema JW, Van der Wall EE, De Roos A. Cardiovascular magnetic resonance and computed tomography of coronary artery bypass grafts. Chapter 21 in: MRI and CT of the cardiovascular system. Second edition. Lippincott Williams & Wilkins 2005.

Curriculum Vitae

De auteur van dit proefschrift werd geboren op 20 mei 1973 te Amsterdam. In 1991 behaalde zij haar VWO-examen aan het Alkwin Kollege te Uithoorn. Aansluitend volgde ze een jaar Medische Informatiekunde aan de Universiteit van Amsterdam, dat ze in 1993 met een propedeuse afsloot. In 1992 begon ze met de studie Geneeskunde, eveneens aan de Universiteit van Amsterdam. In het kader van haar studie liep ze een verpleeghulpstage in het University Hospital in Kuala Lumpur, Maleisië, en een klinisch-wetenschappelijke stage in het AHEPA University Hospital in Thessaloniki, Griekenland. Tijdens een extra-wetenschappelijke stage werkte ze mee aan een onderzoek naar de expressie van interleukine 1β in de nucleus paraventricularis van de hypothalamus bij patiënten met multiple sclerose aan het Nederlands Instituut voor Hersenonderzoek in Amsterdam (Dr. I. Huitinga, Prof. Dr. D.F. Swaab). In 1997 behaalde ze haar doctoraalexamen Geneeskunde en begon ze met de co-assistentschappen in de regio Amsterdam. Haar artsexamen behaalde ze in maart 2000. Vervolgens was ze werkzaam als arts-assistent Cardiologie in het Reinier de Graaf Gasthuis te Delft (Dr. A.J. Withagen) gedurende ruim een jaar. In 2001 startte ze haar promotie-onderzoek in het Leids Universitair Medisch Centrum bij de afdeling Cardiologie (Dr. H.W. Vliegen, Prof. Dr. E.E. van der Wall), in samenwerking met de afdeling Radiologie (Prof. Dr. A. de Roos). In 2005 heeft ze als arts-assistent Cardiologie in het St. Antonius Ziekenhuis te Nieuwegein gewerkt (Dr. W. Jaarsma).

The Road goes ever on and on
Down from the door where it began.
Now far ahead the Road has gone,
And I must follow, if I can,
Pursuing it with eager feet,
Until it joins some larger way
Where many paths and errands meet.
And whither then? I cannot say.

J.R.R. Tolkien